D i s s e r t a t i o n

The effect of tyrosine kinase 2 (Tyk2) deficiency on primary murine macrophages monitored by qualitative and quantitative proteomic analysis

ausgeführt zum Zwecke der Erlangung des akademischen
Grades eines Doktors der Naturwissenschaften
unter der Leitung von

Univ. Prof. Dr. Günter Allmaier
Institut für Chemische Technologien und Analytik
der Technischen Universität Wien

und

Univ. Prof. Dr. Mathias Müller
Institut für Tierzucht und Genetik
der Veterinärmedizinischen Universität Wien

eingereicht an der Technischen Universität Wien
Fakultät für Technische Chemie
von
Mag. Tom Grunert
9500007
Aegidigasse 19/18
1060 Wien

Wien, im Februar 2009

So eine Arbeit wird eigentlich nie fertig.

Man muß sie für fertig erklären,

wenn man nach Zeit und Umständen

das Möglichste getan hat.

Johann Wolfgang von Goethe,

„Italienische Reise"

Caserta, 16. März 1787

Acknowledgements

I would like to thank everybody who helped to make this work possible.

Table of contents

Abstract

Tyrosine kinase 2 (Tyk2) is involved in the intracellular signal transduction of a large number of cytokines. The aim of the presented studies is to improve our understanding of the molecular function of Tyk2 in macrophages using two-dimensional difference gel electrophoresis (2D-DIGE) for protein quantification and matrix-assisted laser desorption/ionisation time-of-flight mass spectrometry (MALDI-TOF-MS) in combination with bioinformatic tools for protein identification. Immunological and enzymatic-colorimetric analyses were employed for further verification and more detailed biological investigations.

The macrophage proteome was investigated before and after treatment with poly(I:C), which mimics the presence of microbial double-stranded RNA. Data emphasise the important role of Tyk2 for the regulation of cellular immune responses and further show that Tyk2 influences the abundance of proteins (incl. isoforms) involved in lipid and carbohydrate metabolism after poly(I:C) treatment. The participation of Tyk2 in metabolic pathways was shown by cholesterol and lactate measurements. The results provide evidence for a novel function of Tyk2 linking metabolic and immune response networks.

This work further contributed to the identification of proteins in Tyk2-deficient macrophages after lipopolysaccharide treatment, a major component of the outer membrane of Gram-negative bacteria. 27 proteins (incl. isoforms) were unambiguously identified by MALDI-TOF-MS/bioinformatics and assigned to various functional categories including immune response, oxidative stress, metabolism and cytoskeleton architecture.

Finally, the fast quality control of protein samples (e.g. derived from body fluids) which are prone to technical artefacts (e.g. enzymatic degradation) was studied by two techniques. SDS-PAGE and capillary gel electrophoresis (CGE)-on-the-chip were both suitable as pre-screening methods for a fast quality evaluation prior to complex MS-based analysis. Differences between samples were easily observed on SDS-PAGE images, but time consumption, sample amount and statistical evaluation were in favour of the technique CGE-on-the-chip.

Zusammenfassung

Tyrosine Kinase 2 (Tyk2) ist an der intrazellulären Signalübertragung bei einer großen Anzahl von Zytokinen beteiligt. Das Ziel der durchgeführten Studie war, das Wissen um die molekulare Funktion von Tyk2 in Makrophagen zu erweitern. Die von uns verwendete Strategie basierte auf 2-dimensionaler differentieller Gel-Elektrophorese (2D-DIGE) für die Proteinquantifizierung und Matrix-unterstützte Laser-Desorption/Ionisation-Flugzeit-Massenspektrometrie (MALDI-TOF-MS) in Kombination mit Bioinformatik für die Proteinidentifizierung. Immunologische und enzymatisch-colorimetrische Analysen wurden für die Verifizierung und für detailliertere biologische Studien angewendet.

Das Proteom der Makrophagen wurde vor und nach Stimulation mit poly(I:C), welches die Anwesenheit mikrobieller doppel-strängiger RNA simuliert, untersucht. Die gewonnenen Daten unterstreichen die bedeutende Rolle von Tyk2 für die Regulation der zellularen Immunantwort. Darüber hinaus konnte gezeigt werden, dass Tyk2 die Regulation von einigen Proteinen und deren Isoformen des Fett- und Kohlenhydratstoffwechsels nach Behandlung mit poly(I:C) beeinflusst. Der Einfluss von Tyk2 auf Stoffwechselwege konnte durch Cholesterin- und Laktatmessungen bestätigt werden. Die Ergebnisse dieser Studie zeigten erstmals, dass Tyk2 bei der molekularen Kommunikation zwischen Immunantwort und Metabolismus eine Rolle spielt.

Des Weiteren trug diese Arbeit zur Identifizierung von Proteinen in Tyk2-defizienten Makrophagen nach Behandlung mit Lipopolysaccharid, einem Hauptbestandteil der äußeren Zellwand von Gram-negativen Bakterien, bei. 27 Proteine inklusive deren Isoformen wurden eindeutig mittels MALDI-TOF-MS und Bioinformatik identifiziert und konnten verschiedenen funktionalen Kategorien (z.B. Immunantwort, oxidativer Stress, Metabolismus und zytoskeletale Architektur) zugeordnet werden.

Zum Schluss wurde ein methodischer Vergleich von zwei schnellen Techniken für die Beurteilung von Proteomproben (z.B. aus Körperflüssigkeiten gewonnen), die besonders anfällig für technische Artefakte (z.B. enzymatischer Abbau) sind, durchgeführt. SDS-PAGE und Kapillargelelektrophorese-am-Chip stellten sich beide als geeignete Methoden für eine schnelle Qualitätskontrolle vor komplexen MS-basierenden Analysen heraus. Unterschiede zwischen den Proteomproben konnten einfacher in der SDS-PAGE visuell beobachtet werden, jedoch Zeitaufwand,

Probenverbrauch und die statistische Auswertung solcher Bilder, geben der Kapillargelelektrophorese-am-Chip den Vorzug.

Introduction

Part I – Biological background

1. Innate immune recognition

A variety of host defence mechanisms have evolutionary developed against microbial pathogens and are basically mediated by two types of immune defence: innate (or natural) and adaptive (or acquired) immunity. The innate immune system serves as first line in defence against pathogenic microbes. Unlike the adaptive immune system, it does not provide exquisite specificity and immunological memory (Medzhitov 2007).

A substantial requirement in the earliest phase of host defence is to recognise invading pathogens. Pathogens exhibit conserved molecular structures, termed as pathogen associated molecular patterns (PAMPs), which are essential for their survival. They are recognised by the host through a limited set of evolutionary conserved pattern recognition receptors (PRRs), which are germ-line encoded and nonclonal. Two different types of PRRs are described based on their cellular location. The well-known family of toll-like receptors (TLRs) detect pathogens at either the cell surface or at lysosomal/endosomal membranes. 13 mammalian members have been identified so far and are implicated in the recognition of a wide range of pathogens, such as bacteria, fungi, protozoa and viruses. For example, TLR1, 2 and 6 detect lipids and carbohydrate compounds of Gram-positive bacterial cell walls, TLR4 recognises lipopolysaccharides (LPS), a cell-wall component of Gram-negative bacteria, and TLR3, 7, 8 and 9 are receptors for nucleic acids. The more recently emerging cytoplasmic PRRs are currently roughly subclassified into nucleotide binding oligomerisation domain (NOD)-like receptors (NLRs) and retinoic acid-inducible gene I (RIG-I)-like receptors (RLRs). These receptors are essential for the recognition of microbial components in the cytoplasma (Akira et al. 2006; Medhzitov et al. 2007; Kumagai et al. 2008; Uematsu et al. 2008).

All PRRs couple ligand binding to cell activation through a distinct set of downstream adapter proteins. Different combinations of adapter molecules ensure specific signal transduction initiated by different types of ligands and PRRs. Subsequently, signals are translated into several distinct intracellular signalling pathways, which finally

converge to activate a common set of transcription factors, most notably nuclear factor-κB (NF-κB) and certain members of the interferon regulatory factor (IRF) family. NF-κB is essential for the production of proinflammatory cytokines, such as interleukin-1 (IL-1), interleukin-6 (IL-6) and tumor necrosis factor α (TNF-α), whereas the most prominent target genes of IRFs are type I interferons (IFNs; IFNα/β). Secreted cytokines act in an autocrine and paracrine manner, induce innate immune effector mechanism and mediate communication between cells of the innate and adaptive immunity (Honda et al. 2006; Kawai et al. 2007).

2. Signalling pathways induced by double-stranded RNA

2.1. Recognition of microbial dsRNA

Double-stranded RNAs (dsRNAs) are PAMPs and their major sources are viral infections. They can be present as viral genomes and released into the cytoplasm during virus entry or appear later during viral life cycles as a replication intermediate of ssRNA viruses or as a by-product during transcription of DNA viruses (Akira et al. 2006). Furthermore, dsRNA can be found in apoptotic bodies from virally infected cells and be released by apoptotic and necrotic cells (Matsumoto et al. 2008). Polyriboinosinic-polyribocytidylic acid (poly(I:C)) is structurally similar to dsRNA and experimentally used to mimic dsRNA. It is synthetically produced and is a highly potent IFNα/β inducer. Poly(I:C) was initially shown to be recognised by membrane-bound TLR3 (Alexopoulou et al. 2001). TLR3 is predominantly, but not exclusively, expressed in cells of the innate immune system. TLR3 is mainly localised in the endosomal compartment, but can also be expressed at the cell surface in some cell-types (Matsumoto et al. 2008). Usually, extracellular poly(I:C) must be internalised to get recognised by endosomal TLR3, a process which is suggested to be mediated by the cell-surface receptor CD14 and by a clathrin-dependent endocytic pathway (Lee et al. 2006; Itoh et al. 2008). In addition to TLR3, the cytoplasmic RLRs, melanoma differentiation associated antigen 5 (MDA-5) and retinoic-acid-inducible protein I (RIG-I), recognize poly(I:C) (Yoneyama et al. 2005). Recent studies suggest that MDA-5 and RIG-I differentially recognise dsRNA in a size dependent manner (Kato 2008; Saito 2008), whereby long dsRNA activates MDA-5 and RIG-I recognises short dsRNA motifs. Poly(I:C) is characterised as long synthetic co-homopolymer RNA and consistently its recognition is triggered in dependence of MDA-5 (Kato et al. 2006). TLR3 and MDA-5/RIG-I dependent core signalling pathways are schematically depicted in Fig. 1 and described below.

2.2. TLR3-dependent signalling

Upon binding of poly(I:C), the adaptor molecule Toll/IL1 receptor (TIR)-domain containing adapter protein-inducing IFNβ (TRIF) is recruited to the TLR3 receptor complex. TRIF interacts with tumor necrosis factor receptor-associated factor 3 (TRAF3), TRAF6 and receptor interacting protein 1 (RIP1). TRAF3 triggers the induction of IFNβ in dependence on interferon regulatory factor 3 (IRF3). IRF3 is

activated by a complex containing the inhibitory κB-kinase signalosome (IKKε) and (TANK)-binding kinase 1 (TBK1), which mediate IRF3 phosphorylation. Activated IRF3 molecules form homodimers, migrate into the nucleus and bind to consensus elements in promoter regions of responsive genes (e.g. IFNβ) (Matsumoto et al. 2008; Takeuchi et al. 2007; Uematsu et al. 2008; Kawai et al. 2007). IRF7 is similarly activated and induces expression of IFNβ and IFNα subtypes, but in most cell-types IRF7 is not constitutively expressed. IRF7 is synthesised in response to type I IFNs and, consequently, leads to auto-amplification of type I IFN expression (Marie et al. 1998). Parallel to IKKε/TBK1 activation, TRAF6 and RIP1 lead to the activation of NF-κB, which is mediated by the ubiquitin-dependent kinase TAK1 complex that targets the IKK complex. Phosphorylated NF-κB translocates into the nucleus and binds to genes containing NF-κB consensus elements in their promoter regions including IFNβ (Matsumoto et al. 2008; Takeuchi et al. 2007; Uematsu et al. 2008; Kawai et al. 2007).

2.3. MDA-5/RIG-I -dependent signalling

MDA-5/RIG-I recognises dsRNA and interacts with the adaptor protein IFNβ promoter stimulator-1 (IPS-1), which is localised on the outer mitochondrial membrane. TRAF3 associates with IPS-1 recruiting IKKε and TBK1 which further cooperate with TRAF family member-associated NF-κB activator (TANK), NAK associated protein 1 (NAP1) and similar to NAP1 TBK1 adaptor (SINTBAD) leading to the activation of IRF3. The IRF3-dependent signalling pathway induced by TLR3 and MDA5/RIG-I overlaps at the level of TRAF3-IKKε/TBK1. In addition to TRAF3, FAS-associated death domain-containing protein (FADD) associates with IPS-1 leading to the cleavage of caspase-8/-10 which downstream induces NF-κB signalling (Takeuchi et al. 2007; Takeuchi et al. 2008; Saito et al. 2008; Yoneyama et al. 2008).
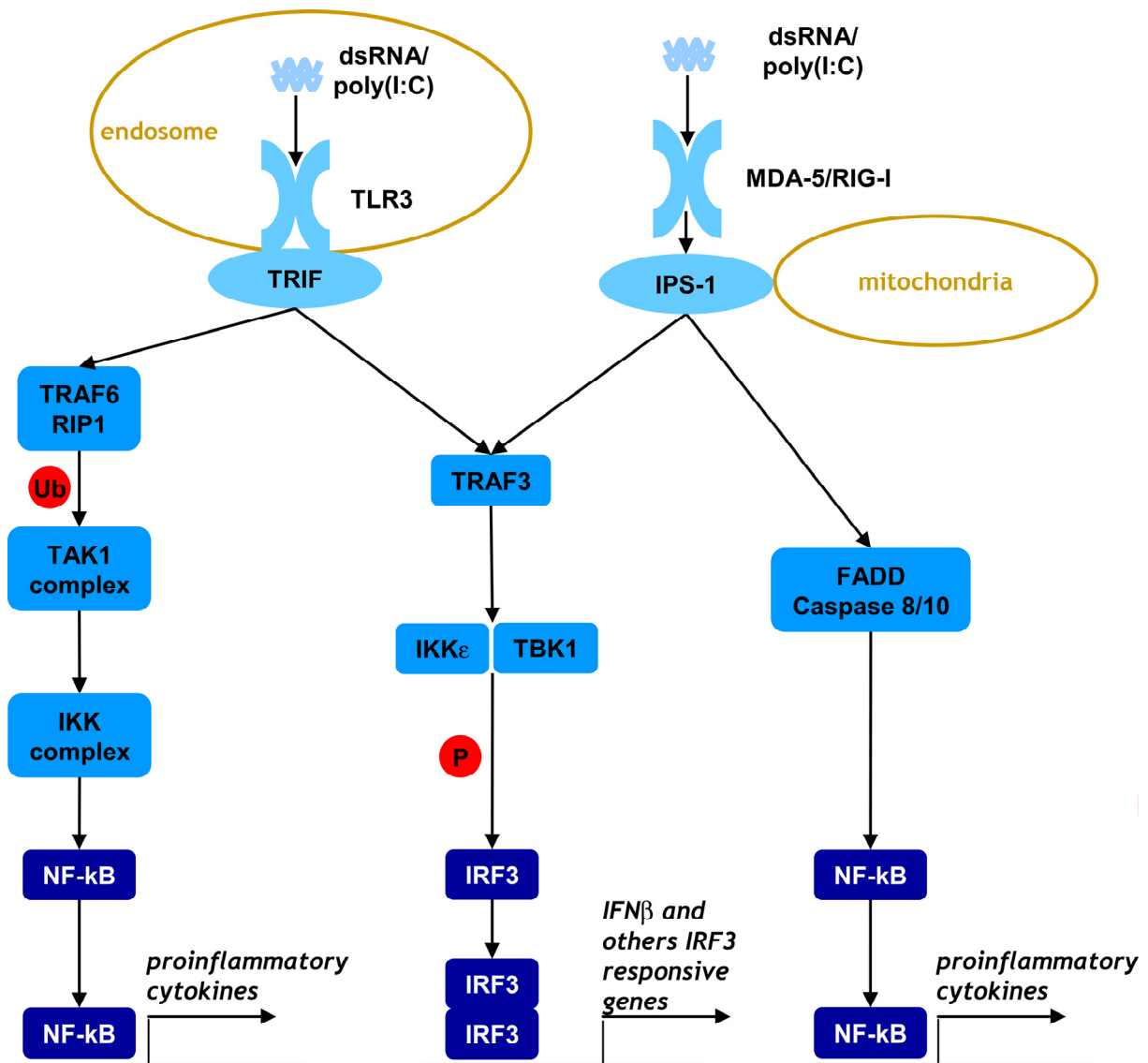
Fig.1 **Poly(I:C) induced core signalling pathways.** dsRNA is recognised by TLR3 and MDA-5/RIG-I and this leads to the production of type I IFNs and proinflammatory cytokines (see text for details).

3. JAK-STAT pathway

3.1. JAK-STAT signalling

The Janus kinase (JAK) - signal transducer and activator of transcription (STAT) signalling pathway is utilised by a variety of cytokines and some growth factors, which are involved in host defence, differentiation, proliferation and oncogenesis. In principle, the JAK-STAT pathway is activated upon cytokine binding to the appropriate receptor and is responsible for the signal transduction from the plasma membrane to the nucleus in order to reprogram gene expression in response to an extracellular stimulus. JAK-STAT signal transduction is performed by a phosphorylation cascade and is described in more detail exemplified for type I IFN signalling (see Fig. 2) (Kisseleva et al. 2002; Schindler et al. 2007).

Type I IFNs bind to the same cell-surface receptor complex, known as type I IFN receptor (IFNAR) that is composed of two subunits, IFNAR1 and IFNAR2. The Janus kinases TYK2 and JAK1 are pre-associated with the IFNAR1 and IFNAR2 chain of the type I IFN receptor, respectively. Following binding of type I IFNs, TYK2 and JAK1 become activated and mediate phosphorylation of receptor tyrosine residues which attract STATs. This leads to the formation of phosphorylated STAT1-STAT2 heterodimers which subsequently associate to IFN regulatory factor 9 (IRF9) forming a complex, called IFN-stimulated gene factor 3 (ISGF3). ISGF3 translocates to the nucleus and binds to specific consensus elements in the promoter region of responsive genes. In addition to ISGF3, which is the main transcription factor complex responsible for type I IFN responses, other STAT homo- and heterodimers and additional signalling cascades can be induced in a cell-type specific manner. JAK-STAT signalling is also negatively regulated at several levels of the signalling cascade, including the receptors, and JAKs and STATs themselves (Decker et al. 2005; Platanias 2005; Schindler et al. 2008).
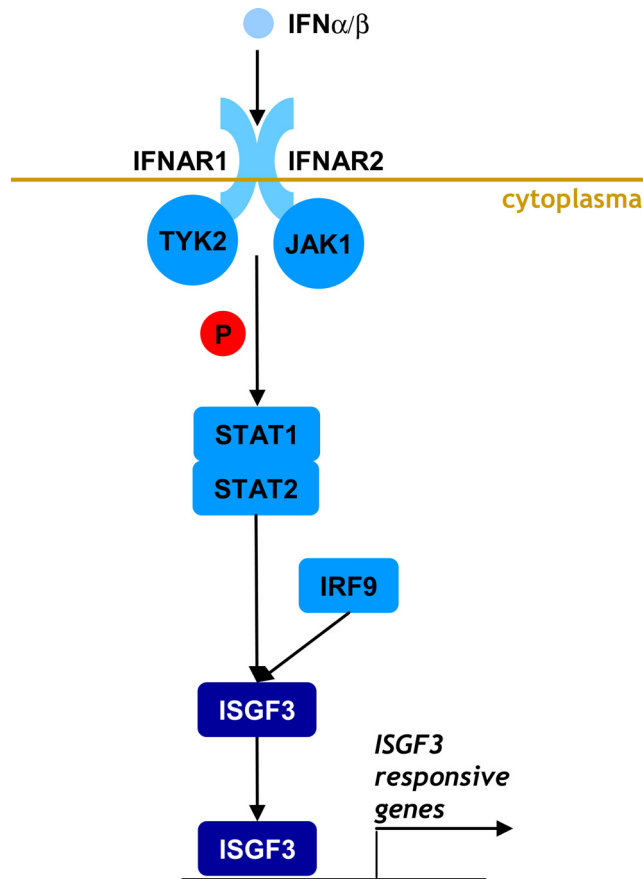
Fig. 2: **Type I IFN signalling: the JAK-STAT pathway.** Type I IFNs activate the JAK-STAT pathway and initiate the induction of target genes (see text for details).

3.2. JAKs and STATs

All four members of the JAK family (JAK1, 2, 3 and TYK2) are non-receptor tyrosine kinases. JAK proteins range in a size from 120-140kDa and feature seven conserved regions of homology, named JAK homology domains (JH1-7). JAKs exhibit at the protein C-terminus a catalytically active kinase domain (JH1) and an adjacent pseudokinase domain (JH2). JAKs are unique among protein tyrosine kinases containing a pseudokinase domain (Ihle 2001). JAK activation requires phosphorylation of tyrosines in the JH1 domain, while JH2 negatively regulates kinase activity. The JH3-7 domains have been implicated in receptor association and specificity (Vainchenker et al. 2008; Schindler et al. 2007; Kisseleva et al. 2002).

At present seven STATs (STATs 1, 2, 3, 4, 5a, 5b, 6) are described with apparent molecular weights of 90-115kDa. They are composed of six different structural and functional domains, most importantly the phosphotyrosine-binding Src homology 2 (SH2) domain for receptor binding and dimerisation. Central for the activation of

STATs is the phosphorylation of a single conserved tyrosine residue near the protein C-terminus, which is required for dimerisation, nuclear translocation and DNA binding (Levy et al. 2002; Brierley et al. 2005; Schindler et al. 2007). All STATs except STAT2 undergo inducible serine phosphorylation, which promotes their transcriptional activity (Decker et al. 2000).

4. Tyrosine kinase 2 (TYK2)

TYK2 was originally described to be essential in type I IFN signalling. Signalling of IFN-α in human fibrosarcoma cells was completely impaired in the absence of TYK2 (Velazquez et al. 1992). Later it was shown that the IFNAR1 subunit of the type I IFN receptor complex requires the expression of TYK2 for transport/stabilisation at the cell surface in human cells (Gauzzi et al. 1997; Ragimbeau et al. 2003; Kumar et al. 2008). In addition to type I IFNs, TYK2 is activated by a large number of other cytokines, including IL-10, IL-6, IL-23 and IL-12 (Kotenko et al. 2000). In contrast to human TYK2, in most cases (including type I IFNs) murine TYK2 is partially required for functional signalling (Shimoda et al. 2000; Karaghisoff et al. 2000).

TYK2-deficient mice are viable, fertile and show normal hematopoietic development (Karaghisoff et al. 2000; Shimoda et al. 2000). The role of TYK2 *in vivo* has been evaluated in various experimental disease models and revealed essential functions of TYK2 as well as detrimental or neutral effects in host responses. Reports concerning antiviral responses showed a selective contribution of TYK2 to the host defence against certain viruses. On one hand, TYK2 is dispensable for survival upon Vesicular Stomatitis Virus (VSV) infection *in vivo* (Karaghiosoff et al. 2000). On the other hand, a protective role of TYK2 *in vivo* was reported for Vaccinia Virus (VV), Lymphocytic Choriomeningitis Virus (LCMV), and Murine Cytomegalovirus (MCMV) (Karaghiosoff et al. 2000; Strobl et al. 2005). Challenge of TYK2-deficient mice with VV resulted in elevated viral replication in spleens as compared to wild-type mice. LCMV infected TYK2-deficient mice revealed a significant reduction of cytotoxic T lymphocyte (CTL) activity (Karaghiosoff et al. 2000). Strongly reduced survival rates were shown in TYK2-deficient mice in response to MCMV. Both, initial control of viral replication and virus clearance from organs at later stages of infection are dependent on TYK2. Furthermore, it was demonstrated that TYK2 is essential for the control of MCMV replication in primary macrophages *in vitro* (Strobl et al. 2005).

In vivo and *in vitro* studies using TYK2-deficient mice underline the importance of TYK2 for the host defence against viral infections and suggest essential molecular functions of TYK2 in promoting antiviral defence mechanisms.

5. References

Akira, S., Uematsu, S., and Takeuchi, O. 2006. Pathogen recognition and innate immunity. Cell 124: 783-801.

Alexopoulou, L., Holt, A.C., Medzhitov, R., and Flavell, R.A. 2001. Recognition of double-stranded RNA and activation of NF-kappaB by Toll-like receptor 3. Nature 413: 732-738.

Brierley, M.M., and Fish, E.N. 2005. Stats: multifaceted regulators of transcription. J Interferon Cytokine Res 25: 733-744.

Decker, T., and Kovarik, P. 2000. Serine phosphorylation of STATs. Oncogene 19: 2628-2637.

Decker, T., Muller, M., and Stockinger, S. 2005. The yin and yang of type I interferon activity in bacterial infection. Nat Rev Immunol 5: 675-687.

Gauzzi, M.C., Barbieri, G., Richter, M.F., Uze, G., Ling, L., Fellous, M., and Pellegrini, S. 1997. The amino-terminal region of Tyk2 sustains the level of interferon alpha receptor 1, a component of the interferon alpha/beta receptor. Proc Natl Acad Sci USA 94: 11839-11844.

Honda, K., and Taniguchi, T. 2006. IRFs: master regulators of signalling by Toll-like receptors and cytosolic pattern-recognition receptors. Nat Rev Immunol 6: 644-658.

Ihle, J.N. 2001. The Stat family in cytokine signaling. Curr Opin Cell Biol 13: 211-217.

Itoh, K., Watanabe, A., Funami, K., Seya, T., and Matsumoto, M. 2008. The clathrin-mediated endocytic pathway participates in dsRNA-induced IFN-beta production. J Immunol 181: 5522-5529.

Karaghiosoff, M., Neubauer, H., Lassnig, C., Kovarik, P., Schindler, H., Pircher, H., McCoy, B., Bogdan, C., Decker, T., Brem, G., Pfeffer, K., Muller, M. 2000. Partial impairment of cytokine responses in Tyk2-deficient mice. Immunity 13: 549-560.

Kato, H., Takeuchi, O., Mikamo-Satoh, E., Hirai, R., Kawai, T., Matsushita, K., Hiiragi, A., Dermody, T.S., Fujita, T., and Akira, S. 2008. Length-dependent recognition of double-stranded ribonucleic acids by retinoic acid-inducible gene-I and melanoma differentiation-associated gene 5. J Exp Med 205: 1601-1610.

Kato, H., Takeuchi, O., Sato, S., Yoneyama, M., Yamamoto, M., Matsui, K., Uematsu, S., Jung, A., Kawai, T., Ishii, K.J., Yamaguchi, O., Otsu, K., Tsujimura, T., Koh, C.S., Reis e Sousa, C., Matsuura, Y., Fujita, T., Akira, S. 2006. Differential roles of MDA5 and RIG-I helicases in the recognition of RNA viruses. Nature 441: 101-105.

Kawai, T., and Akira, S. 2007. Signaling to NF-kappaB by Toll-like receptors. Trends Mol Med 13: 460-469.

Kisseleva, T., Bhattacharya, S., Braunstein, J., and Schindler, C.W. 2002. Signaling through the JAK/STAT pathway, recent advances and future challenges. Gene 285: 1-24.

Kotenko, S.V., and Pestka, S. 2000. Jak-Stat signal transduction pathway through the eyes of cytokine class II receptor complexes. Oncogene 19: 2557-2565.

Kumagai, Y., Takeuchi, O., and Akira, S. 2008. Pathogen recognition by innate receptors. J Infect Chemother 14: 86-92.

Kumar, K.G., Varghese, B., Banerjee, A., Baker, D.P., Constantinescu, S.N., Pellegrini, S., and Fuchs, S.Y. 2008. Basal ubiquitin-independent internalization of interferon alpha receptor is prevented by Tyk2-mediated masking of a linear endocytic motif. J Biol Chem 283: 18566-18572.

Lee, H.K., Dunzendorfer, S., Soldau, K., and Tobias, P.S. 2006. Double-stranded RNA-mediated TLR3 activation is enhanced by CD14. Immunity 24: 153-163.

Levy, D.E., and Darnell, J.E., Jr. 2002. Stats: transcriptional control and biological impact. Nat Rev Mol Cell Biol 3: 651-662.

Marie, I., Durbin, J.E., and Levy, D.E. 1998. Differential viral induction of distinct interferon-alpha genes by positive feedback through interferon regulatory factor-7. EMBO J 17: 6660-6669.

Matsumoto, M., and Seya, T. 2008. TLR3: interferon induction by double-stranded RNA including poly(I:C). Adv Drug Deliv Rev 60: 805-812.

Medzhitov, R. 2007. Recognition of microorganisms and activation of the immune response. Nature 449: 819-826.

Platanias, L.C. 2005. Mechanisms of type-I- and type-II-interferon-mediated signalling. Nat Rev Immunol 5: 375-386.

Ragimbeau, J., Dondi, E., Alcover, A., Eid, P., Uze, G., and Pellegrini, S. 2003. The tyrosine kinase Tyk2 controls IFNAR1 cell surface expression. EMBO J 22: 537-547.

Saito, T., and Gale, M., Jr. 2008. Differential recognition of double-stranded RNA by RIG-I-like receptors in antiviral immunity. J Exp Med 205: 1523-1527.

Schindler, C., Levy, D.E., and Decker, T. 2007. JAK-STAT signaling: from interferons to cytokines. J Biol Chem 282: 20059-20063.

Schindler, C., and Plumlee, C. 2008. Inteferons pen the JAK-STAT pathway. Semin Cell Dev Biol 19: 311-318.

Shimoda, K., Kato, K., Aoki, K., Matsuda, T., Miyamoto, A., Shibamori, M., Yamashita, M., Numata, A., Takase, K., Kobayashi, S., Shibata, S., Asano, Y., Gondo, H., Sekiguchi, K., Nakayama, K., Nakayama, T., Okamura, T., Okamura, S., Niho, Y. 2000. Tyk2 plays a restricted role in IFN alpha signaling, although it is required for IL-12-mediated T cell function. Immunity 13: 561-571.

Strobl, B., Bubic, I., Bruns, U., Steinborn, R., Lajko, R., Kolbe, T., Karaghiosoff, M., Kalinke, U., Jonjic, S., and Muller, M. 2005. Novel functions of tyrosine kinase 2 in the antiviral defense against murine cytomegalovirus. J Immunol 175: 4000-4008.

Takeuchi, O., and Akira, S. 2007. Recognition of viruses by innate immunity. Immunol Rev 220: 214-224.

Takeuchi, O., and Akira, S. 2008. MDA5/RIG-I and virus recognition. Curr Opin Immunol 20: 17-22.

Uematsu, S., and Akira, S. 2008. Toll-Like receptors (TLRs) and their ligands. In: Bauer, S., and Hartmann, G., editors. Toll-Like Receptors (TLRs) and Innate Immunity. Handb Exp Pharmacol. Springer Verlag, Berlin, Heidelberg, Germany. 1-20.

Vainchenker, W., Dusa, A., and Constantinescu, S.N. 2008. JAKs in pathology: role of Janus kinases in hematopoietic malignancies and immunodeficiencies. Semin Cell Dev Biol 19: 385-393.

Velazquez, L., Fellous, M., Stark, G.R., and Pellegrini, S. 1992. A protein tyrosine kinase in the interferon alpha/beta signaling pathway. Cell 70: 313-322.

Yoneyama, M., and Fujita, T. 2008. Structural mechanism of RNA recognition by the RIG-I-like receptors. Immunity 29: 178-181.

Yoneyama, M., Kikuchi, M., Matsumoto, K., Imaizumi, T., Miyagishi, M., Taira, K., Foy, E., Loo, Y.M., Gale, M., Jr., Akira, S., Yonehara, S., Kato, A.,Fujita, T. 2005. Shared and unique functions of the DExD/H-box helicases RIG-I, MDA5, and LGP2 in antiviral innate immunity. J Immunol 175: 2851-2858.

Introduction

Part II - Proteomics

The proteome is defined as all proteins expressed in an organism, tissue, cell or body fluid at a given time under defined conditions. Integrated in the scale-free network of the genome, transcriptome and metabolome, proteome properties are influenced by the resulting multitude of complex interactions and feedbacks (VanRegenmortel 2007). The characterisation of the proteome, termed proteomics, encompasses a variety of technologies to systematically identify proteins in complex samples and to measure differences in protein abundance between samples due to various stimuli like environmental, pharmacological, genetic or pathological changes (Cox et al. 2007; Hamdan et al. 2005). Quantification at the protein level is indispensable as quantities at the transcriptome level can not necessarily be correlated to protein quantities. In addition, possible post-transcriptional (e.g. RNA stability) and post-translational modifications (PTMs; e.g. phosphorylation) determine protein functions, localisations and activities and play an important role in cellular regulations (Hamdan et al. 2005).

The proteomics workflow is a multi-step analysis including sampling, sample preparation and storage, protein separation, protein quantification, protein identification, protein characterisation and verification. The following chapters will give a short overview in sampling, sample preparation and storage, protein quantification and identification and furthermore will particularly focus on methods and techniques which were used within our proteomic workflow (see chapter 2.2. for protein separation and quantification; chapter 3.2. for protein identification).

1. Sampling, sample preparation and storage

1.1. Impact of variables prior to proteomics analysis

Possible specimens of proteome analyses used for animal and human studies are body fluids, tissues and cells including whole cells, cell compartments or biological membranes. Basic requirements for a "perfect sample" include simple access, easy sampling, almost no further sample preparation, no change in protein composition and/or concentration during long-term storage. This would in fact minimise experiment-to-experiment variation and improve the reproducibility giving more confidence in conclusions drawn from a complete proteome study (Molloy et al. 2003). In practice those requirements are rarely fulfilled and at least all substantial factors which may affect the obtained results require observance and/or control to minimise potential variations. Variations can be classified on the basis of their origin, either as biological or technical.

Biological variations derive from features such as gender, age and, in animal studies, genotypes, which are clearly assigned to a subject. In contrast, factors such as nutrition, life style, physical activities and health state are more variable. The latter can be controlled to a large extent for animal studies. However, in human clinical trials they can be standardised only to some degree based on a proper patient selection (Ferguson et al. 2007; Eyk et al. 2008).

All steps of the proteomic workflow are sensitive to technical variations, most notably during sample collection, preparation and storage. Once the sample is removed from the homeostatic environment, biochemical processes are driven to reach an equilibrium adapted to the new environment. During that process proteins are especially susceptible to chemical modification or proteolytic degradation (Ferguson et al. 2007). Therefore, regardless of processing biological fluids, tissue or cell lysates, the time span from sampling to safe storage has to be minimised, protease inhibitors might be added or it has to be strictly stuck to certain incubation times. Additionally, it should be considered that light, temperature, pH, types of sample containers, purity of additives can influence sample integrity during the whole process. The majority of protein samples are stored at -20°C or at -70 to -80°C varying from weeks to several years. For reanalysis the number of freeze-thaw cycles has to be minimised, likewise the time period of freezing and thawing of the samples (Eyk et al. 2008; Hsieh et al. 2006; West-Nielsen et al. 2005).

Many samples have to be particularly prepared before complex proteome analysis according to the specific question that is being addressed in the study. Key options for sample preparation often include sample concentration, sub-cellular fractionation, and minimisation of sample complexity by selective protein enrichment or depletion and removal of excess contaminants. But one has to be aware that each additionally introduced step potentially biases the composition of the proteome (Ferguson et al. 2007; Eyk et al. 2008; Hsieh et al. 2006; Nielsen et al. 2006; Jiang et al. 2008).

1.2. Screening prior to proteomic analysis

Sources of effects prior to analysis have already been recognised for specific analytes in clinical chemistry and diagnostics. Exploring the whole proteome such effects become even more apparent because proteomics methods have high sensitivity and resolution (Ferguson et al. 2007). To overcome this problem, standard sample handling protocols within the laboratory may be implemented. For that the Proteomics Standards Initiative (PSI) tries to provide a good basis by defining community standards for sample preparation and handling between different proteomic laboratories (Taylor et al. 2007) (see chapter 4.).

However, in some cases a pre-screening of samples to check the sample quality is indicated prior to complex, time consuming and expensive proteomic studies to get a well defined and constant starting material. That should be considered for samples derived from *in vivo* experiments having an inherently higher variation compared to *in vitro* experiments, for samples with possible higher technical variations due to certain sample preparations such as pre-fractionation and samples with high proteolytic activity like blood plasma.

A prerequisite for a good screening method is as little sample manipulation as possible, as little time-consumption as possible and easy access to the result without complex data manipulation. Pre-screening requires a method of protein profiling either for comparing protein patterns of high abundance proteins to a reference material or for the assessment of sample homogeneity within the sample pool. Further, the workflow of suspicious samples could be traced back and possible causes are uncovered and removed for future analysis.

2. Global proteomic quantification

2.1. Overview

Global quantitative proteomic approaches can be classified according to different, nevertheless linked strategies (Table 1): (a) gel-based or gel-free separation of proteins and/or peptides (b) non-labelling or labelling of primary structures and (c) spectroscopic-based or mass spectrometry (MS)-based detection (Hamdan et al. 2005).

	Gel-based	Gel-free
Label-based	**Fluorescence labelling (e.g. DIGE)** **Radio isotope labelling** **Stable isotope labelling (e.g. SILAC, ICAT, ITRAQ ICPL)**	**Stable isotope labelling (e.g. SILAC, ICAT, ITRAQ ICPL)**
Label-free	**Non-covalently bound dyes (e.g. fluorescence dyes, Coomassie, silver staining)**	**Global approaches (e.g. MasterMap)** **Targeted approaches (e.g. SRM)**

Table 1: Classification of global quantitative proteomic approaches according to applied separation methods and labelling. DIGE, difference gel electrophoresis; SILAC, stable isotope labelling of amino acids in cell culture; ICAT, isotope coded affinity tags; ITRAQ, isobaric tag for relative and absolute quantification; ICPL, isotope-coded protein labels; SRM, selected reaction monitoring.

(a) Gel-based and -free separation:

Simultaneous quantification of various proteins in a mixture within a wide dynamic range requires separation techniques in order to reduce sample complexity. Two-dimensional gel electrophoresis (2-DE) (O'Farrell 1975), a widely used gel based approach, separates proteins according to their isoelectric points and molecular weights and quantification is done at the protein or peptide level (Patterson et al. 1995; Oda et al. 1999). Gel-free separation approaches are based on

(multidimensional) liquid chromatography (LC) (Gygi et al. 1999; Davis et al. 2001) and capillary electrophoresis (CE) (Cao et al. 1998) combined with quantification only at the peptide level using MS.

The major advantage of quantifying at the protein level is that information about the whole protein (e.g. protein isoform, possible degradation or PTM) remains, whereas by quantifying at the peptide level the association between the particular measured peptides and the proteins is lost. However, gel-free approaches are less labour intensive and especially qualified for high-throughput proteome analysis (Hamdan et al. 2005).

(b) Label-based and -free approaches:

Label-based approaches include any kind of labelling that is introduced into a protein or covalently attached to one or more amino acids of the protein/peptide backbone. Labels can be introduced and detected at the protein or peptide level within the experimental workflow. Ideally, different labels have identical physico-chemical properties, which are important for the separation, but can still clearly be distinguished allowing quantitative analyses. Thus, several differentially labelled samples can be co-processed and distinguished in the same experiment according to their characteristic readout. That allows multiplexing of different targets in the same sample and assaying various samples in parallel ensuring accuracy of analysis and increasing throughput. Label-based approaches can be subdivided in two categories (Hamdan et al. 2005). First, labels are introduced metabolically based on stable isotopes (stable isotope labelling of amino acids in cell culture, SILAC) (Oda et al. 1999; Ong et al. 2002) and radio isotope labelling (Taruvinga et al. 1979) or enzymatically based on stable isotopes ($^{16}O/^{18}O$ exchange) (Yao et al. 2001). Second, in chemical tagging approaches, the label is covalently attached to either specific amino acids (e.g. difference gel electrophoresis, DIGE (Unlu et al. 1998; Knowles et al. 2003); isotope coded affinity tags, ICAT (Gygi et al. 1999); isobaric tag for relative and absolute quantification, ITRAQ (Ross et al. 2004)) or free amino groups of intact proteins (e.g. isotope-coded protein labels, ICPL) (Schmidt et al. 2005). Although labelling based quantification is widely used, several limitations are known including relatively high costs, limited availability of different isotope or fluorescence coded labels and labelling-introduced artefacts (Coiras et al. 2008).

Label-free, MS based quantitative protein profiling would be an attractive alternative. In this approach, different variables, MS- or separation-based, or a combination of

them are used for quantification implying that multiple LC-MS runs are measured under identical conditions with highest possible mass accuracy. In a simple method for approximate quantification, termed "spectral sampling", the number of tandem mass spectra collected from a peptide correlates to peptide concentrations (Liu et al. 2004). More accurate methods are based on global (e.g. MasterMap) or selective (e.g. selected reaction monitoring; SRM) measurements of peptides. In MasterMap, all peptide ion intensities are directly proportional to the initially introduced serial dilution profile and are further linked to results of protein identification (Rinner et al. 2007). In contrast, targeted quantitative approaches based on selected reaction monitoring (SRM) rely on quantifying a predetermined set of peptides. Separation specific values of single ions are used in combination with the specific parent-to-fragment transitions for quantification requiring previous information to define these transitions for each targeted peptide (Lange et al. 2008).

Label-free quantification in combination with 2-DE separation is only provided by non-covalently bound staining of protein spots. Visible (e.g. Coomassie and silver staining) and fluorescence dyes (e.g. Sypro dyes) are used and obtained relative spot intensities are correlated to protein abundance.

(c) Spectroscopic- or MS-based detection:

Label-free and label-based approaches in combination with 2-DE are based on spectroscopic methods measuring the intensity either of absorbed or emitted light that is correlated with the concentration or amount of a given species (Beer's law). Visible and fluorescence spectroscopy are applied to detect quantitative differences of protein expression, using image capturing devices such as laser-based detectors, charge-coupled device (CCD) camera systems and flatbed scanners.

Label-based or -free MS based detection relies on the detection of intact peptides or peptide fragments. Different compositions of introduced stable isotopes allow multiplexing and are used for quantification at the peptide level (e.g. ICAT, SILAC, $^{16}O/^{18}O$ exchange) or upon peptide fragmentation (e.g. ITRAQ). In the former case, identical peptides of different samples are distinguished by a certain mass shift introduced by stable isotopes (e.g. 2 Da shift after $^{16}O/^{18}O$ exchange) and signal intensities of these peptide pairs are correlated to protein abundance. In the latter case, isobaric reporter peptides (no mass shift at the peptide level) are generated which cannot be assigned to their sample origin until they are fragmented allowing

subsequent sample assignment according to distinguishable reporter fragments in the low mass range which intensities can be compared.

Besides other factors, most important for any quantification method is to provide the highest possible dynamic range, the concentration range in which a concentration dependent signal output is produced (Hamdan et al. 2005). For example, samples such as plasma or serum contain proteins in a dynamic range of more than 10 orders of magnitude (Anderson et al. 2002). So far the major advantage of spectroscopic based detection methods (e.g. Fluorescence detection: 3-5 orders of magnitude (Miller et al. 2006)) was a larger dynamic range compared to MS based detection. However, the implementation of novel quantification strategies using MS instruments shifted that aspect, as the dynamic range is now about four orders of magnitude for MS approaches (Blow 2008).

Gel-based and gel-free approaches provide a large number of different strategies for global proteomic quantification, each possessing its specific strength and weakness and especially for MS-based methods a broad spectrum of possibilities exists.

2.2. Protein separation and quantification using 2D-DIGE

2.2.1. Basic principles

In the last decades, 2-DE has been widely used in protein science allowing the separation of several thousand proteins of a single sample (Westermeier et al. 2002). Two dimensional difference gel electrophoresis (2D-DIGE) relies on the same separation principle but with the supplementary introduction of covalently linked, spectrally distinguishable fluorophores prior to electrophoretic separation.

The majority of 2D-DIGE based quantitative comparative proteomic studies uses fluorophores which are attached to lysine residues. Labelling reactions are performed in such a dye-to-protein ratio that only 3-5% of the total number of lysine residues are labelled (minimal labelling). Three fluorescent CyDyes (Cy2, Cy3 and Cy5) with spectrally different excitation and emission wavelengths are commercially available. Each dye carries an intrinsic positive charge with a pK value similar to the ε-amino side group of lysine preserving the isoelectric point (pI) of the protein after the labelling reaction. In practice, a pI shift between labelled and non-labelled proteins has not been demonstrated so far (Hrebicek et al. 2007), but cannot be ruled out. The three fluorophores are also mass matched, adding approximately 450 Da to each protein. Especially at the lower molecular weight range a mass offset of labelled

compared to non-labelled proteins was recognised (Lilley et al. 2006; Hrebicek et al. 2007; Westermeier et al. 2008). Therefore, and to ensure that enough material for subsequent MS based protein identification is provided (see chapter 3), restaining of the gel with MS compatible, visible staining methods is essential (Westermeier et al. 2008).

2.2.2. Experimental design and data analysis

2D-DIGE is capable of comparing relative changes in protein abundance with the advantage of low technical variation due to sample multiplexing. Three different CyDyes are used for three different samples which are then separated within the very same electrophoretic run. One of the CyDyes is used to label an internal standard, i.e. a pool of equal amounts of each single sample present within the given proteomic study. Cy2 is preferably chosen, because it shows slightly different physico-chemical properties compared to Cy3 and Cy5 (Tonge et al. 2001). However, protein-specific dye effects between Cy3 and Cy5 are described in the literature and are explained by differences in the protein-dye binding affinity, in the migration behaviour of dye labelled proteins and in the fluorescent signal and background (Krogh et al. 2007). To circumvent this system bias, the dye combination should be reversed within the experimental set-up, especially because no global normalisation can remove dye effects simultaneously for all protein spots (Krogh et al. 2007). For example, two biological replicates are labelled with either Cy3 or Cy5, and furthermore all samples are randomly analysed on different gel runs. There are a large number of proteomic studies using 2D-DIGE which have demonstrated that the introduction of an internal gel-electrophoretic standard allows proper inter- and intra-gel matching and minimises gel-to-gel variations (Alban et al. 2003; Friedman et al. 2008) (Fig.1).

To ensure statistical significance for data obtained from 2D-DIGE experiments the study of the total experimental variation (including biological and technical variations) is essential for any new application. The calculated experimental variation will suggest the threshold for changes in protein expression which can be expected to be significant changes based on the number of biological replicates at a given confidence level, the so-called minimum of fold change (Karp et al. 2005a/b). Samples carrying different fluorescent dyes are separated within the same gel and detected by fluorescent scanning for each dye separately to prevent signal overlay. Spot signal intensities are normalised to correct dye specific discrepancies arising

from differences due to the scanning process (Alban et al. 2003). In the process, spot pattern of the internal standard are matched across different gels using dedicated software bundles (e.g. DeCyder). Then spot signal intensities derived from different labelled samples are normalised to the internal standard giving standardised abundances. These are further compared for each sample in multi-gel approaches. Thus, spots of interest can be reliably statistically evaluated. Protein spots showing at least a minimum of fold change, according to calculated statistical data, are candidates for further detailed analysis.
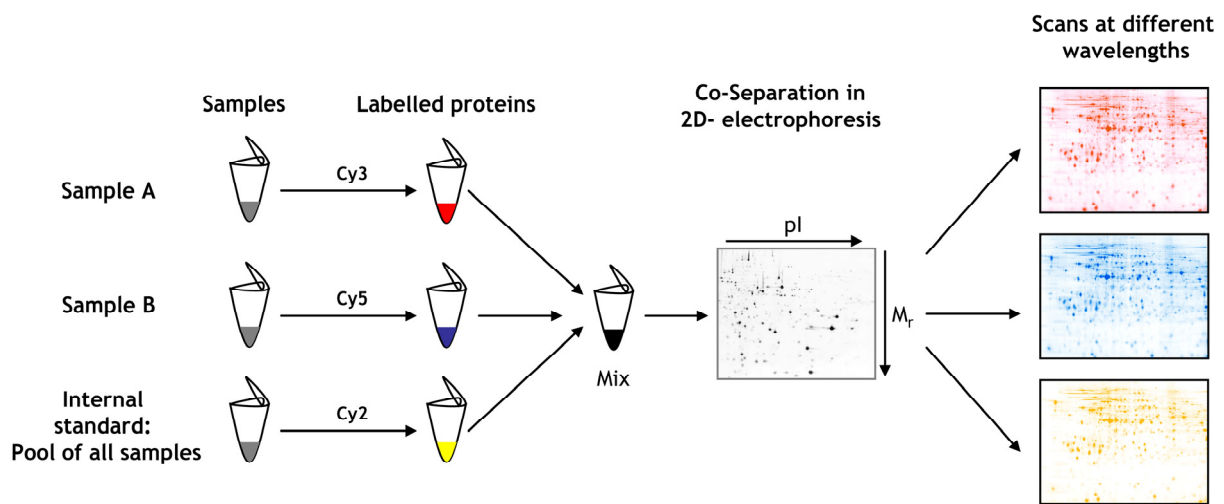
Fig 1. Simplified schematic drawing of a 2D-DIGE study using an internal standard pool (Cy2) (based on (Westermeier et al. 2008)). Proteins of samples to be compared are labelled with either Cy3 (e.g. control sample) or Cy5 (e.g. treated sample). Each 2-DE separation within the study will be performed with the Cy2 standard, combined with the Cy3 and Cy5 labelled samples prior to electrophoresis. Image derived spot intensities from samples labelled with Cy3/5 are normalised based on the corresponding Cy2 spot intensities.

3. Protein identification by mass spectrometry

3.1. Overview

Protein identification is primarily based on protein cleavage and peptide analysis with subsequent database search. Peptides are generated either by chemical or enzymatic cleavage; however, the latter offers mostly better defined cleavage specificities under mild conditions (Liebler 2005). Trypsin is the most commonly used enzyme and preferentially cleaves C-terminally to arginine and lysine residues providing an advantage for MS-based sequencing. The global distribution of arginine and lysine residues within proteins (both have an approx. occurrence in proteins of 5.7 %) results in a selection of peptides of about 5 to 30 amino acids length with only few exceptions (e.g. regions without arginine and lysine residues) (Liebler 2005). Additionally, the molecular weights of the resulting peptides are mostly in a mass-to-charge (m/z) range where adequate accuracy and detection limits are achieved by mass spectrometers.

In general, two different approaches are used for peptide analysis by MS: single stage mass spectrometry experiments (MS), generating m/z data of the intact peptide ions and multi-stage or tandem mass spectrometry experiments (MS/MS), generating sequence information from the precursor peptide ion. Electrospray ionisation (ESI) (Fenn et al. 1989) and matrix-assisted laser desorption/ionisation (MALDI; Karas 1987; Karas et al. 1988; Tanaka et al. 1988) were found to be very efficient for the desorption and ionisation of biomolecules. Both can subsequently be coupled to various mass analysers, most notably time-of-flight (TOF), quadrupole (Q) or ion trap (IT) instruments. Peptide measurements using MALDI are often performed on a reflectron time-of-flight (rTOF) instrument generating mass spectra of peptide ions from a single stage experiment. Additional sequence ion information is obtained either from MALDI-rTOF instruments using post-source decay (PSD; see chapter 3.2.1), a metastable decay of generated ions, or MALDI in combination with Q-RTOF and TOF-rTOF analysers where peptide fragmentation is generated through intended collisions with gas molecules (collision induced dissociation (CID) or collision activated dissociation (CAD)). ESI is mainly performed with mass analysers adapted for tandem or multi-stage MS such as tandem, triple quadrupoles, IT, or Q-rTOFs. Highest mass accuracy, necessary for valuable protein identification solely based on proteolytic peptides, can be achieved by coupling either MALDI or ESI to Orbitrap-

MS (Makarov 2000) and Fourier Transform ion cyclotron resonance (FT ICR) MS (Baldwin 2004).

Peptide mass fingerprinting (PMF) and peptide sequencing were utilised to perform database searching for protein identification. PMF is based on a characteristic signature of peptides derived from the parent protein following specific cleavage (Wada et al. 1983; James et al. 1993; Mann et al. 1993; Pappin et al. 1993; Yates et al. 1993). These experimentally derived peptide masses are compared to peptide masses generated *in silico* from a database of proteins or translated genomic sequences. High mass accuracy of the detected peptide ions is a critical factor for successful matching to database entries because it limits possible compositions of peptides for any given mass (Clauser et al. 1999; Baldwin 2004). Based on the increasing number of database entries, sufficient confidence in protein identification is only achieved by matching a larger number of peptides to a given protein, thus covering a larger percentage of the protein's total sequence in an equal distributed way. Peptide sequencing relies on sequence information by interpretation of fragmented peptide ions derived from PSD (Spengler et al. 1992) or tandem MS experiments (Biemann et al. 1987; Mann et al. 1994; Eng et al. 1994). Spectra derived from any type of peptide fragmentation (e.g. PSD, *in-source* CID or CID) are also suitable to search against comprehensive protein sequence databases using again different search algorithms. For example, the "peptide sequence tag" (Clauser et al. 1994) approach extracts a partial stretch of an amino acid sequence from the spectrum which is a highly specific identifier for the peptide and compares it to the sequence tags of all proteins in a database. In the advanced version, "probability based matching" (Perkins et al. 1999), the experimentally observed fragment ions are compared to all predicted fragments from peptide sequences of the appropriate mass in the database. From this comparison the statistical significance of the match is calculated by comparing the PSD or CID spectrum and the sequences in the database. The probability of a correct identification is correlated to the number of peptides being attributed to any protein and the resulting sequence coverage. Difficulties are raised if e.g. species are studied with yet uncharacterised or only partly characterised genomes hence observed data cannot be matched to the database. In that case *de-novo* peptide sequencing (Taylor et al. 1997) based on known fragmentation rules (Roepstorff et al. 1984; Johnson et al. 1987) is the method of choice implying a sufficient spectrum quality.

Similar to the requirement for protein quantification, sample complexity of protein or peptide mixtures should be reduced by a separation step to clearly identify proteins. In gel-free approaches complex protein mixtures are cleaved, the resulting peptides subsequently separated by liquid chromatography and analysed by MS. A special implementation of the so called "shotgun" approach incorporates multidimensional high performance liquid chromatography, termed multidimensional protein identification technology (MudPIT) (Link et al. 1999). Here, peptides are separated according to at least two different separation principles based on different physico-chemical characteristics (e.g. hydrophobicity and charge) of the analytes prior to mass spectrometry.

Characteristic gel-based workflows for protein identification are: (a) proteins are separated by 2-DE, visualised and protein areas of interest are excised from the gel. Proteins are then proteolytically *in-gel* digested and obtained peptides are directly submitted to MS (Cordwell 1995) (Jensen et al. 1999) (see chapter 3.2.); (b) proteins are separated in a 1-DE gel from which individual bands that may contain multiple proteins are cut out, digested and peptides are analysed by LC-MS (Huang et al. 2002).

3.2. Protein identification using MALDI-rTOF-MS

3.2.1. Basic principles of MALDI-rTOF-MS

In MALDI-MS experiments the analyte is mixed with an excess of matrix, a low molecular weight, photon-absorbing compound, and is co-crystallised on a target (e.g. a stainless steel plate). The target is placed into the high vacuum of the ion source of the mass spectrometer and energy provided by pulsed laser shots is deposited into the co-crystallites. The matrix absorbs the photon energy of the laser light and subsequently the analyte is transferred into gas phase and ionised. The ionised analytes are accelerated in an electric field using a high-voltage grid or lens and separated by drifting along the field-free TOF mass analyser until they reach the detector that counts arriving ions and amplifies signals. M/z values are calculated by measuring the flight time of the ions through the drift tube to the detector based on the following equations.

The kinetic energy E_k of an accelerated ion is calculated by

$$E_k = \frac{m\,v^2}{2} = z\,e_0\,U.$$

     m = mass
     v = velocity
     z = number of charges
     e_0 = elementary electric charge
     U = acceleration voltage

The velocity for the ion is given by

$$v = \frac{L}{t}.$$

     L = drift length
     t = drift time

Replacing v by its value in the previous equation and subsequent conversion to m/z results in

$$\frac{m}{z} = \frac{2\,e_0\,U}{L^2}\,t^2.$$

Assuming a constant flight distance (L) and a given acceleration voltage (U), the m/z value is proportional to the square of the drift time for an ion (de Hofmann et al. 2002; Lottspeich et al. 2006).

Unambiguous protein identification largely depends on mass measurement resolution and accuracy in the MS analysis. Slight differences in the distribution of the kinetic energies of ions with identical molecular weights introduced during the desorption/ionisation process and the early acceleration phase can cause signal broadening leading to poor resolution. Over the years two additional devices were introduced, that could significantly improve mass resolution by compensating this energy distribution. First, delayed extraction or time lag focusing (Wiley et al. 1955) a technique which turns on the accelerating high electric field with a time delay after the pulsed laser desorption/ionisation process was initiated. Ions of the same m/z value achieve variable distances from the plate during the desorption/ionisation process which correlates to their initial kinetic energy. Upon acceleration voltage is turned on, the energy acquired by these ions depends on their position (Hamdan et al. 2005). Ions with higher initial velocities cover a longer distance during the time delay, but gain a lower kinetic energy from the activated electric field compared to ions with lower initial velocities. Second, applying a reflector instrument (Mamyrin et

al. 1973), ions of the same m/z drifting in the TOF analyser at different locations (again caused by energy distribution) are decelerated in an electric field and reflected under a small angle to the detector. Isobaric ions exhibiting a higher kinetic energy penetrate the applied electrical field more deeply than ions with lower kinetic energy having therefore a longer distance to reach the detector. Hence, after passing the reflector, the kinetic energy of isobaric ions is again equalised and mass resolution improved (due to energy focusing and a longer flight path).

MALDI-rTOF-MS peptide sequencing is performed using PSD which is based on metastable fragmentation. It occurs when excess of internal energy, introduced during the desorption/ionisation process, leads to further, post-source, dissociation of the ions while passing the TOF mass analyser before reaching the detector. During their drift they dissociate into smaller ion products, so-called fragments, with comparable velocities, but different kinetic energies ($E = mv^2/2$). These fragments are not distinguishable if a simple TOF analyser (without reflectron) is used. However, in the reflectron mode, mass differences are resolvable, because fragments with different kinetic energies have different penetration depths into the reflector and impinge the detector at different time.

3.2.2. Protein Identification

Identification using MALDI-rTOF-MS is primarily based on recorded PMF mass spectra resulting in a peak list of m/z values. Raw data are corrected for known autolytic tryptic peptides, contaminations (e.g. keratin) and matrix clusters (Smirnov et al. 2004; Mattow et al. 2004). The remaining m/z list is submitted to different search algorithms (e.g. MASCOT (Perkins et al. 1999)), which compare experimentally obtained m/z values with those derived from theoretical calculations of tryptic peptides of proteins from different applied databases (e.g. SwissProt). Protein sequence coverage of more than 20% is likely to be significant, but does not identify proteins unambiguously (Biron et al. 2006). Therefore, several peptides probably belonging to the protein are selected for further PSD fragment ion analysis. A single peptide may not produce an unique result, because frequently a fragmentation pattern, particularly obtained from small peptides (< 10 amino acids), results in several distinct amino sequences all with statistical significant scores. At least the combination of two search algorithms in two different databases obtained from PMF and/or PSD experiments, which are independently exceeding their algorithm's

significance threshold, are necessary to correctly identify a protein (Lubec et al. 2007). Additionally, the primary protein characteristics, namely the useful physicochemical attributes (*pI* and MW) obtained from the prior separation steps (e.g. 2-DE) can be compared to theoretical values found in protein databases. But this is limited by the fact, that additives in the separation process (e.g. urea, reducing agents) can alter *pI* and MW of certain proteins. Nevertheless, the confidence in protein identification can hereby be increased and first indications for possible post-translational modifications or unwanted protein cleavages are available. A considerable drawback of 2-DE gel-based protein identification is that, to some extent, an apparently well resolved protein spot can contain multiple proteins which disable any quantification result (Gygi et al. 2000; Yang et al. 2007). As Western blot analysis with highly specific antibodies represents a complementary identification/verification method to mass spectrometry it can further corroborate mass spectrometric results and is therefore highly recommended for validated protein identification.

4. Guidelines for reporting the use of gel electrophoretic and mass spectrometric data in proteomics

Proteomics experiments comprise many different methods of high complexity. Results and data interpretation will differ depending on how the experimental and analytical parameters were chosen. Recently, community-based standards and guidelines for the analysis and documentation of proteomic experiments were developed known as the "minimum information about a proteomics experiment" (MIAPE). On that base the following criteria for analysis and documentation have been defined for gel electrophoresis and mass spectrometry (Taylor et al. 2007; Gibson et al. 2008; Binz et al. 2008) and were tried to be fulfilled throughout this thesis.

Gel electrophoresis

- General features (e.g. type of electrophoresis)
- Sample preparation (e.g. labels and sample loading)
- Gel matrix and electrophoresis (e.g. dimension, properties of the gel matrix)
- Inter-dimension process (e.g. equilibration, protein reduction and alkylation)
- Detection process (e.g. protein staining, immunoblotting)
- Image acquisition (e.g. equipment and procedure used for image digitalisation)
- Image properties (e.g. resolution, bit-depth)
- Quantification (e.g. DIGE)

Mass spectrometry

- MS-instrument features including components of ion source, separation and detection (e.g. ESI, MALDI; TOF, TOF/rTOF, ion trap)
- Proteolytic cleavage (e.g. tryptic digest)
- Peptide separation, concentration and purification (e.g. HPLC, ZipTip-technology)
- Information on MS and MS/MS database search (e.g. name and version of software and databases, mass tolerance for precursor or fragment ions)
- Quantification (e.g. ITRAQ, ICAT, SILAC)

5. References

Alban, A., David, S.O., Bjorkesten, L., Andersson, C., Sloge, E., Lewis, S., and Currie, I. 2003. A novel experimental design for comparative two-dimensional gel analysis: two-dimensional difference gel electrophoresis incorporating a pooled internal standard. Proteomics 3: 36-44.

Anderson, N.L., and Anderson, N.G. 2002. The human plasma proteome: history, character, and diagnostic prospects. Mol Cell Proteomics 1: 845-867.

Baldwin, M.A. 2004. Protein identification by mass spectrometry: issues to be considered. Mol Cell Proteomics 3: 1-9.

Biemann, K., and Scoble, H.A. 1987. Characterization by tandem mass spectrometry of structural modifications in proteins. Science 237: 992-998.

Binz, P.A., Barkovich, R., Beavis, R.C., Creasy, D., Horn, D.M., Julian, R.K., Jr., Seymour, S.L., Taylor, C.F., and Vandenbrouck, Y. 2008. Guidelines for reporting the use of mass spectrometry informatics in proteomics. Nat Biotechnol 26: 862.

Biron, D.G., Brun, C., Lefevre, T., Lebarbenchon, C., Loxdale, H.D., Chevenet, F., Brizard, J.P., and Thomas, F. 2006. The pitfalls of proteomics experiments without the correct use of bioinformatics tools. Proteomics 6: 5577-5596.

Blow, N. 2008. Mass spectrometry and proteomics: hitting the mark. Nat Methods 5: 741-747.

Clauser, K.R., Baker, P., and Burlingame, A.L. 1994. Peptide fragmention tags from MALDI/PSD for error-tolerant searching of genomic databases. In: Proc. 44th ASMS Conf. Mass Spectrom. Allied Topics, May 12–16, Portland, OR, USA., 365.

Clauser, K.R., Baker, P., and Burlingame, A.L. 1999. Role of accurate mass measurement (+/- 10 ppm) in protein identification strategies employing MS or MS/MS and database searching. Anal Chem 71: 2871-2882.

Coiras, M., Camafeita, E., Lopez-Huertas, M.R., Calvo, E., Lopez, J.A., and Alcami, J. 2008. Application of proteomics technology for analyzing the interactions between host cells and intracellular infectious agents. Proteomics 8: 852-873.

Cordwell, S.J., Wilkins, M.R., Cerpa-Poljak, A., Gooley, A.A., Duncan, M., Williams, K.L., and Humphery-Smith, I. 1995. Cross-species identification of proteins separated by two-dimensional gel electrophoresis using matrix-assisted laser desorption ionisation/time-of-flight mass spectrometry and amino acid composition. Electrophoresis 16: 438-443.

Cox, J., and Mann, M. 2007. Is proteomics the new genomics? Cell 130: 395-398.

Davis, M.T., Beierle, J., Bures, E.T., McGinley, M.D., Mort, J., Robinson, J.H., Spahr, C.S., Yu, W., Luethy, R., and Patterson, S.D. 2001. Automated LC-LC-MS-MS platform using binary ion-exchange and gradient reversed-phase chromatography for improved proteomic analyses. J Chromatogr B Biomed Sci Appl 752: 281-291.

de Hoffmann, E., and Stroobant, V. 2002. Mass Spectrometry. Principles and Applications. Wiley, Chichester, England.

Eng, J.K., McCormack, A.L., and Yates, J.R. 1994. An approach to correlate tandem mass spectral data of peptides with amino acid sequences in a protein database. J. Amer. Soc. Mass Spectrom. 5: 976-989.

Eyk, J.v.D., M.J. 2008. Clinical Proteomics. From Diagnosis to Therapy. Wiley, Weinheim, Germany.

Fenn, J.B., Mann, M., Meng, C.K., Wong, S.F., and Whitehouse, C.M. 1989. Electrospray ionization for mass spectrometry of large biomolecules. Science 246: 64-71.

Ferguson, R.E., Hochstrasser, D.F., and Banks, R.E. 2007. Impact of preanalytical variables on the analysis of biological fluids in proteomic studies. Proteomics Clin. Appl. 1: 739–746.

Gibson, F., Anderson, L., Babnigg, G., Baker, M., Berth, M., Binz, P.A., Borthwick, A., Cash, P., Day, B.W., Friedman, D.B., Garland, D., Gutstein, H.B., Hoogland, C., Jones, N.A., Khan, A., Klose, J., Lamond, A.I., Lemkin, P.F., Lilley, K.S., Minden, J., Morris, N.J., Paton, N.W., Pisano, M.R., Prime, J.E., Rabilloud, T., Stead, D.A., Taylor, C.F., Voshol, H., Wipat, A., Jones, A.R. 2008. Guidelines for reporting the use of gel electrophoresis in proteomics. Nat Biotechnol 26: 863-864.

Gygi, S.P., Corthals, G.L., Zhang, Y., Rochon, Y., and Aebersold, R. 2000. Evaluation of two-dimensional gel electrophoresis-based proteome analysis technology. Proc Natl Acad Sci USA 97: 9390-9395.

Gygi, S.P., Rist, B., Gerber, S.A., Turecek, F., Gelb, M.H., and Aebersold, R. 1999. Quantitative analysis of complex protein mixtures using isotope-coded affinity tags. Nat Biotechnol 17: 994-999.

Hamdan, M., and Righetti, P.G. 2005. Proteomics today. Wiley, Hoboken, NJ, USA.

Hrebicek, T., Durrschmid, K., Auer, N., Bayer, K., and Rizzi, A. 2007. Effect of CyDye minimum labeling in differential gel electrophoresis on the reliability of protein identification. Electrophoresis 28: 1161-1169.

Hsieh, S.Y., Chen, R.K., Pan, Y.H., and Lee, H.L. 2006. Systematical evaluation of the effects of sample collection procedures on low-molecular-weight serum/plasma proteome profiling. Proteomics 6: 3189-3198.

Huang, L., Baldwin, M.A., Maltby, D.A., Medzihradszky, K.F., Baker, P.R., Allen, N., Rexach, M., Edmondson, R.D., Campbell, J., Juhasz, P., Martin, S.A., Vestal, M.L.,Burlingame, A.L. 2002. The identification of protein-protein interactions of the nuclear pore complex of Saccharomyces cerevisiae using high throughput matrix-assisted laser desorption ionization time-of-flight tandem mass spectrometry. Mol Cell Proteomics 1: 434-450.

James, P., Quadroni, M., Carafoli, E., and Gonnet, G. 1993. Protein identification by mass profile fingerprinting. Biochem Biophys Res Commun 195: 58-64.

Jensen, O.N., Wilm, M., Shevchenko, A., and Mann, M. 1999. Sample preparation methods for mass spectrometric peptide mapping directly from 2-DE gels. Methods Mol Biol 112: 513-530.

Jiang, X., Ye, M., and Zou, H. 2008. Technologies and methods for sample pretreatment in efficient proteome and peptidome analysis. Proteomics 8: 686-705.

Johnson, R.S., Martin, S.A., Biemann, K., Stults, J.T., and Watson, J.T. 1987. Novel fragmentation process of peptides by collision-induced decomposition in a tandem mass spectrometer: differentiation of leucine and isoleucine. Anal Chem 59: 2621-2625.

Karas, M. 1987. Matrix-assisted ultraviolet laser desorption of non volatile compounds. Int J Mass Spectrom Ion Proc 78: 53-68.

Karas, M., and Hillenkamp, F. 1988. Laser desorption ionization of proteins with molecular masses exceeding 10,000 daltons. Anal Chem 60: 2299-2301.

Karp, N.A., and Lilley, K.S. 2005. Maximising sensitivity for detecting changes in protein expression: experimental design using minimal CyDyes. Proteomics 5: 3105-3115.

Karp, N.A., Spencer, M., Lindsay, H., O'Dell, K., and Lilley, K.S. 2005. Impact of replicate types on proteomic expression analysis. J Proteome Res 4: 1867-1871.

Knowles, M.R., Cervino, S., Skynner, H.A., Hunt, S.P., de Felipe, C., Salim, K., Meneses-Lorente, G., McAllister, G., and Guest, P.C. 2003. Multiplex proteomic analysis by two-dimensional differential in-gel electrophoresis. Proteomics 3: 1162-1171.

Krogh, M., Liu, Y., Waldemarson, S., Valastro, B., and James, P. 2007. Analysis of DIGE data using a linear mixed model allowing for protein-specific dye effects. Proteomics 7: 4235-4244.

Lange, V., Picotti, P., Domon, B., and Aebersold, R. 2008. Selected reaction monitoring for quantitative proteomics: a tutorial. Mol Syst Biol 4: 222.

Liebler, D.C. 2005. Essential elements of a proteomics laboratory. In: Liebler D.C., editor. Proteomics in Cancer Research. Wiley, Hoboken, NJ, USA. 1-16.

Lilley, K.S., and Dupree, P. 2006. Methods of quantitative proteomics and their application to plant organelle characterization. J Exp Bot 57: 1493-1499.

Link, A.J., Eng, J., Schieltz, D.M., Carmack, E., Mize, G.J., Morris, D.R., Garvik, B.M., and Yates, J.R., 3rd. 1999. Direct analysis of protein complexes using mass spectrometry. Nat Biotechnol 17: 676-682.

Liu, H., Sadygov, R.G., and Yates, J.R., 3rd. 2004. A model for random sampling and estimation of relative protein abundance in shotgun proteomics. Anal Chem 76: 4193-4201.

Lottspeich, F., and Engels, J.W. 2006. Bioanalytik. Spektrum Akademischer Verlag, Heidelberg, Berlin, Germany.

Lubec, G., and Afjehi-Sadat, L. 2007. Limitations and pitfalls in protein identification by mass spectrometry. Chem Rev 107: 3568-3584.

Makarov, A. 2000. Electrostatic axially harmonic orbital trapping: a high-performance technique of mass analysis. Anal Chem 72: 1156-1162.

Mamyrin, B.A., Karataev, V.I., Shmikk, D.V., Zagulin, V.A. 1973. The mass-reflectron, a new nonmagnetic time-of-flight mass spectrometer with high resolution. Sov. Phys. JETP 37: 45–48.

Mann, M., Hojrup, P., and Roepstorff, P. 1993. Use of mass spectrometric molecular weight information to identify proteins in sequence databases. Biol Mass Spectrom 22: 338-345.

Mann, M., and Wilm, M. 1994. Error-tolerant identification of peptides in sequence databases by peptide sequence tags. Anal Chem 66: 4390-4399.

Mattow, J., Schmidt, F., Hohenwarter, W., Siejak, F., Schaible, U.E., and Kaufmann, S.H. 2004. Protein identification and tracking in two-dimensional electrophoretic gels by minimal protein identifiers. Proteomics 4: 2927-2941.

Miller, I., Crawford, J., and Gianazza, E. 2006. Protein stains for proteomic applications: which, when, why? Proteomics 6: 5385-5408.

Molloy, M.P., Brzezinski, E.E., Hang, J., McDowell, M.T., and Van Bogelen, R.A. 2003. Overcoming technical variation and biological variation in quantitative proteomics. Proteomics 3: 1912-1919.

Oda, Y., Huang, K., Cross, F.R., Cowburn, D., and Chait, B.T. 1999. Accurate quantitation of protein expression and site-specific phosphorylation. Proc Natl Acad Sci USA 96: 6591-6596.

O'Farrell, P.H. 1975. High resolution two-dimensional electrophoresis of proteins. J Biol Chem 250: 4007-4021.

Ong, S.E., Blagoev, B., Kratchmarova, I., Kristensen, D.B., Steen, H., Pandey, A., and Mann, M. 2002. Stable isotope labeling by amino acids in cell culture, SILAC, as a simple and accurate approach to expression proteomics. Mol Cell Proteomics 1: 376-386.

Pappin, D.J., Hojrup, P., and Bleasby, A.J. 1993. Rapid identification of proteins by peptide-mass fingerprinting. Curr Biol 3: 327-332.

Patterson, S.D., and Aebersold, R. 1995. Mass spectrometric approaches for the identification of gel-separated proteins. Electrophoresis 16: 1791-1814.

Perkins, D.N., Pappin, D.J., Creasy, D.M., and Cottrell, J.S. 1999. Probability-based protein identification by searching sequence databases using mass spectrometry data. Electrophoresis 20: 3551-3567.

Rinner, O., Mueller, L.N., Hubalek, M., Muller, M., Gstaiger, M., and Aebersold, R. 2007. An integrated mass spectrometric and computational framework for the analysis of protein interaction networks. Nat Biotechnol 25: 345-352.

Roepstorff, P., and Fohlman, J. 1984. Proposal for a common nomenclature for sequence ions in mass spectra of peptides. Biomed Mass Spectrom 11: 601.

Ross, P.L., Huang, Y.N., Marchese, J.N., Williamson, B., Parker, K., Hattan, S., Khainovski, N., Pillai, S., Dey, S., Daniels, S., et al. 2004. Multiplexed protein quantitation in Saccharomyces cerevisiae using amine-reactive isobaric tagging reagents. Mol Cell Proteomics 3: 1154-1169.

Schmidt, A., Kellermann, J., and Lottspeich, F. 2005. A novel strategy for quantitative proteomics using isotope-coded protein labels. Proteomics 5: 4-15.

Smirnov, I.P., Zhu, X., Taylor, T., Huang, Y., Ross, P., Papayanopoulos, I.A., Martin, S.A., and Pappin, D.J. 2004. Suppression of alpha-cyano-4-hydroxycinnamic acid matrix clusters and reduction of chemical noise in MALDI-TOF mass spectrometry. Anal Chem 76: 2958-2965.

Spengler, B., Kirsch, D., Kaufmann, R., and Jaeger, E. 1992. Peptide sequencing by matrix-assisted laser-desorption mass spectrometry. Rapid Commun Mass Spectrom 6: 105-108.

Tanaka, K., Waki, H., Ido, Y., Akita, S., Yoshida, Y., Yoshida, T.,Matsuo, T. 1988. Protein and polymer analyses up to m/z 100 000 by laser ionization time-of-flight mass spectrometry. Rapid Commun Mass Spectrom 2:151-153.

Taruvinga, M., Jackson, A.A., and Golden, M.H. 1979. Comparison of 15N-labelled glycine, aspartate, valine and leucine for measurement of whole-body protein turnover. Clin Sci (Lond) 57: 281-283.

Taylor, C.F., Binz, P.A., Aebersold, R., Affolter, M., Barkovich, R., Deutsch, E.W., Horn, D.M., Huhmer, A., Kussmann, M., Lilley, K., Macht, M., Mann, M., Muller, D., Neubert, T.A., Nickson, J., Patterson, S.D., Raso, R., Resing, K., Seymour, S.L., Tsugita, A., Xenarios, I., Zeng, R., Julian, R.K., Jr. 2008. Guidelines for reporting the use of mass spectrometry in proteomics. Nat Biotechnol 26: 860-861.

Taylor, C.F., Paton, N.W., Lilley, K.S., Binz, P.A., Julian, R.K., Jr., Jones, A.R., Zhu, W., Apweiler, R., Aebersold, R., Deutsch, E.W., Dunn, M.J., Heck, A.J., Leitner, A., Macht, M., Mann, M., Martens, L., Neubert, T.A., Patterson, S.D., Ping, P., Seymour, S.L., Souda, P., Tsugita, A., Vandekerckhove, J., Vondriska, T.M., Whitelegge, J.P., Wilkins, M.R., Xenarios, I., Yates, J.R., 3rd, Hermjakob, H. 2007. The minimum information about a proteomics experiment (MIAPE). Nat Biotechnol 25: 887-893.

Taylor, J.A., and Johnson, R.S. 1997. Sequence database searches via de novo peptide sequencing by tandem mass spectrometry. Rapid Commun Mass Spectrom 11: 1067-1075.

Tonge, R., Shaw, J., Middleton, B., Rowlinson, R., Rayner, S., Young, J., Pognan, F., Hawkins, E., Currie, I., and Davison, M. 2001. Validation and development of fluorescence two-dimensional differential gel electrophoresis proteomics technology. Proteomics 1: 377-396.

Unlu, M., Morgan, M.E., and Minden, J.S. 1997. Difference gel electrophoresis: a single gel method for detecting changes in protein extracts. Electrophoresis 18: 2071-2077.

Van Regenmortel, M.H. 2007. The rational design of biological complexity: a deceptive metaphor. Proteomics 7: 965-975.

Wada, Y., Hayashi, A., Masanori, F., Katakuse, I., Ichihara, T., Nakabushi, H., Matsuo, T., Sakurai, T., and Matsuda, H. 1983. Characterization of a new fetal hemoglobin variant, Hb F Izumi A gamma 6 Glu replaced by Gly, by molecular secondary ion mass spectrometry. Biochim Biophys Acta 749: 244-248.

Westermeier, R., and Naven, T. 2002. Proteomics in Practice. A Laboratory Manual of Proteome Analysis, Wiley, Weinheim, Germany.

Westermeier, R., and Scheibe, B. 2008. Difference gel electrophoresis based on lys/cys tagging. Methods Mol Biol 424: 73-85.

West-Nielsen, M., Hogdall, E.V., Marchiori, E., Hogdall, C.K., Schou, C., and Heegaard, N.H. 2005. Sample handling for mass spectrometric proteomic investigations of human sera. Anal Chem 77: 5114-5123.

Wiley, W.C., and McLaren, I.H. 1955. Time-of-Flight Mass Spectrometer with Improved Resolution. Rev Sci Instr 26: 1150-1157.

Yang, Y., Thannhauser, T.W., Li, L., and Zhang, S. 2007. Development of an integrated approach for evaluation of 2-D gel image analysis: impact of multiple proteins in single spots on comparative proteomics in conventional 2-D gel/MALDI workflow. Electrophoresis 28: 2080-2094.

Yao, X., Freas, A., Ramirez, J., Demirev, P.A., and Fenselau, C. 2001. Proteolytic 18O labeling for comparative proteomics: model studies with two serotypes of adenovirus. Anal Chem 73: 2836-2842.

Yates, J.R., 3rd, Speicher, S., Griffin, P.R., and Hunkapiller, T. 1993. Peptide mass maps: a highly informative approach to protein identification. Anal Biochem 214: 397-408.

Aims of the thesis

This work was conducted with the following objectives:

(1) Identifying novel molecular functions of Tyk2 in macrophages using a proteomics approach.

    (a) The aim was to compare Tyk2-deficient and wild-type (control) bone marrow-derived murine macrophages before and after poly(I:C) stimulation. Whole cell extracts were isolated and differentially regulated proteins were found using two-dimensional difference gel electrophoresis (2D-DIGE). Selected protein spots were identified using mass spectrometry followed by immunological and enzymatic as well as colorimetric analyses.

    (b) An additional purpose of this work was to contribute to the identification of differentially regulated protein spots in response to lipopolysaccharide (LPS) in macrophages. Selected spots were submitted to protein identification by mass spectrometry based on peptide mass fingerprinting and sequence tags.

(2) Finding a suitable method for fast pre-screening of samples prior to complex proteomics analysis.

    The focus was to analyse a set of thirteen mouse sera for sample homogeneity using fast and easy-to-handle analytical methods. SDS-PAGE and CGE-on-the-chip were investigated focusing on sample and time consumption and significance for detecting differences.

Manuscripts and accepted publications

1. Proteome analysis of wild-type and tyrosine kinase 2 (TYK2)-deficient primary murine macrophages before and after stimulation with poly(I:C)

J Proteomics, Manuscript in preparation 2009

Proteome analysis of wild-type and tyrosine kinase 2 (TYK2)-deficient primary murine macrophages before and after stimulation with poly(I:C)

Tom Grunert[1, 2], Birgit Strobl[1], Martina Marchetti-Deschmann[2], Ingrid Miller[3], Marta Radwan[1, 3], Claus Vogl[1], Thomas Kolbe[4], Dagmar Kratky[5], Manfred Gemeiner[3], Günter Allmaier[2] and Mathias Müller[1, 4]

[1] Institute of Animal Breeding and Genetics, University of Veterinary Medicine Vienna, Vienna, Austria

[2] Institute of Chemical Technologies and Analytics, Vienna University of Technology, Vienna, Austria

[3] Institute of Chemistry, Biochemistry and Physics, University of Veterinary Medicine Vienna, Vienna, Austria

[4] University Center Biomodels Austria, University of Veterinary Medicine Vienna, Vienna, Austria

[5] Institute of Molecular Biology and Biochemistry, Center of Molecular Medicine, Medical University of Graz, Graz, Austria

Abstract

Tyrosine kinase 2 (TYK2) is an integral part of the Janus kinase - signal transducer and activator of transcription (JAK-STAT) pathway and is involved in intracellular signal transduction of various cytokines. We have recently reported that TYK2 contributes to host defence mechanisms against certain viruses. Here, we investigated the impact of TYK2 on the macrophage proteome using the double-stranded RNA analogue polyinosinic acid-polycytidylic acid (poly(I:C)) as a model to mimic viral infections. 2D-DIGE in connection with MALDI-reflectron-TOF MS identified eighteen protein spots corresponding to sixteen different proteins as being differentially expressed in the absence of TYK2 with/without poly(I:C) treatment. The majority of these proteins are functionally assigned to the cellular immune response and metabolism. We showed that induced protein expression of T-cell specific GTPase is partially dependent on TYK2. In contrast, we found a negative regulatory role of TYK2 on selected lipid and carbohydrate metabolic enzyme levels upon poly(I:C) treatment. Further investigations showed that TYK2 is required for the up-regulation of cellular total cholesterol and extracellular lactate in response to poly(I:C). These combined results provide evidence for a novel function of TYK2 at the molecular interface between innate immunity and lipid as well as carbohydrate metabolism.

1. Introduction

Protein kinases are involved in the regulation of a large number of cellular processes and dysregulated kinase activity is a frequent cause of diseases. Tyrosine kinase 2 (TYK2) is a member of the Janus kinase family of intracellular non-receptor tyrosine kinases transducing signals via the JAK-STAT (Janus kinase - signal transducer and activator of transcription) pathway [1]. TYK2 was originally isolated in a genetic screen to find components involved in type I interferon (IFN; IFNα/β) and type II IFN (IFNγ) signalling [2]. IFNs are widely expressed cytokines that have potent antiviral activity. Further studies revealed that TYK2 plays a role in signal transduction via a number of other cytokines and some growth factors [3]. We have recently shown a selective requirement of TYK2 in host defence against certain virus infections in vivo. TYK2-deficient mice were capable to survive infections with Vesicular Stomatitis Virus (VSV) [4]. In contrast, they were more susceptible to Lymphocytic Choriomeningitis Virus (LCMV), Vaccinia Virus (VV) [4] and Murine Cytomegalovirus (MCMV) [5]. These selected requirements of TYK2 imply specific molecular and/or cellular functions of TYK2 in the defence against different viruses. In vitro, it was shown that macrophages infected with MCMV require TYK2 for the control of virus replication [5].

To further study the contribution of TYK2 to macrophage activity we used synthetic polyinosinic acid-polycytidylic acid (poly(I:C)) to mimic the presence of double-stranded RNA (dsRNA), a known (by-) product of virus replication. Poly(I:C) is recognized by pattern recognition receptors, including Toll-like receptor 3 (TLR3) and retinoic-acid-inducible gene I (RIG-I)-like receptors (RLRs). Subsequently, signals are translated into several distinct intracellular signalling pathways which finally result in the activation of a common set of transcription factors, including members of the interferon-regulatory factor (IRF) family. This leads to the production and release of

type I IFNs. Following binding of IFNα/β to the type I IFN receptor (IFNAR), an assembly of the two subunits IFNAR1 and IFNAR2, TYK2 and JAK1 are activated. JAKs phosphorylate downstream STATs which then translocate to the nucleus and induce expression of IFN responsive genes [6-9].

In a previous study, we used a proteomic approach to investigate the molecular role of TYK2 in macrophages in response to lipopolysaccharide (LPS), a structural membrane component of Gram-negative bacteria recognised by TLR4 [10]. The absence of TYK2 showed complex consequences on the macrophage proteome and implied regulatory roles of TYK2 at the mRNA and post-transcriptional level before and after treatment with LPS.

In the current work, we performed a global proteome analysis of TYK2-deficient and wild-type primary murine macrophages to identify novel molecular functions of TYK2 in response to poly(I:C). Consistent with our proteomic study using LPS, we can show that TYK2 is essential for the regulation of cellular immune responses. Data further suggest novel roles of TYK2 in the regulation of cellular lipid and carbohydrate metabolism.

2. Material and Methods

2.1. Materials

All chemicals were of analytical grade or of higher purity unless stated otherwise. Poly(I:C) (Amersham Biosciences, Piscataway, NJ, USA) was annealed prior to use to ensure a high yield of double-stranded configuration. Purified (≥ 90 % by SDS-PAGE) recombinant murine IFN-β (Calbiochem, San Diego, CA, USA) was diluted in PBS containing 0.1% BSA.

2.2. Animals, cells and cell lysates

TYK2 knock out (TYK2-/-) [4] and IFNAR1 knock out (IFNAR1-/-) [11] mice have been previously described and were on C57BL/6 background. Mice were kept under specified pathogen-free (SPF) conditions and were sex-and age-matched (8-12 weeks) for each experiment. Bone marrow-derived macrophages (BMM) from wild-type (WT, control), TYK2 (TYK2-/-) and IFNAR deficient (IFNAR1-/-) mice were isolated and grown as described previously [12]. Following cultivation for 6-7 days, cells were incubated with 50 µg/mL poly(I:C) or 500 units/ml IFN-β for the times indicated. Whole cell lysates were prepared as previously described [10] and used for 2D-DIGE and Western blot analysis. Protein concentration was measured by the Coomassie G-250 (dye reagent, Bio-Rad laboratories, Hercules, CA, USA) protein binding assay [13].

2.3. 2D-DIGE and statistical analysis

2D-DIGE experiments were designed to comprise three biological replicates per genotype (WT vs. TYK2-/- BMM) and treatment (with or without poly(I:C) for 18h). DIGE labelling, 2-DE separation and evaluation was performed as previously described [10]. Briefly, samples were minimally labelled with CyDye DIGE[TM]

fluorescent dyes (GE Healthcare Life Sciences, Munich, Germany). Proteins were separated in the first dimension on 24 cm IPG Dry strips with linear pH gradients of pH 4-7 and pH 6-9 using the IPGphor III system (all GE Healthcare). The second dimension was performed on isocratic SDS-PAGE gels (10%T, 25.5 x 20.5 cm) according to Laemmli [14] using an Ettan Dalt Six electrophoresis chamber (GE Healthcare). Fluorescence images of the gels were acquired on a Typhoon 9400 scanner (GE Healthcare). Image analysis including spot detection, matching, normalisation and quantification was performed using DeCyder software Version 5.02 (GE Healthcare).

Statistical analysis of all spots was based on spot volume ratios. Differentially regulated spots between genotypes (WT and TYK2-/-) were selected according to volume ratio and Student's *t*-test. Spot matching and spot quality of proteins of interest were manually checked to avoid false positives. As we are mainly interested in genotype-specific differences between WT and TYK2-/- BMM, untreated samples were labelled with Cy3 and treated samples were labelled with Cy5. Differentially regulated spots between WT and TYK2-/- were crosschecked for dye labelling bias based on reverse labelling experiments (untreated/Cy5, treated/Cy3). A pool of equal amounts of protein from all samples was used as internal standard and labelled with Cy2.

2.4. Protein identification by MALDI-reflectron TOF-MS

Protein spots were detected by acidic silver nitrate staining as previously described using a MS-compatible protocol [15], manually excised and used for MS analysis. In some cases semipreparative 2-DE gels (150 µg protein load) were used to recover sufficient material for mass spectrometric analysis. Spot destaining, *in-gel* tryptic

digestion and sample preparation using ZipTip$_{\mu\text{-C18}}$ (Millipore, Billerica, MA, USA) was performed as previously described [10].

Peptide mass fingerprinting (PMF) and seamless post source decay (PSD) fragment ion analysis experiments were performed on a MALDI-reflectron TOF (time-of-flight) instrument (AXIMA-CFR*plus*, Shimadzu Biotech Kratos Analytical, Manchester, UK) equipped with a nitrogen-laser (λ = 337 nm). Monoisotopic values of the matrix cluster trimer at [3M+H]$^+$ *m/z* 568.15 and autolytic tryptic products at [M+H]$^+$ *m/z* 805.41, [M+H]$^+$ *m/z* 1153.57 and [M+H]$^+$ *m/z* 2163.05 were used for internal calibration. Autolytic tryptic product ions, matrix cluster ions [16], keratin and gel blank artefacts [17] were sorted out from the obtained PMF mass spectra. The resulting monoisotopic list of *m/z* values were submitted to search engines MASCOT [18], revision 2.1.0 to 2.2.0, and ProFound [19] searching the databases SWISSPROT (version 53.2 of 05-May-2007 to 56.5 of 25-Nov-2008) and NCBI (sequence Release 23 of 08-May-2007 to 32 of 10-Nov-2008) restricting to *Mus musculus* taxonomy. Search parameters: mass accuracy - 50 ppm, fixed modification - carbamidomethylation, variable modifications - methionine oxidation and acetylation at the protein N-terminal end, missed cleavages: one. Based on the measured PMF at least two peptides were selected for PSD experiments. Search parameters for PSD experiments were identical to PMF experiments, except for: Peptide mass accuracy - 100 ppm and product ion tolerance - 1.0 Da. A protein was considered as identified, if the scores of database searches clearly exceeded the algorithm's significance threshold ($p < 0.05$) for PMF data and for PSD fragment ion analyses of at least one peptide.

2.5. Western blot analysis

1D Western blots were performed on small-sized SDS-PAGE gels as previously described [5]. The following antibodies were used: goat anti-TGTP (A-20) and goat anti-ACSL4 (N-18) (all Santa Cruz Biotechnology, Santa Cruz, CA, USA); rabbit anti-ACLY (Cell Signalling, Danvers, MA, USA); mouse anti-extracellular signal regulated kinase (pan-ERK) (BD Biosciences Transduction Laboratories, Lexington, KY, USA); donkey anti-rabbit IgG-HRP F(ab)´$_2$ fragment; sheep anti-mouse IgG-HRP F(ab)´$_2$ fragment; ECL Western Blotting Detection reagents (all GE Healthcare Life Sciences, Munich, Germany).

2.6. Metabolite Analysis – Lactate, Cholesterol and Triacylglycerol

Supernatants from BMM were collected for extracellular lactate measurements using a kit from Greiner Diagnostics (Bahlingen, Germany) following the manufacturer's instructions. Briefly, 10 µL of supernatant were incubated with 1 ml of lactate reagent at room temperature for 5 min and the absorbance was measured at 500 nm.

Lipids were extracted from BMM for total cholesterol (TC) and triacylglycerol (TAG) quantitative analysis. Briefly, BMM washed three times with PBS and incubated with hexane/isopropanol (60/40, v/v) for 1 h at 4 °C with gentle mixing. Lipid extracts were transferred to sample vials and evaporated to dryness in a vacuum centrifuge. The residue was dissolved in chloroform/methanol (66/33, v/v) and aliquots were taken for TC and TAG analysis. For TAG quantifications 0.3 % Triton X-100 was added for complete solubilisation. Samples were vacuum dried before determining cellular TAG (Greiner Diagnostics, Bahlingen, Germany) and TC (Diagnostic Systems, Holzheim, Germany) concentrations by enzymatic assays following manufacturer's instructions. For total protein content determination (Coomassie G-250 protein binding assay [13]) 0.3 M NaOH was added to the cell culture plates after lipid extraction and incubated

for 2 h at room temperature. Cell culture plates were kept at -20 °C overnight and for 4 h at room temperature before the protein assay was performed. Data of metabolite (lactate, TC and TAG) measurements were normalised to cellular total protein content. Statistical evaluation was performed using the software package SPSS version 14.0 (SPSS, Chicago, IL, USA). ANOVA and linear regression were used for statistical analysis. The experiment was treated as random factor. A design matrix of zeros and ones was used to obtain contrasts between genotypes within a treatment and between treatments for each genotype. Results were reported as means ± standard error (SE).

3. Results and Discussion

3.1. Overview of the results and statistical evaluation of protein spot expression obtained from 2D-DIGE analysis

Differences in protein patterns in whole cell lysates were compared between WT and TYK2-/- BMM with and without poly(I:C) treatment. 2D-DIGE was used at two different pH gradients (pH 4-7 and pH 6-9) to cover a broad pH range and representative 2-DE protein pattern are shown in Fig.1. A total number of six analytical gels per pH range was analysed compromising three biological replicates per genotype and treatment. Only protein spots which were present in all images, were included in the further data analysis (pH 4-7: 505 spots and pH 6-9: 490 spots). Experimental variation was assessed based on spot volume ratios which resulted in a mean SD of ±0.079 and ±0.087 for pH 4-7 and pH 6-9, respectively. On average, spot expression differences of more than 29% (pH 4-7) and 31% (pH 6-9) will produce significant results ($p \leq 0.05$) in 90% of the cases with our experimental set-up (sample size per group = 3). These findings, showing highly reproducible 2D-DIGE spot pattern from whole cell lysates of primary murine macrophages, are in agreement with our previous study [10]. For further analysis, we only considered differentially regulated spots between the genotypes showing at least 30% change.

The study focused on the impact of TYK2 on the macrophage proteome in the untreated state and after poly(I:C) treatment. Statistical analysis indicated that 156 protein spots were significantly changed (minimum 1.3-fold; $p \leq 0.05$) in TYK2-/- compared to WT macrophages (Tab. 1). 56 spots were up-regulated and 54 were down-regulated in the absence of TYK2 after poly(I:C) treatment. 14 spots were up-regulated and 32 down-regulated without treatment showing that TYK2 positively and negatively regulates cellular protein expression in basal state and after poly(I:C) stimulation.

3.2. Differentially expressed proteins can be assigned to several distinct functional protein groups

Among the 156 spots showing expression differences, 26 were selected for protein identification based on selection criteria, i.e. spot quality and quantity, spot traceability on silver stained gels as previously described [10]. 18 protein spots (Fig. 1) were unambiguously identified by MALDI-reflectron-TOF mass spectrometry based on PMF and amino acid sequence tags derived from PSD fragment ion analysis and are listed in detail in Tab. 2. For spot 3 and 18 two highly sequence homologous protein variants were identified showing nearly identical theoretical pI- and M$_r$-values. In both cases, one unique peptide was assigned to the most probable variant; therefore either this protein variant or a mixture of both protein variants is contained in the spot. For two proteins multiple spots were identified located at similar M$_r$, but at different pI-positions (spots 4/5 and spots 10/11). This can be explained by post-translational modifications, which were not further investigated within the presented study. The remaining eight differentially expressed spots could not be successfully identified because database searching with PMFs and PSD spectra did not yield significant results. This can be explained either by insufficient amount of protein and/or incomplete peptide cleavage/extraction (hydrophobic interactions with gel matrix) combined with non-optimal fragmentation behaviour.

Identified proteins can be grouped on the basis of their major cellular function according to the PANTHER classification system [20], gene ontology (GO) [21] and UniProtKB databases [22] (Tab. 2). Interestingly, the majority of proteins are metabolic enzymes showing consistently an increased expression by 1.40- to 2.29-fold in absence of TYK2 upon poly(I:C) treatment. All of them are involved in cellular lipid or carbohydrate metabolic processes, or both. Long-chain-fatty-acid-CoA ligase 4 (ACSL4), peroxisomal multifunctional enzyme type 2 (DHB4) and peroxisomal 3-

ketoacyl-CoA thiolase A or B (THIKA/B) are enzymes of the fatty acid degradation pathway (β-oxidation) [22, 23]. DHB4 and THIKA/B are exclusively allocated to peroxisomal and ACSL4 to mitochondrial and peroxisomal subcellular compartments. In addition, the enzyme catalase (CATA) degrades H_2O_2, which is produced as a result of peroxisomal β-oxidation [24]. The following identified proteins are involved in different carbohydrate metabolic processes: (a) glycolytic/gluconeogenesis pathway: triosephosphate isomerase (TPIS), fructose-bisphosphate aldolase A (ALDOA) and α-enolase (ENOA); (b) acetyl-CoA formation: ATP-citrate lyase (ACLY) and (c) tricarboxylic acid cycle (citrate cycle): aconitate hydratase (ACON). TPIS and ACLY are enzymes linking carbohydrate and lipid metabolic processes. TPIS participates in the production of glycerol a precursor for the synthesis of triacylglycerol (TAG), whereas ACLY is involved in the glucose-dependent lipogenesis [22, 23]. In summary, the presented results show a substantial impact of TYK2 after poly(I:C) treatment on the expression of proteins mainly involved in fatty acid degradation and glycolysis which was not observed in our previous study using LPS [10].

Furthermore we identified four proteins which are known as IFN regulated proteins: T-cell specific GTPase (TGTP), proteasome activator complex subunit 1 (PSME1), interferon-induced protein with tetratricopeptide repeats 3 (IFIT3) and interferon-activable protein 205-B (IFI5B). All of them showed a decreased protein expression in the absence of TYK2 in the basal state and/or after poly(I:C) stimulation. This is in line with the role of TYK2 in IFN signalling and data emphasize the important role of TYK2 for the regulation of at least a subset of IFN inducible proteins.

From all identified proteins we selected several candidates which are known to be involved in immune response, carbohydrate and lipid metabolic pathways for more detailed examinations using 1D Western blotting, provided that specific antibodies for targeted proteins were available. Due to the impact of TYK2 on a remarkable number

of proteins involved in metabolic pathways we additionally investigated potentially influenced metabolites (Fig. 2): cellular triacylglycerol (TAG), total cholesterol (TC), and extracellular lactate.

3.3. TYK2 is a positive regulator of poly(I:C) induced T-cell specific GTPase (TGTP) protein expression in macrophages

TGTP (synonym: Mg21; proposed new gene/protein name: IRGb6 [25]) is a member of the 47-kDa GTPase family ([26-28]) and was discovered to be selectively induced by IFNγ in macrophages and T-cells [29]. TGTP possesses specific antiviral activity, is induced upon MCMV infection [30] and is implicated in cell survival after infection with VSV, but not herpes simplex virus [31]. In addition, it was shown that transfected poly(I:C) efficiently induces TGTP in fibroblast cell lineages in an IFNα/β-dependent manner [31].

After treatment with poly(I:C) for 18h, TGTP was more than eight-fold induced in WT, but only to half of the extent in TYK2-/- macrophages (Fig. 3A). TYK2-dependend induction of TGTP by poly(I:C) treatment could be clearly confirmed by 1D Western blotting (Fig. 3B). The expression of TGTP was rapidly increased in WT macrophages reaching a maximum of expression after 8 h. In TYK2-/- macrophages the induction of TGTP protein expression was delayed and did not reach the level of WT cells until 18 h of poly(I:C).

Thus, we could show that TGTP is induced in a TYK2-dependent manner upon poly(I:C) in murine primary macrophages. Since poly(I:C) is known to be a strong inducer of IFNα/β and TYK2 is a positive regulator of type I IFN-induced signalling, it is most likely that TGTP induction is dependent on autocrine/paracrine type I IFN signalling.

3.4. ACSL4 and ACLY

ACSL4 belongs to the large family of long-chain acyl-CoA synthetases (ACSLs) [32], which are essential for *de novo* lipid synthesis, fatty acid degradation and phospholipid remodelling of membranes. Membrane-bound ACSL proteins catalyze ATP-dependent the activation of hydrophobic long-chain fatty acid to hydrophilic acyl-CoA, whereas ACSL4 specifically prefers arachidonate as substrate [33]. According to the presented 2D-DIGE data, ACSL4 showed 1.9-fold higher levels in TYK2-/-BMM upon poly(I:C) treatment (Fig. 3A). In 2D-DIGE we detected ACSL4 in a spot at approx. 80 kDa (Fig. 1, spot number 1) which corresponds well to the theoretical M_r of 79.2 kDa. Applying the same samples used for 2D-DIGE analysis, 1D Western blotting experiments identified three protein bands at different M_r (approx. 35 kDa, 65 kDa and 75 kDa) (Fig. 3B). The protein band at approx. 75 kDa was assigned to the ACSL4 protein due to a similar M_r derived from the 2D-DIGE data. Poly(I:C) treated WT cells showed a less intense signal compared to TYK2-/- cells, which would be in line with the results obtained from 2D-DIGE experiments. Signal intensities of the additional two protein bands remained unchanged across the different genotypes and treatments. The appearance of these protein bands can be explained by unspecific binding of the primary and/or secondary antibody or by specific binding to proteolytic cleavage products of ACSL4. Further experiments are needed either to optimize the binding specifity of the anti-ACSL4 antibody and/or to analyse possibly existent ACSL4 fragments.

ACLY is a cytosolic enzyme that catalyzes the conversion of citrate to oxaloacetate and acetyl-CoA during glucose metabolism. Acetyl-CoA is a precursor for the synthesis of fatty acids, cholesterols and isoprenoids [23]. ACLY was shown to be transcriptionally regulated [34] and post-translationally modified [35]. Cells lacking ACLY activity displayed decreased cytokine-stimulated cell proliferation, but they

could resist cell death by cytokine withdrawal [36]. ACLY was 1.57-fold upregulated in TYK2-/- as compared to WT BMM after poly(I:C) treatment (Fig. 3A). Samples used for 2D-DIGE were again subjected to Western blot analysis, but signal intensities decreased only slightly to moderately in WT compared to TYK2-/- cells upon poly(I:C) treatment (Fig. 3B).

In summary, preliminary results obtained from Western blot analysis for ACSL4 and ACLY give first evidence for a consistent behaviour of expression pattern in 2D-DIGE and 1D Western blotting. However, protein expression differences obtained from 2D-DIGE experiments are not directly transferable to results from 1D Western blotting. 1D Western blotting provides information about the total protein expression at a given M_r, whereas differences in spot abundance in 2D-DIGE experiments can be additionally attributed to possible post-translational modifications. Moreover, the relatively modest changes in protein expression require a more suitable signal detection of Western blot analysis for a confident differentiation of changes in protein expression of less than 2.0-fold. Further experiments are in progress to gain additional information including time course experiments, examination of at least two more independent biological experiments and possibly 2D- Western blotting.

3.5. TYK2 is required for the upregulation of cellular total cholesterol and extracellular lactate in macrophages

Experiments were conducted to asses the impact of TYK2 on cellular TC, TAG and extracellular lactate amounts. Since TYK2 is associated to type I IFN signalling, we additionally included BMM from IFNAR1-/- mice. Furthermore we treated cells with recombinant IFNβ to address the questions, if type I IFN signalling is required and/or if IFNβ alone is sufficient for the effects observed after poly(I:C) treatment.

Cellular TC concentration (Fig. 4A) is only slightly (1.16-fold), but significantly increased in WT cells after poly(I:C) induction. TC levels of both, TYK2-/- and IFNAR1-/- macrophages, are significantly decreased relative to WT cells and showed no induction in presence of poly(I:C). TC levels after IFNβ treatment remained unchanged in all three genotypes. This points to the fact that IFNAR1 and TYK2 are required, but IFNβ alone is not sufficient for poly(I:C) induced changes in cellular TC. Fig. 4B demonstrates that cellular TAG concentration is significantly increased (1.35-fold) in WT macrophages upon poly(I:C) treatment. For IFNAR1-/- but not TYK2-/- cells a decreased TAG content was observed compared to WT cells. In the presence of IFNβ no significant effects across the genotypes were observed. It is shown that the increased cellular TAG level induced by poly(I:C) is dependent on intact type I IFN signalling. Additionally, TYK2 does not contribute to effects observed with poly(I:C) and IFNβ alone is not sufficient for poly(I:C) induced changes in cellular TAG concentration. However, due to the chosen sample size and the higher technical variation caused by the addition of Triton X-100 for TAG quantifications, minor differences are not detectable.

The link between innate immunity and lipid metabolism in activated macrophages is not surprising [37], but the precise molecular mechanisms are still under investigation. In earlier studies, bacterial and viral infections have been supposed to contribute to macrophage differentiation into lipid-laden foam cells, which drive the disease progress in atherosclerosis [38, 39]. Furthermore, it was demonstrated that TLR3 and TLR4 ligands can block macrophage cholesterol efflux [40]. This leads to an increased cellular cholesterol level which corresponds to our findings. In addition, it was suggested that the transcriptional activity of liver X receptors (LXRs), which are responsible for the synthesis of cholesterol efflux mediators (e.g. ATP-binding cassette transporter 1 (ABCA1)), does not require the production of type I IFNs [40].

Our data suggest that TC accumulation upon treatment with poly(I:C) is depending on intact type I IFN signalling and TYK2. Fatty acids mobilised from TAGs are a major source of cellular energy [23]. Earlier studies revealed that macrophages accumulate TAGs after LPS [41, 42], but not after poly(I:C) stimulation [42]. This is in contrast to our presented findings showing TAG accumulation after poly(I:C) treatment.

For extracellular lactate content it was found that it is about 3-fold increased in WT cells after induction with poly(I:C) (Fig. 4C). Extracellular lactate levels in TYK2-/- and IFNAR1-/- cells are decreased to a similar extent compared to WT cells. However, TYK2-/- and IFNAR1-/- cells also showed an approx. 2-fold increase compared to untreated cells. Macrophages stimulated with IFNβ showed a modest up-regulation of extracellular lactate concentration, which was dependent on the presence of TYK2 and IFNAR1. It was concluded that TYK2 and intact IFN signalling are required for full lactate release. Our data further suggest that additional factors activated by poly(I:C) must contribute to the increase in lactate levels.

In most cells, glycolysis serves to convert glucose to pyruvate and then generate ATP by oxidative phosphorylation (OXPHOS). At low oxygen level pyruvate is converted to lactate (anaerobic glycolysis) to produce ATP, however with less efficiency [43]. Moreover, a strongly increased extracellular lactate level was found in macrophages stimulated with LPS [44, 45] and could be further extended by our findings after poly(I:C) treatment. We assume a shift from OXPHOS to increased glycolysis in activated macrophages. Furthermore, we provide evidence that macrophage glycolytic function is partially mediated by type I IFN signalling. It is interesting to note that earlier studies suggested effects of IFNs on OXPHOS [46].

4. Concluding remarks

The presented data show that the absence of TYK2 reveals significant changes on cellular protein abundance in macrophages in basal state and upon poly(I:C) stimulation, which is in line with our recently published study [10]. We observed an explicit impact of TYK2 on the abundance of lipid and carbohydrate metabolic enzymes. The contribution of TYK2 to cellular lipid and carbohydrate metabolic pathways was supported at the metabolite level. Data emphasize the importance of TYK2 for the regulation of cellular immune responses and provide evidence for a novel function of TYK2 linking metabolic and innate immune networks.

Acknowledgements

Legends to Figures

Figure 1

Representative silver stained 2-DE protein patterns of macrophages.

Whole cell extracts obtained from 2D-DIGE experiments were separated on pH range (A) 4-7 and (B) 6-9. Numbered spots indicate proteins which have been identified by PMFs and sequence tags applying MALDI mass spectrometry.

Figure 2

Overview of identified metabolic enzymes within the metabolic pathways.

Scheme showing the location of interaction of identified differentially regulated metabolic enzymes functionally related to their metabolic pathways and the connection to specific metabolites (triacylglycerides, cholesterol and lactate). TCA cycle, Tricarboxylic acid cycle; OXPHOS, Oxidative phosphorylation; (a) Triosephosphate isomerase, TPIS; (b) Fructose-bisphosphate aldolase A, ALDOA; (c) α-enolase, ENOA; (d) ATP-citrate lyase, ACLY; (e) Aconitate hydratase, ACON; (f) Long-chain-fatty-acid-CoA ligase 4, ACSL4; (g) Peroxisomal multifunctional enzyme type 2, DHB4; (h) Peroxisomal 3-ketoacyl-CoA thiolase A or B, THIKA/B; (i) Catalase, CATA.

Figure 3

Effect of TYK2 deficiency on expression levels of TGTP, ACSL4 and ACLY proteins.

Macrophages were treated with poly(I:C) (0, 4, 8 and 18 h) and whole cell lysates were analysed by 2D-DIGE and Western blotting. (A) 2D-DIGE analysis. Expression levels given as fold ratios relative to unstimulated WT cells. Represented values are mean values ± SD of three biological replicates. (B) Western blot analysis. 10 µg (TGTP, ACSL4) and 20 µg (ACLY) protein per lane were separated by SDS-PAGE

(10%T for TGTP, 8%T for ACSL4 and 6.5%T for ACLY). TGTP: Data are representatives of three independent experiments; ACSL4 and ACLY: Data are representatives of three biological replicates used for 2D-DIGE experiments. #1 and #2 indicate cells derived from different mice. The upper panel shows protein expression of respective proteins, the lower panel shows panERK levels for protein loading control.

Figure 4

Effects of TYK2 and IFNAR1 deficiency on (A) TC, (B) TAG and (C) lactate concentration.

Cells were incubated either with poly(I:C) or IFNβ for 18 h. Values of measured metabolite concentrations were normalized on cellular total protein content. Results are mean values ± SE of the following number of independent experiments: TC, n = 7; TAG, n = 3; lactate, n = 4. Significance levels of genotype specific differences for each treatment are indicated with * $p < 0.05$ and ** $p < 0.01$. Significance levels not indicated in the figures: TC, WT(untreated) vs. WT(polyI:C) $p \leq 0.01$; TAG, WT(untreated) vs. WT(polyI:C) $p \leq 0.05$; Lactate, WT(untreated) vs. WT(polyI:C) $p \leq 0.01$, WT(untreated) vs. WT(IFNβ) $p \leq 0.05$.

References

[1] Darnell J E Jr., Kerr I M, Stark G R. Jak-STAT pathways and transcriptional activation in response to IFNs and other extracellular signaling proteins. Science 1994;264:1415-1421.

[2] Velazquez L, Fellous M, Stark G R, Pellegrini S. A protein tyrosine kinase in the interferon alpha/beta signaling pathway. Cell 1992;70:313-322.

[3] Schindler C. Cytokines and JAK-STAT signaling. Exp Cell Res 1999;253:7-14.

[4] Karaghiosoff M, Neubauer H, Lassnig C, Kovarik P, Schindler H, Pircher H, McCoy B, Bogdan C, Decker T, Brem G, Pfeffer K, Muller M. Partial impairment of cytokine responses in Tyk2-deficient mice. Immunity 2000;13:549-560.

[5] Strobl B. Bubic I, Bruns U, Steinborn R, Lajko R, Kolbe T, Karaghiosoff M, Kalinke U, Jonjic S, Muller M. Novel functions of tyrosine kinase 2 in the antiviral defense against murine cytomegalovirus. J Immunol 2005;175:4000-4008.

[6] Matsumoto M, Seya T. TLR3: interferon induction by double-stranded RNA including poly(I:C). Adv Drug Deliv Rev 2008;60:805-812.

[7] Takeuchi O, Akira S. MDA5/RIG-I and virus recognition. Curr Opin Immunol 2008;20:17-22.

[8] O'Shea J J, Gadina M, Schreiber R D. Cytokine signaling in 2002: new surprises in the Jak/Stat pathway. Cell 2002;109 Suppl:121-131.

[9] Schindler C, Plumlee C. Inteferons pen the JAK-STAT pathway. Semin Cell Dev Biol 2008;19:311-318.

[10] Radwan M, Miller I, Grunert T, Marchetti-Deschmann M, Vogl C, O'Donoghue N, Dunn M J, Kolbe T, Allmaier G, Gemeiner M, Müller M,Strobl B. The impact of tyrosine kinase 2 (Tyk2) on the proteome of murine macrophages and their response to lipopolysaccharide (LPS). Proteomics 2008;8:3469-3485.

[11] Muller U, Steinhoff U, Reis L F, Hemmi S, Pavlovic J, Zinkernagel R M, Aguet M. Functional role of type I and type II interferons in antiviral defense. Science 1994;264:1918-1921.

[12] Baccarini M, Bistoni F, Lohmann-Matthes M L. In vitro natural cell-mediated cytotoxicity against Candida albicans: macrophage precursors as effector cells. J Immunol 1985;134:2658-2665.

[13] Bradford M M. A rapid and sensitive method for the quantitation of microgram quantities of protein utilizing the principle of protein-dye binding. Anal Biochem 1976;72:248-254.

[14] Laemmli U K. Cleavage of structural proteins during the assembly of the head of bacteriophage T4. Nature 1970;227:680-685.

[15] Blum H, Gross H J, Beier H. The expression of the TMV-specific 30-kDa protein in tobacco protoplasts is strongly and selectively enhanced by actinomycin. Virology 1989;169:51-61.

[16] Smirnov I P, Zhu X, Taylor T, Huang Y, Ross P, Papayanopoulos I A, Martin S A, Pappin D J. Suppression of alpha-cyano-4-hydroxycinnamic acid matrix clusters and reduction of chemical noise in MALDI-TOF mass spectrometry. Anal Chem 2004;76:2958-2965.

[17] Mattow J, Schmidt F, Hohenwarter W, Siejak F, Schaible U E, Kaufmann S H. Protein identification and tracking in two-dimensional electrophoretic gels by minimal protein identifiers. Proteomics 2004;4:2927-2941.

[18] Perkins D N, Pappin D J, Creasy D M, Cottrell J S. Probability-based protein identification by searching sequence databases using mass spectrometry data. Electrophoresis 1999;20:3551-3567.

[19] Zhang W, Chait B T. ProFound: an expert system for protein identification using mass spectrometric peptide mapping information. Anal Chem 2000;72:2482-2489.

[20] Thomas P, Campbell M J, Kejariwal A, Mi H, Karlak B, Daverman R, Diemer K, Muruganujan A, Narechania A. PANTHER: a library of protein families and subfamilies indexed by function. Genome Res 2003;13:2129-2141.

[21] Ashburner M, Ball C A, Blake J A, Botstein D, Butler H, Cherry J M, Davis A P, Dolinski K, Dwight S S, Eppig J T, Harris M A, Hill D P, Issel-Tarver L, Kasarskis A, Lewis S, Matese J C, Richardson J E, Ringwald M, Rubin G M, Sherlock G. Gene ontology: tool for the unification of biology. The Gene Ontology Consortium. Nat Genet 2000;25:25-29.

[22] The UniProt Consortium. The universal protein resource (UniProt). Nucleic Acids Res 2008;36:D190-195.

[23] Michal G. Biochemical Pathways. An atlas of biochemistry and molecular biology. New York: John Wiley & Sons; 1999.

[24] Schrader M, Yoon Y. Mitochondria and peroxisomes: are the 'big brother' and the 'little sister' closer than assumed? Bioassays 2007;29:1105-1114.

[25] Martens S, Howard J. The interferon-inducible GTPases. Annu Rev Cell Dev Biol 2006;22:559-589.

[26] Taylor G A, Feng C G, Sher A. p47 GTPases: regulators of immunity to intracellular pathogens. Nat Rev Immunol 2004;4:100-109.

[27] MacMicking J D. Immune control of phagosomal bacteria by p47 GTPases. Curr Opin Microbiol 2005;8:74-82.

[28] Howard J. The IRG proteins: a function in search of a mechanism. Immunobiology 2008;213:367-375.

[29] Carlow D A, Marth J, Clark-Lewis I, Teh H S. Isolation of a gene encoding a developmentally regulated T cell-specific protein with a guanine nucleotide triphosphate-binding motif. J Immunol 1995;154:1724-1734.

[30] van den Pol A N, Robek M D, Ghosh P K, Ozduman K, Bandi P, Whim M D, Wollmann G. Cytomegalovirus induces interferon-stimulated gene expression and is attenuated by interferon in the developing brain. J Virol 2007;81:332-348.

[31] Carlow D A, Teh S J,Teh H S. Specific antiviral activity demonstrated by TGTP, a member of a new family of interferon-induced GTPases. J Immunol 1998;161:2348-2355.

[32] Soupene E, Kuypers F A. Mammalian long-chain acyl-CoA synthetases. Exp Biol Med (Maywood) 2008;233:507-521.

[33] Kang M J, Fujino T, Sasano H, Minekura H, Yabuki N, Nagura H, Iijima H, Yamamoto T T. A novel arachidonate-preferring acyl-CoA synthetase is present in steroidogenic cells of the rat adrenal, ovary, and testis. Proc Natl Acad Sci USA 1997;94:2880-2884.

[34] Towle H C, Kaytor E N, Shih H M. Regulation of the expression of lipogenic enzyme genes by carbohydrate. Annu Rev Nutr 1997;17:405-433.

[35] Berwick D C, Hers I, Heesom K J, Moule S K, Tavare J M. The identification of ATP-citrate lyase as a protein kinase B (Akt) substrate in primary adipocytes. J Biol Chem 2002;277:33895-33900.

[36] Bauer D E, Hatzivassiliou G, Zhao F, Andreadis C, Thompson C B. ATP citrate lyase is an important component of cell growth and transformation. Oncogene 2005;24:6314-6322.

[37] Gordon S. Do macrophage innate immune receptors enhance atherogenesis? Dev Cell 2003;5:666-668.

[38] Pepys M B, Hirschfield G M. C-reactive protein: a critical update. J Clin Invest 2003;111:1805-1812.

[39] Bukrinsky M, Sviridov D. Human immunodeficiency virus infection and macrophage cholesterol metabolism. J Leukoc Biol 2006;80:1044-1051.

[40] Castrillo A, Joseph S B, Vaidya S A, Haberland M, Fogelman A M, Cheng G, Tontonoz P. Crosstalk between LXR and toll-like receptor signaling mediates bacterial and viral antagonism of cholesterol metabolism. Mol Cell 2003;12:805-816.

[41] Funk J L, Feingold K R, Moser A H, Grunfeld C. Lipopolysaccharide stimulation of RAW 264.7 macrophages induces lipid accumulation and foam cell formation. Atherosclerosis 1993;98:67-82.

[42] Kazemi M R, McDonald C M, Shigenaga J K, Grunfeld C, Feingold K R. Adipocyte fatty acid-binding protein expression and lipid accumulation are increased during activation of murine macrophages by toll-like receptor agonists. Arterioscler Thromb Vasc Biol 2005;25:1220-1224.

[43] Kawaguchi T, Veech R L, Uyeda K. Regulation of energy metabolism in macrophages during hypoxia. Roles of fructose 2,6-bisphosphate and ribose 1,5-bisphosphate. J Biol Chem 2001;276:28554-28561.

[44] Haji-Michael PG, Ladriere L, Sener A, Vincent J L, Malaisse W J. Leukocyte glycolysis and lactate output in animal sepsis and ex vivo human blood. Metabolism 1999;48:779-785.

[45] Cramer T, Yamanishi Y, Clausen B E, Forster I, Pawlinski R, Mackman N, Haase V H, Jaenisch R, Corr M, Nizet V, Firestein G S, Gerber H P, Ferrara N, Johnson R S. HIF-1alpha is essential for myeloid cell-mediated inflammation. Cell 2003;112:645-657.

[46] Nagano Y, Kojima Y, Sawa I, Hagihara B, Kobayashi S, Shirasaka M, Haneishi T. The effect of the virus inhibiting factor on oxidative phosphorylation. Jpn J Exp Med 1966;36:341-362.

Figure 1

Figure 2

Figure 3

TGTP   ACSL4   ACLY

A

B
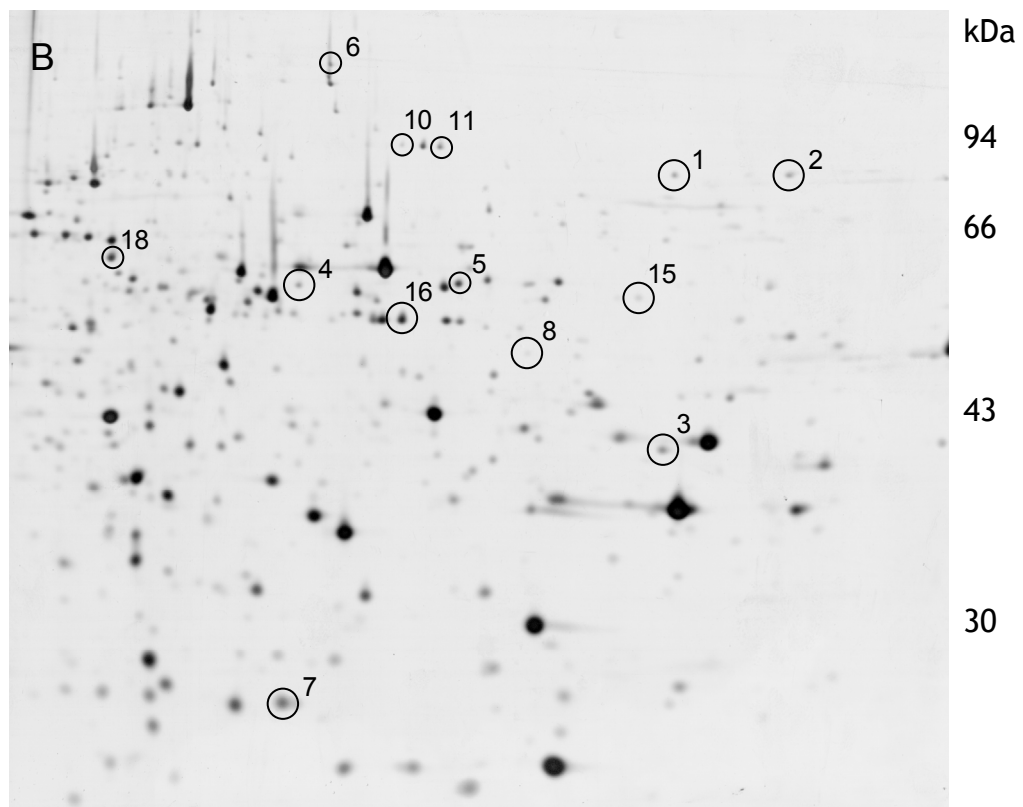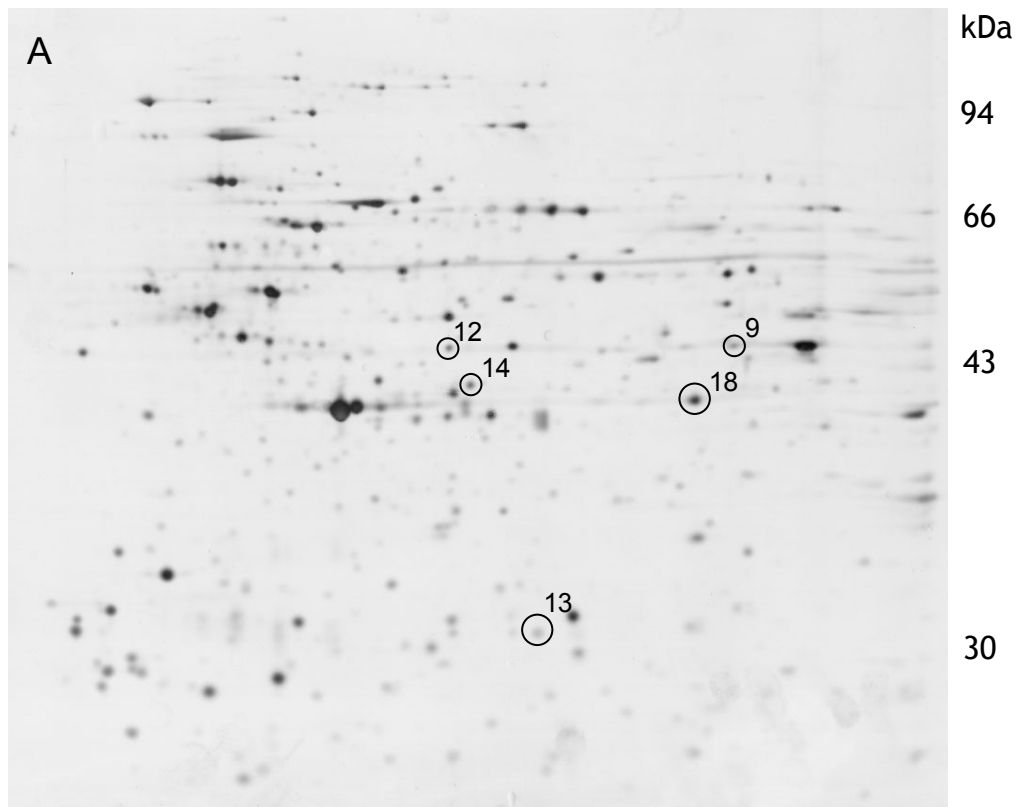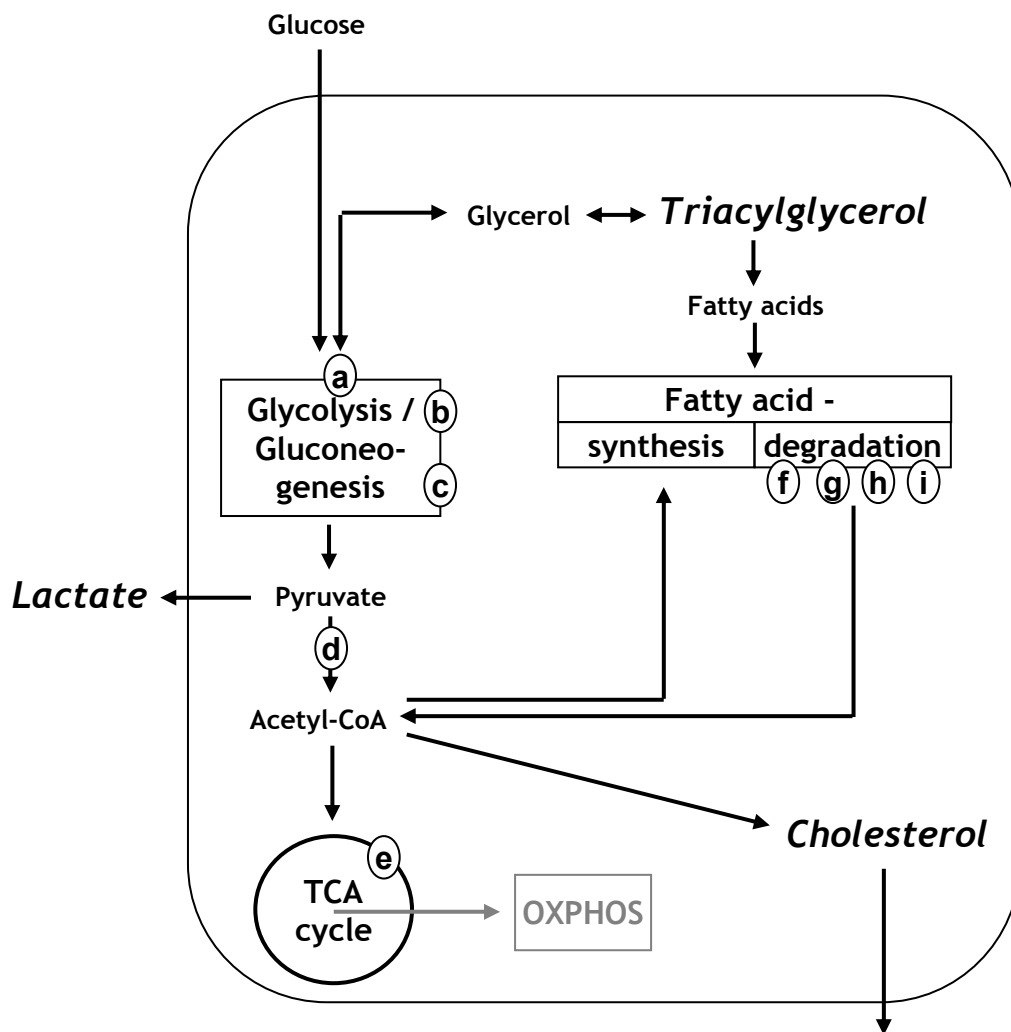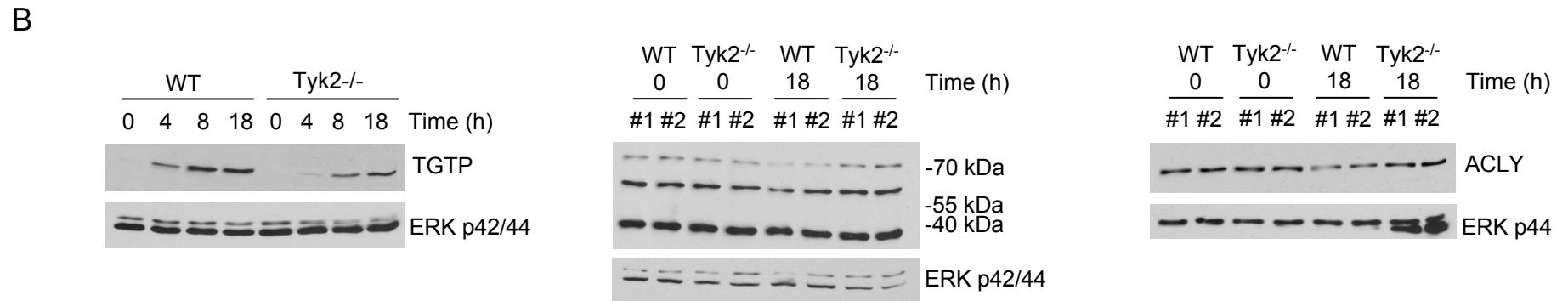
Figure 4

A
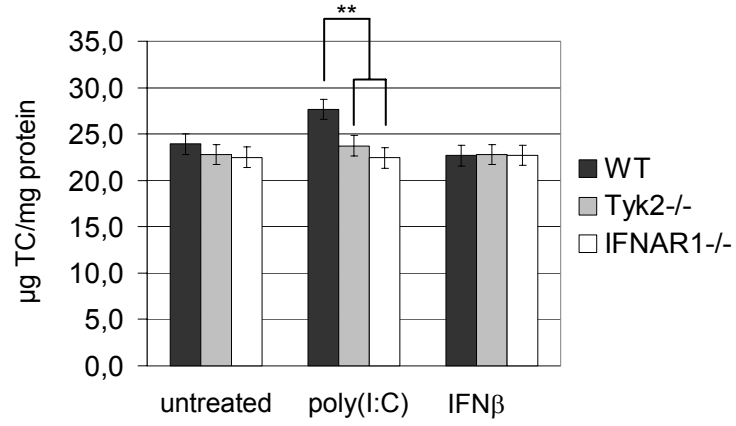
B
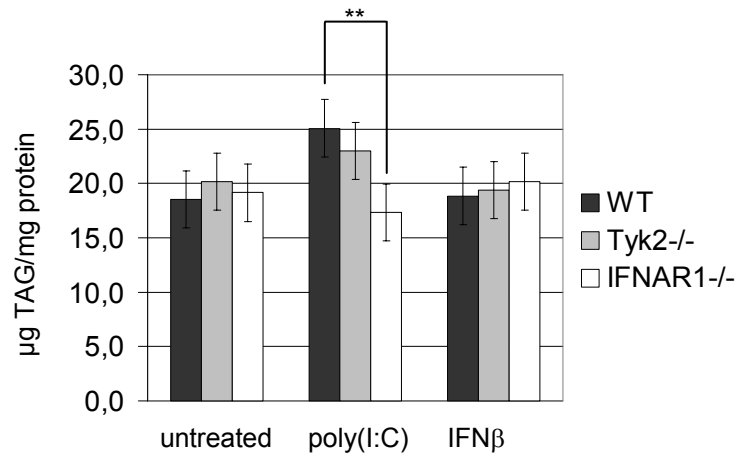
C
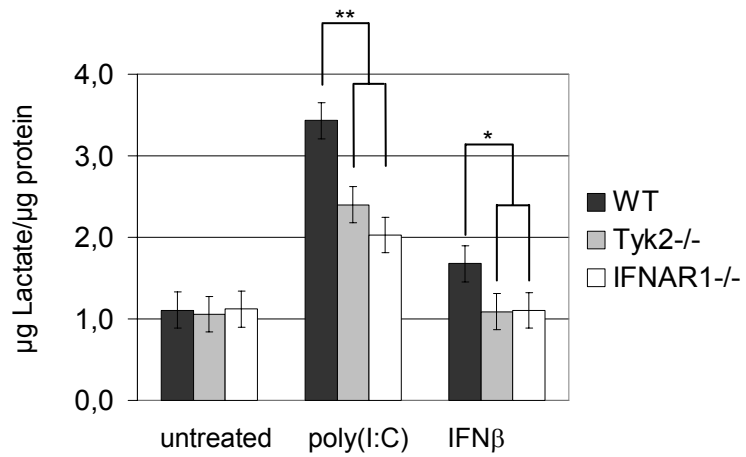
Table 1 - Numbers of differentially expressed spots *).			
Treatment	Total	up-regulated	down-regulated
- poly(I:C)	46	14	32
+ poly(I:C)	110	56	54

*) min. 1.3-fold change in TYK2-/- compared to WT BMM; p≤0.05 (*t*-Test).

Table 2 - Summary of differentially regulated proteins in TYK2-deficient macrophages.

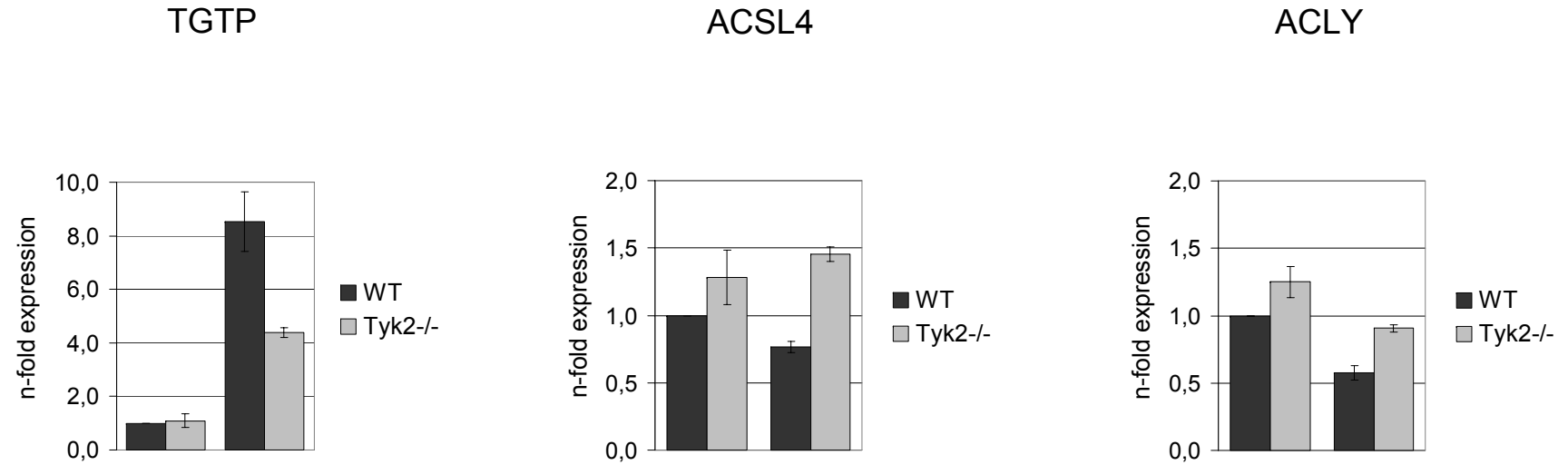| Spot #	Protein Name / Function	SWISSPROT accession #	WT	Tyk2-/-	WT + poly(I:C) treatment	Tyk2-/- + poly(I:C) treatment	Average ratio Tyk2-/- vs. WT + poly(I:C) treatment	p(gt) a)	p(gt x tr) b)	MWt (kDa) theor.	pI theor.	Peptide Mass Fingerprint Probability based MOWSE Score	Sequ. Cov. %	Matched/ unmatched peptides	Sequencing Probability based MOWSE Score	Precursor Ion(s) m/z (observed) and charge state	Peptide Sequence(s)
	METABOLISM																
1	Long-chain-fatty-acid-CoA ligase 4 (ACSL4)	Q9QUJ7	1	1,28	0,76	1,45	1,90	ns c)	5,62E-05	79.22	8.51	97	18	9/7	99	1002.20 + 1557.62 + 1628.89 +	FEIPIKVR TAEDYCVDENGQR YNFPLVTLYATLGR
2	Peroxisomal multifunctional enzyme type 2 (DHB4)	P51660	1	1,07	0,62	0,90	1,44	ns	7,28E-03	79.95	8.76	218	26	16/2	63	1283.52 + 1323.47 + 1529.67 +	IDVVVNNAGILR DATSLNQAALYR HVLQQFADNDVSR
3	3-ketoacyl-CoA thiolase A, peroxisomal (THIKA) d)	Q921H8	1	1,07	0,68	1,56	2,29	ns	8,28E-04	43.95	8.74	157	36	11/7	159	1569.73 + 2043.37 +	FPQASASDVVVVHGR IAQFLSGIPETVPLSTVNR
	3-ketoacyl-CoA thiolase B, peroxisomal (THIKB) d)	Q8VCH0								43.99	8.82	67	20	6/12	68	2043.37 +	IAQFLSGIPETVPLSTVNR
4	Catalase (CATA)	P24270	1	1,40	0,99	1,44	1,45	9,05E-03	3,58E-02	59.77	7.72	70	13	5/2	55	1277.44 + 1392.53 +	LAQEDPDYGLR NFTDVHPDYGAR
5	Catalase (CATA)	P24270	1	1,42	0,58	1,22	2,12	1,34E-02	3,97E-03	59.77	7.72	139	22	10/2	81	1277.44 + 1392.53 +	LAQEDPDYGLR NFTDVHPDYGAR
6	ATP-citrate synthase (ACLY)	Q91V92	1	1,25	0,58	0,91	1,57	2,03E-02	7,06E-04	119.73	7.13	185	18	15/2	55	875.01 + 1568.84 +	EAGVFVPR TIAIIAEGIPEALTR
7	Triosephosphate isomerase (TIM,TPIS)	P17751	1	1,21	0,73	1,13	1,56	8,26E-04	7,95E-04	26.71	6.90	244	65	14/4	128	1248.34 + 1540.71 +	SNVNDGVAQSTR DLGATWVVLGHSER
8	Fructose-bisphosphate aldolase A (ALDOA)	P05064	1	1,21	0,83	1,47	1,76	5,26E-03	5,89E-04	39.36	8.30	118	25	7/1	191	2108.36 + 2259.38 +	IGEHTPSALAIMENANVLAR YTPSGQSGAAASESLFISNHAY
9	α-enolase (ENOA)	P17182	1	1,33	0,86	1,20	1,40	2,72E-02	1,63E-02	47.14	6.37	120	19	8/1	63	704.80 + 1440.60 +	GVPLYR YITPDQLADLYK
10	Aconitate hydratase, mitochondrial (ACON)	Q99KI0	1	1,11	0,48	0,78	1,63	4,11E-02	3,21E-03	85.46	8.08	86	11	8/5	92	1464.62 + 1602.73 +	SQFTITPGSEQIR NAVTQEFGPVPDTAR
11	Aconitate hydratase, mitochondrial (ACON)	Q99KI0	1	1,23	0,82	1,19	1,46	5,40E-04	1,08E-03	85.46	8.08	311	33	23/4	157	1464.62 + 1602.73 +	SQFTITPGSEQIR NAVTQEFGPVPDTAR

Table 2 (continued)

Spot #	Protein Name / Function	SWISSPROT accession #	WT	Tyk2-/-	WT + poly(I:C) treatment	Tyk2-/- + poly(I:C) treatment	Average ratio Tyk2-/- vs. WT + poly(I:C) treatment	p(gt) a)	p(gt x tr) b)	MWt (kDa) theor.	pI theor.	Peptide Mass Fingerprint			Sequencing		
												Probability based MOWSE Score	Sequ. Cov. %	Matched/ unmatched peptides	Probability based MOWSE Score	Precursor Ion(s) m/z (observed) and charge state	Peptide Sequence(s)
	IMMUNE RESPONSE																
12	T cell-specific GTPase (TGTP)	NP_035709 e)	1	1,09	8,53	4,39	0,51	ns	3,15E-03	47.15	5.49	311	54	20/0	164	1679.87 + 1867.08 +	FGEYDFFIIISATR DIESAPLHIAVTGETGAGK
13	Proteasome activator complex subunit 1 (PSME1)	P97371	1	0,70	1,53	1,37	0,89	1,07E-04	ns	28.67	5.73	270	71	18/3	146	1396.63 + 1873.03 +	NAYAVLYDIILK QLVHELDEAEYQEIR
14	Interferon-induced protein with tetratricopeptide repeats 3 (IFIT3)	Q64345	1	0,66	7,15	4,78	0,67	3,61E-03	1,36E-03	47.93	5.51	241	52	22/7	242	1741.90 + 1891.12 +	STVNNSPLYSLVMCR KSEDLAALECLLQFPR
15	Interferon-activable protein 205-B (IFI5B)	Q08619	1	0,26	2,76	3,15	1,14	3,61E-06	2,80E-01	47.59	8.38	58	11	6/5	155	1361.48 + 1772.04 +	QMIEVPNCITR GILEINETSSVLEAAPK
	OTHERS																
16	Immune-responsive protein 1 (IRG-1)	P54987	1	1,16	34,73	58,59	1,69	ns	4,05E-03	54.01	7.09	71	13	5/2	79	1169.23 + 1579.68 +	SDTFYGHWR LSSMSSFDHTTLPR
17	UMP-CMP kinase 2, mitochondrial (CMPK2) (Thymidylate kinase LPS-inducible member - TYKi)	Q3U5Q7	1	0,84	13,96	8,03	0,58	ns	1,26E-03	50.03	6.89	196	34	13/3	157	1102.32 + 1622.73 +	VLELIQSSGR LSSMSSFDHTTLPR
18	EH domain-containing protein 1 (EHD1) d)	Q9WVK4	1	1,34	2,03	3,18	1,57	ns	5,00E-04	60.60	6.35	180	32	15/3	148	1237.38 + 1675.80 + 2015.27 +	LNAFGNAFLNR LLDTVDDMLANDIAR VYIGSFWSHPLLIPDNR
	EH domain-containing protein 3 (EHD3) d)	Q9QXY6								60.87	6.03	69	16	7/11	81	1237.38 + 2015.27 +	LNAFGNAFLNR VYIGSFWSHPLLIPDNR

a) p-values for the differences between genotypes (gt) under basal conditions.

b) p-values for the differences between genotypes in response to poly(I:C) treatment (gt x tr).

c) not significant (p-value >0.05).

d) proteins with high sequence homology.

e) Accession # from NCBI nr database.

2. The impact of tyrosine kinase 2 (Tyk2) on the proteome of murine macrophages and their response to lipopolysaccharide (LPS)

Proteomics 2008, *8*, 3469–3485

RESEARCH ARTICLE

The impact of tyrosine kinase 2 (Tyk2) on the proteome of murine macrophages and their response to lipopolysaccharide (LPS)

Marta Radwan[1, 2, 3], Ingrid Miller[2]*, Tom Grunert[1, 4], Martina Marchetti-Deschmann[4], Claus Vogl[1], Niaobh O'Donoghue[5], Michael J. Dunn[5], Thomas Kolbe[3], Günter Allmaier[4], Manfred Gemeiner[2], Mathias Müller[1, 3] and Birgit Strobl[1]

[1] Institute of Animal Breeding and Genetics, University of Veterinary Medicine Vienna, Vienna, Austria
[2] Institute of Medical Chemistry, University of Veterinary Medicine Vienna, Vienna, Austria
[3] University Center Biomodels Austria, University of Veterinary Medicine Vienna, Vienna, Austria
[4] Institute of Chemical Technologies and Analytics, Vienna University of Technology, Vienna, Austria
[5] UCD Conway Institute of Biomolecular and Biomedical Research, University College Dublin, Dublin, Ireland

Tyrosine kinase 2 (Tyk2) belongs to the Janus kinase (Jak) family and is involved in signalling *via* a number of cytokines. Tyk2-deficient mice are highly resistant to lipopolysaccharide (LPS)-induced endotoxin shock. Macrophages are key players in the pathogenesis of endotoxin shock and, accordingly, defects in the LPS responses of Tyk2$^{-/-}$ macrophages have been reported. In the present study, the molecular role of Tyk2 is investigated in more detail using a proteomics approach. 2-D DIGE was applied to compare protein patterns from wild-type and Tyk2$^{-/-}$ macrophages and revealed significant differences in protein expression patterns between the genotypes before and after LPS treatment. Twenty-one proteins deriving from 25 differentially expressed spots were identified by MALDI/ESI MS. Among them, we show for N-myc interactor that its mRNA transcription/stability is positively influenced by Tyk2. In contrast, LPS-induced expression of plasminogen activator 2 protein but not mRNA is strongly enhanced in the absence of Tyk2. Our data furthermore suggest an influence of Tyk2 on the subcellular distribution of elongation factor 2 and on LPS-mediated changes in the peroxiredoxin 1 spot pattern. Thus, our results imply regulatory roles of Tyk2 at multiple levels and establish novel connections between Tyk2 and several cellular proteins.

Keywords:
2-D DIGE / Jaks / LPS / MS / Murine macrophages

Correspondence: Dr. Birgit Strobl, Institut für Tierzucht und Genetik, Veterinärmedizinische Universität Wien, Veterinärplatz 1, A-1210 Wien, Vienna, Austria
E-mail: birgit.strobl@vu-wien.ac.at
Fax: +43-1-25077-5693

Abbreviations: EF2, elongation factor 2; **ERK,** extracellular signal regulated kinase; **GAPDH,** glyceraldehyde-3-phosphate dehydrogenase; **IFIT,** interferon-induced protein with tetratripeptide repeats; **IFN,** interferon; **IN35,** interferon-induced protein 35 kD homologue; **Jak,** Janus kinase; **LPS,** lipopolysaccharide; **NMI,** N-myc interactor; **PAI2,** plasminogen activator inhibitor 2; **PRDX1,** peroxiredoxin 1; **RT-qPCR,** reverse transcription–quantitative PCR; **SP1,** transcription factor Sp1; **STAT,** signal transducer and activator of transcription; **Tyk2,** tyrosine kinase 2; **UBE2D2,** ubiquitin-conjugating enzyme E2 D2; **uPA,** urokinase plasminogen activator

1 Introduction

Tyrosine kinase 2 (Tyk2) belongs to the Janus kinase (Jak) family of nonreceptor tyrosine kinases. Jaks associate with the intracellular domains of cytokine receptors and are activated upon ligand binding by auto- and/or transphosphorylation. Activated Jaks phosphorylate signal transducers and activators of transcription (STATs), which then translocate to the nucleus as activated homo- or heterodimers where they affect the expression of responsive genes [1, 2]. Type I interferons (IFNs) were the first cytokines described to utilise Tyk2 for signal transduction and subse-

---

* Additional corresponding author; Ingrid Miller,
   E-mail: ingrid.miller@vu-wien.ac.at

quently activation of Tyk2 has been shown for a number of other cytokines and some growth factors [3–5]. Cells derived from mice lacking Tyk2 revealed a partial requirement for Tyk2 for IFNα/β and interleukin 12 (IL-12) signalling [6, 7]. *In vivo*, Tyk2 plays an important role in the host defence against microbial pathogens. Tyk2 deficient mice show increased susceptibility to murine cytomegalovirus [8], *Leishmania major* [9] and *Listeria monocytogenes* [10]. In contrast, a negative role of Tyk2 was shown for disease progression in lipopolysaccharide (LPS) and ischemia/reperfusion-induced shock models [11–13]. LPS is the major structural component of the outer membrane of Gram-negative bacteria and a potent activator of immune cells. Macrophages and monocytes are of primary importance for the recognition of and the response to LPS. Activated macrophages produce a variety of cytokines, ROS and other inflammatory mediators that contribute to the effective eradication of invading pathogens. Excessive or deregulated production of these cytokines and mediators, however, can be harmful for the host and lead to the endotoxic shock syndrome [14, 15]. The high resistance of Tyk2$^{-/-}$ mice to LPS prompted us to further investigate the molecular role of Tyk2 for macrophage functions. LPS signalling in macrophages is induced through the Toll-like receptor 4 (TLR4) complex. Basically, LPS treatment leads to the activation of two independent signalling cascades *via* distinct adaptor proteins bound to the cytoplasmic moiety of the receptor chains: one resulting mainly in the activation of nuclear factor-κB (NF-κB) and in the production of pro-inflammatory cytokines and mediators. The second cascade induces gene expression, most prominently IFNβ, *via* activation of members of the interferon regulatory factor (IRF) family. Subsequently, IFNβ activates Tyk2 and Jak1 in an autocrine or paracrine manner and triggers the expression of IFN responsive genes. The successive and concerted action of signalling cascades and their cross-influence determines the complex cellular responses initiated by LPS recognition [16–18].

Proteomics studies on human and murine macrophages have been performed since early days of 2-DE, using cell lines and primary cells of different sources. MS later on allowed the identification of differentially expressed spots when comparing 2-DE patterns under different conditions, and to attribute protein regulations to various stimuli. In a few studies primary murine macrophages (peritoneal or bone marrow-derived) were analysed, *e.g.* under ionising radiation [19], infection with bacteria or protozoa [20], IFNγ activation [21] or LPS stimulation [22, 23].

In our study, we focused on the influence of Tyk2 on the macrophage proteome both in the untreated and the LPS treated state. Using 2-D DIGE technology we show complex consequences of the lack of a single protein on the overall protein expression pattern. We identified by MALDI and ESI MS 21 different proteins from 25 spots, which are either up- or downregulated in the absence of Tyk2. Proteins from various functional categories were identified, thereby suggesting an influence of Tyk2 on various cellular processes. More

detailed analyses on selected proteins showed that this is exerted at mRNA and/or protein level further underscoring the importance of proteomics studies.

2 Materials and methods

2.1 Animals and cells

Tyk2 knockout mice have been described previously [6] and were on C57BL/6 background. Animals were housed under specific pathogen-free conditions and were sex- and age-matched (8–12 wk) for each experiment. Bone marrow-derived macrophages were isolated and grown in the presence of macrophage colony-stimulating factor 1 (CSF-1) derived from L929 cells as described previously [24]. After cultivation for 6 days cells were treated with 100 ng/mL LPS (*Escherichia coli* serotype 055:B5, Sigma, St. Louis, MO, USA).

2.2 Sample preparation

2.2.1 Whole cell lysates

Cells (5×10^6) were lysed in 100 µL lysis buffer (50 mM Tris-HCl pH 8.0; 10% glycerol v/v; 0.5% NP-40 v/v; 0.1 mM EDTA; 150 mM NaCl; 2 mM DTT; phosphatase inhibitors: 2 mM sodium orthovanadate; 25 mM sodium fluoride and protease inhibitors: 2 mM PMSF; 2 µg/mL aprotinin; 2 µg/mL leupeptin; 2 µg/mL pepstatin). Cell debris was removed by centrifugation at $14\,000 \times g$. For 2-D DIGE samples were lyophilised and dissolved in DIGE lysis buffer (7 M urea; 2 M thiourea; 4% CHAPS w/v; 30 mM Tris-HCl pH 8.5).

2.2.2 Nuclear extracts

Nuclear extracts were produced as previously described [25] with a few modifications. Cells (1.5×10^7) were collected in 1 mL PBS and pelleted by centrifugation at $1500 \times g$ for 5 min. The pellets were resuspended in 1.5 mL cold buffer A (10 mM HEPES pH 7.9; 10 mM KCl; 0.1 mM EDTA; 0.1 mM EGTA; 2 mM DTT and phosphatase/protease inhibitors as described above). They were allowed to swell on ice for 15 min, NP-40 was added to a final concentration of 0.6% v/v. The mixtures were vortexed vigorously for 10 s followed by spinning at $13\,000 \times g$ for 1 min at 4°C. The nuclear pellets were washed with cold PBS and then incubated with benzonase (1000 units; Sigma, purity >90%) in 15 µL H$_2$O *per* sample for 15 min at room temperature. Pellets were resuspended in 1 mL cold buffer B (20 mM HEPES pH 7.9; 400 mM NaCl; 1 mM EDTA; 1 mM EGTA; 2 mM DTT and protease inhibitors) and incubated for 45 min at 4°C with vigorous shaking. Insoluble material was removed by centrifugation at $13\,000 \times g$ for 5 min at 4°C, and the supernatants were kept for further analysis ('nuclear extracts').

2.2.3 TCA precipitation

Nuclear extracts (whole sample from 1.5×10^7 cells) were mixed with 0.25 volumes of ice-cold 6.1 M TCA solution. DTT was added to a final concentration of 20 mM. The extracts were incubated for 2 h on ice to allow complete pre-cipitation. The samples were centrifuged at $10\,000 \times g$ for 10 min at 4°C. The supernatant was discarded and the pellet was washed three times with 1 mL ice-cold acetone contain-ing 20 mM DTT. The pellet was air-dried and dissolved in DIGE lysis buffer (7 M urea; 2 M thiourea; 4% CHAPS w/v; 30 mM Tris) by shaking overnight at 4°C. The pH of the samples was adjusted to pH 8.5 with 100 mM Tris. Prior to separation on 2-DE, nuclear extracts were tested for repro-ducibility and quality with western blot analyses, using tran-scription factor Sp1 (SP1) as a nuclear and glyceraldehyde-3-phosphate dehydrogenase (GAPDH) as a cytosolic marker protein. Protein concentration in both, whole cell and nuclear extracts was determined by the Coomassie G-250 protein binding assay [26].

2.3 DIGE labelling

Twenty-five micrograms of protein *per* sample were labelled with CyDye Fluor minimal dyes (GE Healthcare Life Sci-ences, Munich, Germany) according to the manufacturer's instructions, except for a lower coupling rate. For whole cell lysates 4 nmol dye/mg protein were used (as described pre-viously [27]), for nuclear extracts 2 nmol dye/mg protein were found optimal to avoid artefacts due to multiple label-ling of lysine residues. Three biological replicates were used *per* experiment. Untreated samples from wild-type and Tyk2$^{-/-}$ macrophages were labelled with Cy3, corresponding treated samples with Cy5. The internal standard, prepared by pooling 25 µg of protein from each sample included in an experimental set, was labelled with Cy2. Two samples (Cy3, Cy5) and the internal standard (Cy2) were separated on each gel.

2.4 2-DE separation

The first dimension was carried out on an IPGphor III sys-tem using 24 cm IPG Dry strips with linear pH gradients (all GE Healthcare). The IPG strips pH 4–7 were loaded with the samples through passive in-gel rehydration for 10 h at room temperature. The three labelled samples were mixed and the volume was adjusted to 450 µL with rehydration buffer (7 M urea; 2 M thiourea; 4% CHAPS w/v; 70 mM DTT; 1% IPG buffer 4–7 v/v). For IPG strips pH 6–9 samples were applied by anodic cup loading. The strips were rehydrated overnight in 450 µL rehydration buffer (7 M urea; 2 M thiourea; 4% CHAPS w/v; 150 mM DTT; 2% IPG buffer 6–11 v/v). The mixed samples were adjusted to 50 µL in rehydration buffer and loaded onto the strips *via* loading cups. The proteins were focused for 30 kV·h in a step gradient with a maximum of 3500 V. The focused IPG strips were reduced 10 min

(1.25% DTT w/v) and alkylated 10 min (2.5% w/v iodoacet-amide) in equilibration buffer (6 M urea; 30% glycerol v/v; 75 mM Tris-HCl pH 8.8; 2% SDS w/v). The equilibrated strips were placed onto 10%T or 11.5%T polyacrylamide gels and sealed with 0.5% agarose in SDS running buffer. SDS-PAGE was performed according to Laemmli [28]. Gels were run overnight at 13 mA *per* gel in an Ettan Dalt Six electro-phoresis chamber (GE Healthcare).

2.5 2-DE evaluation

All gels were scanned at 100 µm resolution on a Typhoon 9400 imager and analysed with DeCyder software V5.02 (all GE Healthcare). Evaluation was based on volume ratios (sample spot volume divided by the corresponding internal standard spot volume). Protein spots differentially expressed between groups were extracted, using volume ratios and Student's *t*-test as selection criteria. Based on reverse label-ling experiments spots showing dye labelling bias were excluded from the candidate list. For figures and tables, expression levels were calculated relative to unstimulated wild-type cells ±SD.

2.6 Statistical analysis

For statistical analyses the volume ratios were used. A lin-ear model was fitted with genotype (*gt*), LPS-treatment (*tr*), and the interaction between these two (*gt* × *tr*) as fixed effects. The influence of the individuals was considered as a random effect. Significance of the effects was tested using a moderated *t*-test [29]. The residual variances of all spots from one experiment were assumed to be prior F-distributed. In an empirical Bayes fashion, the parameters for these F-distributions were estimated from the data using maximum likelihood. The moderated variance of each gene was set to the posterior maximum. With this variance, a moderated *t*-value was calculated for the two relevant fixed effects *gt* and *gt* × *tr*. The moderated *t*-test method strikes a balance between using a *t*-test, where the interference of the variance is compromised by the low sample size for each gene, and using a fold-change approach, where differences among spots in variance are ignored entirely.

2.7 MS

Protein spots were detected by acidic silver nitrate staining as previously described [30], making it MS-compatible by omitting glutaraldehyde from the sensitiser and form-aldehyde from the silver nitrate solution. Spots of interest were manually excised and pooled for MS analyses. Semi-preparative 2-DE gels with a protein load of 150–200 µg were used to recover enough material for MS-analysis of faint spots. All spots were destained as previously described [31].

2.7.1 Protein identification by MALDI-MS

In-gel digestion was performed according to [32] with slight modifications. Gel pieces were equilibrated with 25 mM ammonium bicarbonate, washed with ACN, dried in a vacuum centrifuge and rehydrated in 25 mM ammonium bicarbonate containing 12.5 ng/µL sequencing grade trypsin (Roche, Mannheim, Germany) at 4°C for 30 min. Excess of trypsin working solution was removed, samples were covered with 25 mM ammonium bicarbonate and incubated overnight at 37°C. Supernatant was collected and the elution of the peptides was performed twice with 66% ACN/33% 0.1% TFA. The combined aliquots were dried in a vacuum centrifuge and dissolved in 0.1% TFA. Samples were purified and concentrated with ZipTip$_{µ-C18}$ pipette tips (Millipore, Billerica, MA, USA) and analysed on a MALDI-TOF/reflectron TOF-instrument (TOF^2; Shimadzu Biotech Kratos Analytical, Manchester, UK) in the positive ion mode with delayed extraction applying a thin layer preparation technique as described earlier [33]. External calibration was performed using monoisotopic values of the singly charged ions of an aqueous solution of standard peptides (bradykinin fragment 1–7, human angiotensin II, P14R, ACTH fragment 18–39). Autolytic tryptic products, matrix clusters [34], keratin and gel blank artefacts [35] were removed from the mass spectra and the resulting monoisotopic list of *m/z* values was submitted to search engines MASCOT (Revision 2.1.0 to 2.2.0) [36] and ProFound [37] searching the databases Swiss-Prot (Version 50.6 of 05-Sep-2006 to 54.5 of 04-Nov-2007) and NCBI (Sequence Release 19 of 10-Sep-2006 to 26 of 13-Nov-2007). Search criteria were: taxonomy, *Mus musculus*; mass accuracy, 200 ppm; fixed modifications, carbamidomethylation; variable modifications, methionine oxidation and acetylation at the protein N-terminus, maximum one missed cleavage site. PSD experiments were performed on selected peptides from the measured PMFs. MS/MS database searches have been performed using the same restrictions as for PMF, additionally a product ion tolerance of ± 1 Da was defined. A hit was considered significant, if the scores of at least two database searches, obtained for PMF data and/or PSD data, independently exceeded the algorithm's significance threshold ($p < 0.05$).

2.7.2 Protein identification by ESI-MS

Spot plugs were digested with trypsin as previously described [31]. All samples were run on an LTQ linear ion mass spectrometer (Thermo Scientific, San Jose, CA, USA) connected to a Surveyor chromatography system incorporating an autosampler as previously described [38]. Tryptic peptides were resuspended in 0.1% formic acid and were separated by means of a SurveyorLC system (Thermo Scientific) connected directly to the source of the LTQ. Each sample was loaded onto a Biobasic C18 Picofrit™ column (100 mm length, 75 µm id) at a flow rate of 30 nL/min. The samples were then eluted from the C18 Picofrit™ column by an increasing ACN gradient. The mass spectrometer was operated in positive ion mode with a

capillary temperature of 200°C, a capillary voltage of 46 V, a tube lens voltage of 140 V and with a potential of 1800 V applied to the frit. All data were acquired with the mass spectrometer operating in automatic data-dependent switching mode. A zoom scan was performed on the five most intense ions to determine charge state prior to MS/MS analysis. All MS/MS spectra were analysed using BioworksBrowser (Version 3.2; Thermo) using the TurboSEQUEST® algorithm under default settings. The MS/MS spectra were searched against the Swiss-Prot database (Uniprot_sprot; Release 10.0). The following search parameters were used: precursor ion mass tolerance of 1.5 Da, fragment ion tolerance of 1.0 Da with methionine oxidation and cysteine carboxy-amidomethylation specified as differential modifications and a maximum of two missed cleavage sites allowed.

2.8 Western blot analysis

1-D Western blots were performed on small-size SDS-PAGE gels as previously described [8].

2-D Western blot: 2-DE was performed as above except that we used 10 cm laboratory-made pH 6–10 IPG strips [39] with 50 µg protein applied by anodic cup loading. Focusing was carried out without oil for a total of 13 kV·h on a Multiphor II system (GE Healthcare). The second dimension on $14 \times 14 \times 0.15$ cm^3 gels and semidry blotting were performed as previously described [27].

The following antibodies were used: goat anti-NMI, rabbit anti-PAI2, rabbit anti-SP1, donkey anti-goat IgG-HRP (all Santa Cruz Biotechnology, Santa Cruz, CA, USA); rabbit anti-EF2 (Cell Signalling, Danvers, MA, USA); goat anti-PRDX1 (R&D Systems, Wiesbaden-Nordenstadt, Germany); mouse anti-extracellular signal regulated kinase (ERK) (BD Biosciences Transduction Laboratories, Lexington, KY, USA); rabbit anti-GAPDH (Biotrend, Cologne, Germany); donkey anti-rabbit IgG-HRP F(ab)$_2'$ fragment; sheep anti-mouse IgG-HRP F(ab)$_2'$ fragment (all GE Healthcare).

2.9 Reverse transcription–quantitative PCR (RT-qPCR)

Total RNA was isolated from 10^6 cells using TRIzol (Invitrogen Life Technologies, Lofer, Austria) according to the manufacturer's instructions. RNA was treated with DNase I (Promega Corporation, Mannheim, Germany) to eliminate genomic DNA. Total RNA (1.5 µg) was used for cDNA synthesis using iScript (BioRad Laboratories, Vienna, Austria). Primers and probes were designed using Primer Express (Applied Biosystems, Vienna, Austria) software. Probes (Genexpress, Wiener-Neudorf, Austria) were labelled with 6-carboxyfluorescein (FAM) and Blackhole Quencher 1 (BHQ1) at the 5′ and 3′ ends, respectively. The following primers (Invitrogen Life Technologies) and probes were used, all 5′ to 3′ direction: *PAI2* fwd: ACTCAGATCCTA-GAACTTCCGCAT; rev: AAAGTTTATTTCACTTTCCAG-CAATTC; probe: CATGCTCCTGTTGCTTCCCGATGAGA;

NMI fwd: GCCAAGCGCTCATCACCTT; rev: CCTTCCATC
TGCACGACATG; probe: AGAAGTCGCACAAAATGTGA-
TATCGATGGG; *PRDX1* fwd: CTAGTCCAGGCCTTC-
CAGTTCA; rev: TCAGGCTTGATGGTATCACTGC; probe:
AACATGGTGAAGTGTGTCCAGCTGGCTG. RT-qPCR was
performed in duplicate on Eppendorf realplex4 (Eppendorf,
Vienna, Austria). Gene expression was calculated as pre-
viously described [11] except that ubiquitin-conjugating en-
zyme E2 D2 (*UBE2D2*) was used as endogenous control [8].
Expression levels were calculated relative to unstimulated
wild-type cells ± standard error (SE).

3 Results

3.1 2-D DIGE protein patterns of primary murine macrophages are highly reproducible

We compared protein patterns of wild-type and Tyk2$^{-/-}$ bone
marrow-derived macrophages before and after LPS treat-

ment in whole cell lysates and in nuclear extracts, respec-
tively. Both types of cell extracts were analysed in two differ-
ent pH gradients (pH 4–7 and 6–9, respectively), thus yield-
ing four 2-D DIGE experiments. Each experiment comprised
three biological replicates *per* genotype and treatment
resulting in six analytical gels. Representative 2-DE protein
patterns are shown in Fig. 1. Depending on the specific
experiment, we detected 478–792 spots that were present in
all images (Table 1) and only those spots were included in the
further examinations. Spot volume ratios of biological repli-
cates showed low variability with mean SDs between ±0.073
and ±0.085 (Table 1 and Fig. S1 of Supporting Information).
For a given statistical power of 0.9, a *p*-value of ≤0.05 (two-
sided), the sample size of three, and the respective mean SD,
the resulting minimal detectable differences (effect size) in
expression levels were between 26.2 and 30.5%. Thus, on
average, differences in expression values of around 30% can
be detected with our experimental set-up.

Nuclear extracts comprised about 10% of total proteins
found in whole cell lysates and protein patterns were clearly
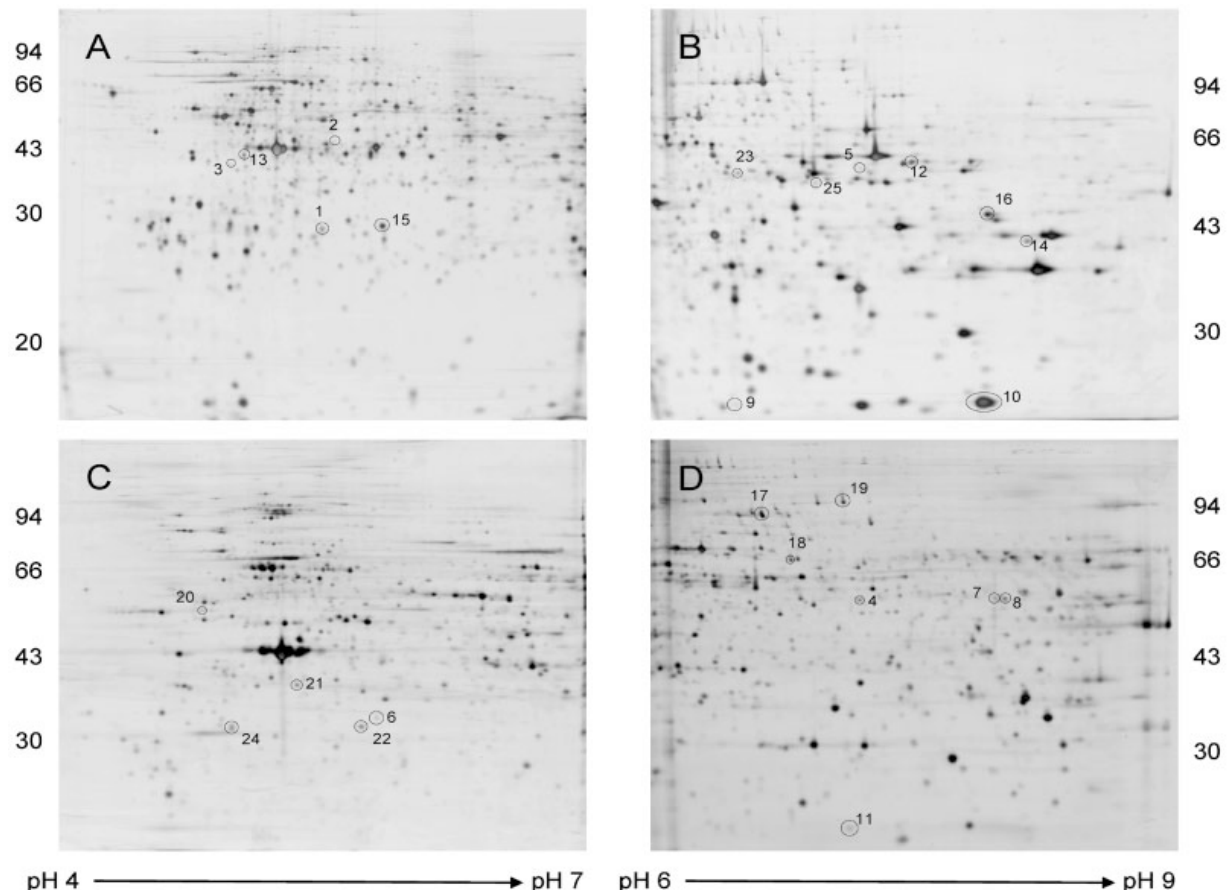
Figure 1. Representative 2-DE protein patterns of Tyk2$^{-/-}$ macrophages. Analytical gels (75 µg protein each) visualised by MS-compatible silver stain after 2-D DIGE. Identified proteins are indicated by the spot numbers used in Table 3. Whole cell lysates: (A) pH gradient 4–7, 11.5%T SDS-PAGE; (B) pH 6–9, 10%T SDS-PAGE. Nuclear extracts: (C) pH 4–7; (D) pH 6–9; both: 10%T SDS-PAGE.

Table 1. Experiments performed and their statistical properties

	Whole cell lysates ±18 h LPS		Nuclear extracts ±8 h LPS	
pH	4–7	6–9	4–7	6–9
Number of spots in all 18 images	579	478	731	792
Mean SD	0.073	0.078	0.085	0.085
Minimal detectable difference	26.2%	28.0%	30.5%	30.5%

different, although with some overlaps (Fig. 1). This standard protocol for the preparation of nuclear extracts does not result in the complete extraction of nuclear proteins and can also lead to copurification of proteins from other compartments, *e.g.* plasma membrane, ER, cytoskeletal fragments and large cytoplasmic protein complexes. Nevertheless, extracts showed good reproducibility and enrichment of a subset of cellular proteins, which might not be detected in whole cell extracts. Western blot analysis with specific marker proteins showed hardly detectable levels of GAPDH, a cytosolic marker protein, and high amounts of SP1, a nucleus specific protein (see Fig. S2 of Supporting Information).

3.2 Absence of Tyk2 significantly alters the protein expression pattern in macrophages

The analyses with respect to the impact of Tyk2 deficiency on the macrophage proteome were performed with an emphasis on the effects on basal protein expression (genotype effects) and on LPS mediated changes in expression levels (genotype × treatment effects). Statistically significant differences were found for a large number of spots in both cases (see Fig. S3 of Supporting Information). We filtered these spots for differences between wild-

type and Tyk2$^{-/-}$ cell extracts of at least 40% before and/ or after LPS treatment. Forty-six spots in whole cell lysates and seventy-three in nuclear extracts met these criteria (Table 2), this corresponds to 3–6% of spots examined, depending on the specific experiment. Positive as well as negative effects of Tyk2 deficiency on expression levels were found with similar distribution in all cases. Among the 119 differentially expressed spots, 75 spots displayed genotype effects, 13 spots genotype × treatment effects and 31 spots showed both effects. A similar predominant genotype effect was found if data were analysed without filtering for the minimal difference of 40% (see Fig. S3 of Supporting Information).

3.3 Differentially expressed proteins exert various functions

From among the 119 differentially expressed spots, 34 spots were selected for protein identification. The selection was based on a combination of the following criteria: expression pattern in the 2-D DIGE analysis (extent of difference between the genotypes before and after treatment), stainability of spots with silver (for colorimetric visualisation on the gels enabling manual spot cutting), spot quantity (spot density in silverstained patterns supplying sufficient amounts for MS analysis) and spot quality (shape and compactness of spots, nonoverlap with others). Usually selection criteria were used with equal emphasis, where impossible, the most common denominator of selectable criteria was used for decision making.

Using LC-ESI- and MALDI-MS/MS, 25 of the 34 selected spots gave interpretable MS spectra, which equates to a success rate of 73.5%. In these spots, 21 different proteins were identified (see Fig. 2 for 2-D DIGE spot images and Table S1 of Supporting Information for details of MS analysis). The differentially expressed proteins (listed in Table 3) were classified according to their gene ontology annotation. Identified proteins belong to various functional categories including

Table 2. Numbers of differentially expressed and identified spots[a]

Experiment	Total	gt[b]		gt × tr[c]		gt + gt × tr[d]		ID[e]
		Up[f]	Down[f]	Up	Down	Up	Down	
Whole cell lysates (pH 4–7)	17	2	–	3	–	7	5	5
Whole cell lysates (pH 6–9)	29	4	5	5	4	6	5	8
Nuclear extracts (pH 4–7)	33	22	14	–	1	1	2	5
Nuclear extracts (pH 6–9)	40	11	17	–	–	2	3	7
Total	119	39	36	8	5	16	15	25 (21 proteins)

a) At least 40% difference in expression ± LPS treatment between genotypes, $p \leq 0.05$.
b) Genotype effect (significant differences between genotypes under basal conditions).
c) Genotype × treatment effect (significant differences between genotypes in response to LPS treatment).
d) Genotype and genotype × treatment effect.
e) Identified spots.
f) Up/downregulated in the absence of Tyk2.
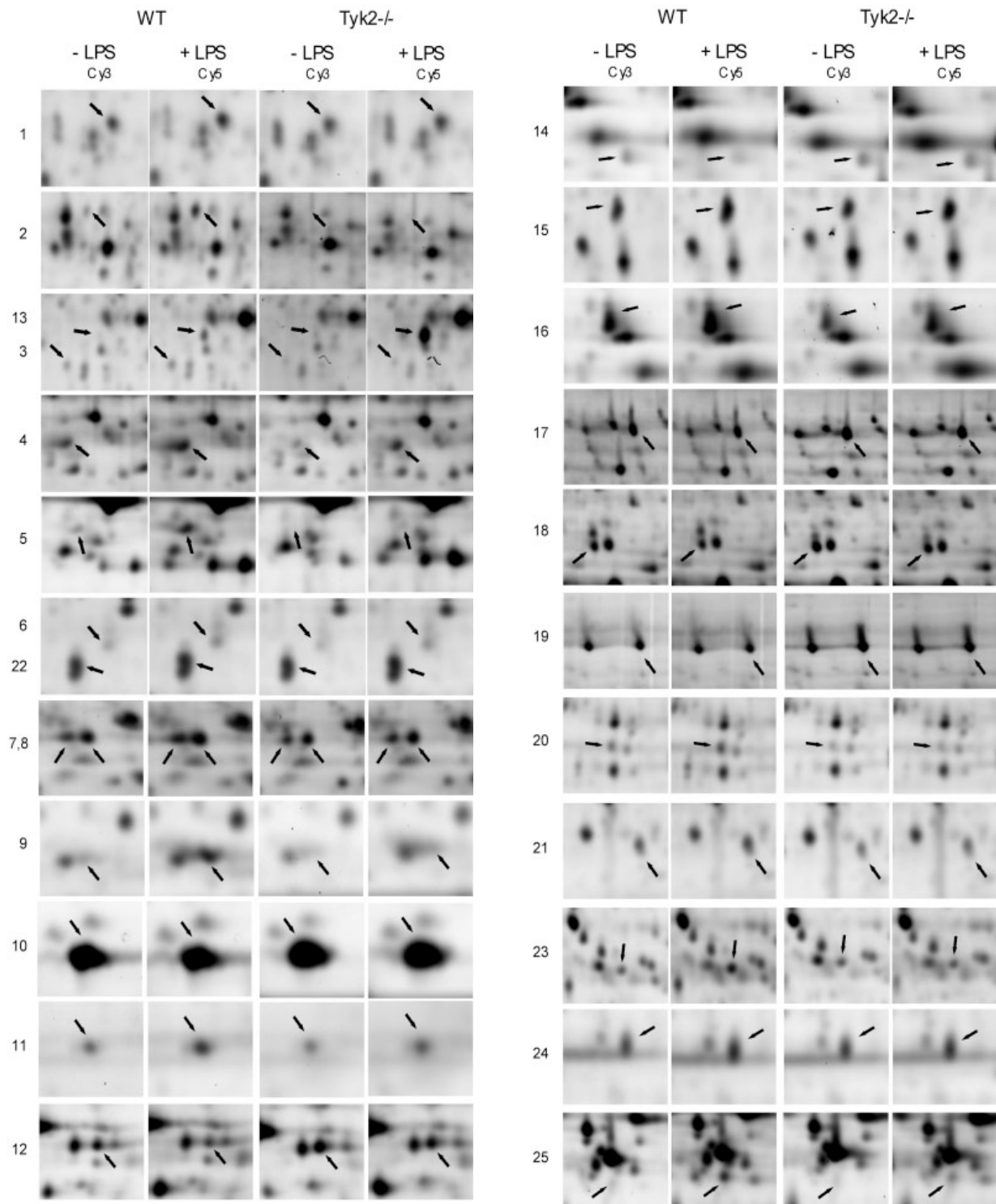
Figure 2. Comparison of proteome pattern in wild-type *versus* Tyk2$^{-/-}$ macrophages with or without LPS treatment. Selected regions from 2-D DIGE images are shown (compare Fig. 1 for exact spot location on the whole gel images). Cy3/Cy5 images converted to grey scale for all 25 spots identified (indicated by arrows and the spot numbers used in Fig. 1 and Table 3) are depicted. See legend to Fig. 1 and Table 3 for details on protein extracts and electrophoretic conditions.

Table 3. Differentially expressed proteins in Tyk2$^{-/-}$ macrophages

Spot no.	Protein name	Accession no. Swiss-Prot	WT	WT + LPS	Tyk2$^{-/-}$	Tyk2$^{-/-}$ + LPS	p (gt)[a]	p (gt × tr)[b]	M_r (kDa) theoret.	pI theoret.	MS method	Protein extract[c]
Immune response												
1	Proteasome activator complex subunit 2 (PSME2)	P97372	1	1.30	0.76	0.92	0.0033	ns[d]	27	5.5	ESI	A
2	Interferon-induced protein with tetratripeptide repeats 3 (IFIT3)	Q64345	1	3.12	0.51	0.65	0.0021	0.0021	47.2	5.5	ESI	A
3	N-myc-interactor (NMI)	O35309	1	1.27	0.59	0.48	0.0004	0.0025	35.2	5	ESI MALDI	A
4	Interferon-induced protein with tetratripeptide repeats 1 (IFIT1)	Q64282	1	1.65	0.38	0.73	0.0006	ns	53.7	7.2	MALDI	D
5	Interferon-induced protein with tetratripeptide repeats 1 (IFIT1)	Q64282	1	3.95	0.67	0.62	ns	0.0010	53.7	7.2	MALDI	B
6	Interferon-induced protein 35 kD homologue (IIN35)	Q9D8C4	1	1.26	0.54	0.73	0.0002	0.0468	31.8	5.6	MALDI	C
7	Interferon-activable protein 205 (IFI5) or interferon-activable protein 204 (IFI4)[e]	Q08619/P15092	1	1.31	0.60	1.03	0.0014	0.0129	47/71.6	8.4/9	MALDI	D
8	Interferon-activable protein 205 (IFI5) or interferon-activable protein 204 (IFI4)[e]	Q08619/P15092	1	1.27	0.56	0.97	0.0014	0.0129	47/71.6	8.4/9	MALDI	D
Oxidative stress response												
9	Peroxiredoxin-1 (PRDX1)	P35700	1	3.94	1.19	1.99	0.0221	0.0012	22.2	8.3	MALDI	B
10	Peroxiredoxin-1 (PRDX1)	P35700	1	0.68	1.08	1.28	ns	0.0044	22.2	8.3	MALDI	B
11	Peroxiredoxin-1 (PRDX1)	P35700	1	1.78	0.98	1.06	ns	0.0197	22.2	8.3	MALDI	D
12	Catalase (CATA)	P24270	1	0.60	1.48	1.13	0.0024	0.0257	59.8	7.7	MALDI	B
Apoptosis												
13	Plasminogen activator inhibitor 2 (PAI2)	P12388	1	4.73	1.97	30.0	0.0010	0.0006	46.3	5	MALDI	A
Metabolism												
14	3-Ketoacyl-CoA thiolase A (THIKA) or 3-ketoacyl-CoA thiolase B (THIKB)[e]	Q921H8/Q8VCH0	1	0.54	1.12	1.04	ns	0.0036	44	8.7	MALDI	B
15	Purine nucleoside phosphorylase (PNPH)	P23492	1	1.56	0.66	0.99	0.0013	ns	32.2	5.8	ESI	A
16	Argininosuccinate synthase (ASSY)	P16460	1	1.55	0.60	0.98	0.0024	ns	46.6	8.4	MALDI	B
Translation, transcription												
17	Elongation Factor 2 (EF2)	P58252	1	0.84	1.59	1.37	0.0016	ns	95.3	6.4	MALDI	D
18	Phenylalanyl-tRNA-synthase β chain (SYFB)	Q9WUA2	1	0.79	1.34	1.24	0.0064	ns	65.7	6.7	MALDI	D

Table 3. Continued

Spot no.	Protein name	Accession no. Swiss-Prot	WT	WT + LPS	Tyk2$^{-/-}$	Tyk2$^{-/-}$ + LPS	p (gt)[a]	p (gt × tr)[b]	M_r (kDa) theoret.	pI theoret.	MS method	Protein extract[c]
19	Staphylococcal nuclease domain-containing protein 1 (SND1)	Q78PY7	1	0.87	1.54	1.38	0.0006	ns	102.1	7.1	MALDI	D
Cytoskeleton												
20	Vimentin (VIME)	P20152	1	1.35	0.55	0.60	0.0002	ns	53.7	5.1	MALDI	C
21	F-actin capping protein subunit α-1 (CAZA1)	P47753	1	1.29	0.70	0.77	0.0011	ns	32.9	5.3	MALDI	C
22	F-actin capping protein subunit β (CAPZB)	P47757	1	1.20	0.68	0.75	0.0014	ns	31.3	5.5	MALDI	C
23	Adenyl cyclase-associated protein 1 (CAP1)	P40124	1	1.92	1.23	1.19	0.0102	0.0007	51.6	7.2	MALDI	B
Others												
24	EF-hand domain containing protein 2 (EFHD2)	Q9D8Y0	1	1.38	0.73	0.78	0.0016	ns	26.8	5	MALDI	C
25	Immune-responsive protein 1 (IRG1)	P54987	1	4.42	0.75	1.90	ns	0.0014	53.8	7.1	MALDI	B

a) *p*-Values for the differences between genotypes under basal conditions.
b) *p*-Values for the differences between genotypes in response to LPS treatment.
c) Protein extracts: A, whole cell lysates pH 4–7; B, whole cell lysates pH 6–9; C, nuclear extracts pH 4–7; D, nuclear extracts pH 6–9.
d) Not significant (*p*-value>0.05).
e) Proteins with high sequence homology.

oxidative stress and immune responses, metabolism and cytoskeleton architecture. In several cases we identified the same protein in different spots on one gel or in both protein extracts. For instance, interferon-induced protein with tetratripeptide repeats 1 (IFIT1) was identified in whole cell lysates and nuclear extracts located at pI 7.2 and M_r of 60 kDa (spots 4 and 5 in Table 3, Figs. 1B, D and 2). Both spots showed upregulation by LPS treatment in wild-type cells, whereas the effect of Tyk2 deficiency on basal expression and LPS induction was different for the two spots. Interferon-activable protein 204 or 205 (IFI4/5) was found in two neighbouring spots showing identical expression patterns (spots 7 and 8 in Table 3, Figs. 1D and 2). We could not distinguish between IFI4 and IFI5 since they display high sequence homology and only peptides in common were found in MS. Six known IFN-inducible proteins (proteasome activator complex subunit 2 (PSME2), IFIT1, IFIT3, IFI4/5, interferon-induced protein 35 kD homologue (IN35), N-myc-interactor (NMI)) were identified. All of them showed upregulation upon LPS treatment in wild-type cells. Interestingly, all of them displayed reduced basal expression levels and, except for PSME2, reduced or even absent LPS-mediated upregulation in Tyk2-deficient cells in at least one of the corresponding spots (spots 1–8 in Table 3 and Fig. 2).

From the list of differentially regulated proteins (Table 3 and Fig. 2) we selected several candidates based on their regulation patterns or their molecular functions for further investigations. We performed time course studies of protein and mRNA expression using 1-D Western blotting and RT-qPCR, respectively. When a complex spot pattern was assumed for a particular protein 2-D Western blots were performed in addition.

3.3.1 Tyk2 is required for efficient expression of NMI protein and mRNA

According to the 2-D DIGE analysis, NMI showed approximately 0.6-fold expression levels before and after LPS treatment in Tyk2$^{-/-}$ as compared to wild-type cells (spot 3 in Table 3 and Figs. 2 and 3A). We subsequently used 1-D Western blot analysis for validation of expression patterns. The amount of NMI protein was clearly reduced in Tyk2$^{-/-}$ cells upon 0 and 18 h LPS treatment (Fig. 3B). The relatively modest upregulation of NMI protein upon LPS treatment in wild-type cells found with 2-D DIGE technology (1.3-fold) was only just about detectable with Western blot analysis. Similar results were obtained in a more extensive time course experiment (data not shown). We next examined by RT-qPCR whether the reduced protein level in Tyk2$^{-/-}$ cells
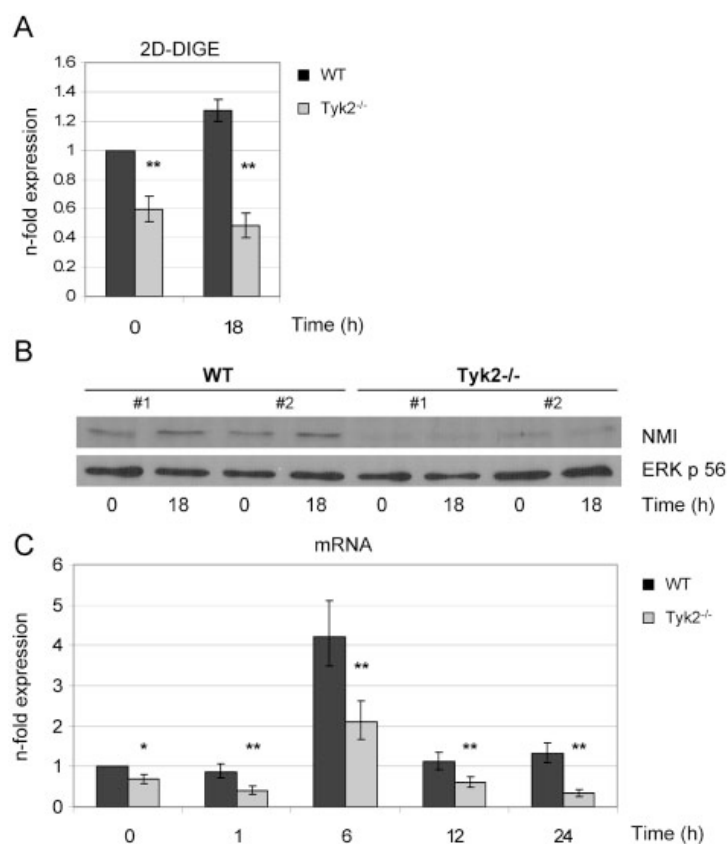
Figure 3. Effect of Tyk2 deficiency on the expression of NMI protein (A, B) and mRNA (C). Macrophages were treated with LPS for the indicated times and whole cell lysates or total RNA were subjected to 2-D DIGE analysis (A), Western blotting (B) or RT-qPCR (C). (A) 2-D DIGE: expression levels are given as fold ratios relative to unstimulated wild-type (WT) cells. Mean values ±SD of three biological replicates are shown. (B) Western blot analysis: 20 µg protein *per* lane were separated by 10%T SDS-PAGE. Protein loading was controlled by reprobing with an anti-panERK antibody. Data are representative of at least three independent experiments. Nos. 1 and 2 indicate that the cells were derived from independent mice. (C) mRNA expression was analysed by RT-qPCR. *UBE2D2* was used as endogenous control, expression levels were calculated relative to untreated WT cells. Mean values ±SE from at least three independent experiments are depicted. * $p \leq 0.05$, ** $p \leq 0.01$.

is due to lower mRNA expression. A modest and transient upregulation of mRNA was detectable upon 6 h of LPS treatment in both wild-type and Tyk2$^{-/-}$ macrophages (Fig. 3C). However, mRNA levels were consistently lower in the absence of Tyk2 throughout the time course investigated.

3.3.2 Tyk2 negatively regulates plasminogen activator inhibitor 2 (PAI2) protein but not mRNA expression

Expression levels of PAI2 were particularly interesting since Tyk2$^{-/-}$ macrophages displayed elevated basal expression as well as a strongly enhanced LPS mediated upregulation (spot 13 in Table 3 and Figs. 2 and 4A). Strong induction of PAI2 protein by LPS treatment was detectable in both genotypes and enhanced expression in the absence of Tyk2 could be clearly confirmed by 1-D Western blot analysis (Fig. 4B). PAI2 protein expression could be detected from 8 h LPS stimulation onwards (data not shown) with stable maximal expression from about 18–24 h of treatment (Fig. 4B). Increased PAI2 protein level in Tyk2$^{-/-}$ cells was observed throughout all time points with detectable PAI2 expression (Fig. 4B and data not shown). In both 2-D DIGE and 1-D Western blot analysis we detected PAI2 with the M_r of approximately 42 kDa, which resembles the nonglycosylated form of PAI2 reported in the literature [40]. PAI2 mRNA

expression was not affected by the absence of Tyk2 (Fig. 4C). Expression was rapidly induced in wild-type as well as Tyk2$^{-/-}$ macrophages, reached maximal expression levels at around 6–12 h LPS treatment and modestly declined thereafter (Fig. 4C).

3.3.3 Absence of Tyk2 affects peroxiredoxin 1 (PRDX1) spot patterns

PRDX1 was identified in three spots with similar molecular weight (23 kDa) but distinct p*I*s of about 6.5, 7.2 and 8 (Table 3, spots 9–11). Two spots were identified from whole cell lysates (spots 9 and 10 in Table 3, Figs. 1B and 2) and one from nuclear extracts (spot 11 in Table 3, Figs. 1D and 2). For validation experiments, we concentrated on whole cell lysates in order to define the total spot composition rather than to address possible differences in subcellular distributions. According to the 2-D DIGE data, spot 9 was upregulated and spot 10 was downregulated by LPS treatment in wild-type cells (Table 3 and Fig. 5A). In the absence of Tyk2, spot 9 showed slightly elevated basal expression and reduced upregulation upon LPS treatment. In contrast, spot 10 was only modestly but conversely regulated by LPS in wild-type and Tyk2$^{-/-}$ cells resulting in a 1.9-fold higher level in Tyk2$^{-/-}$ cells as compared to stimulated wild-type cells (Table 3 and Fig. 5A). Surprisingly, we could not find an
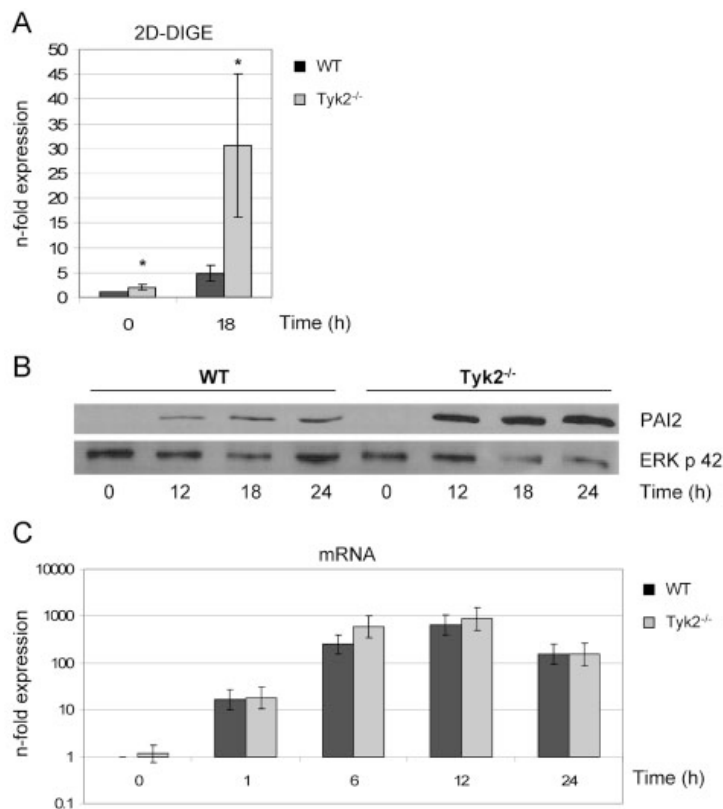
Figure 4. Effect of Tyk2 deficiency on the expression of PAI2 protein (A, B) and mRNA (C). Macrophages were treated with LPS for the indicated times and whole cell lysates or total RNA were subjected to 2-D DIGE analysis (A), Western blotting (B) or RT-qPCR (C). (A) 2-D DIGE: expression levels are given as fold ratios relative to unstimulated WT cells. Mean values ±SD of three biological replicates are shown. (B) Western blot analysis: 5 μg protein *per* lane were separated by 10%T SDS-PAGE. Protein loading was controlled by reprobing with an anti-panERK antibody. Data are representative of at least three independent experiments. (C) mRNA expression was analysed by RT-qPCR. *UBE2D2* was used as endogenous control, expression levels were calculated relative to untreated WT cells. Mean values ±SE from at least three independent experiments are depicted. * $p \leq 0.05$, ** $p \leq 0.01$.
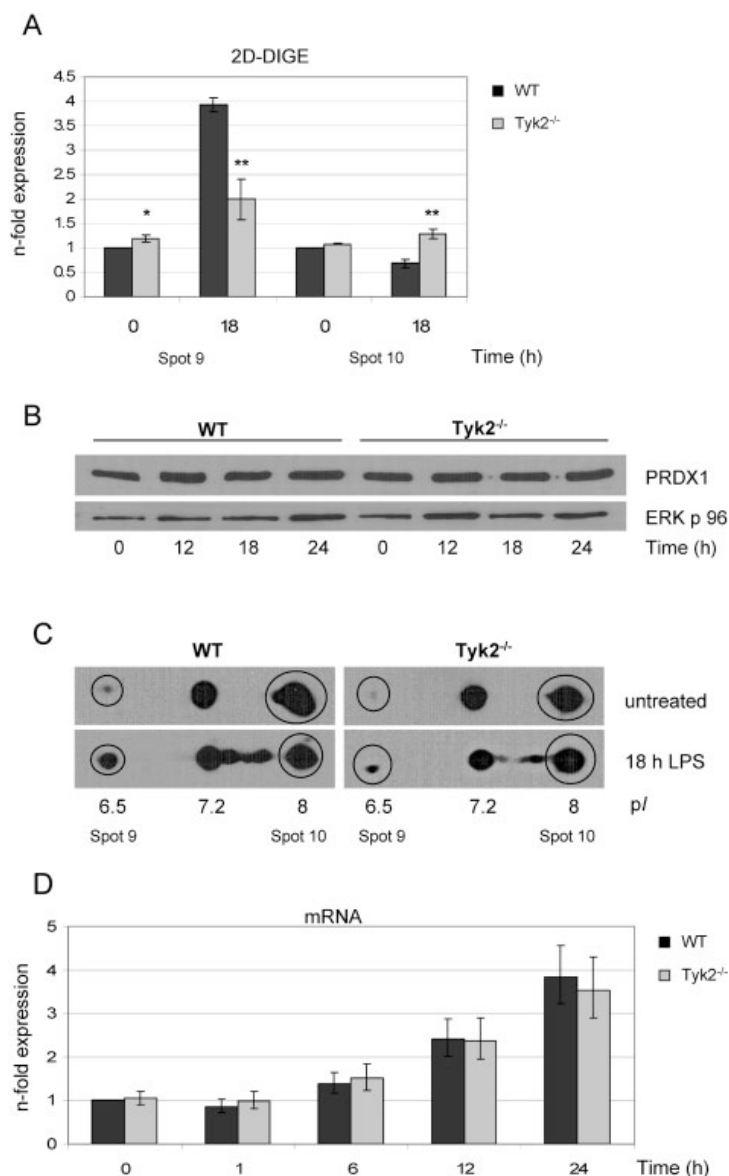
Figure 5. Effect of Tyk2 deficiency on the expression of PRDX1 protein (A–C) and mRNA (D). Macrophages were treated with LPS for the indicated times and whole cell lysates or total RNA were subjected to (A) 2-D DIGE analysis, (B, C) Western blotting or (D) RT-qPCR. (A) 2-D DIGE: expression levels are given as fold ratios relative to unstimulated WT cells. Mean values ±SD of three biological replicates are shown. (B) 1-D Western blot: 5 μg protein *per* lane were separated by 12%T SDS-PAGE. Protein loading was controlled by reprobing with an anti-panERK antibody. Data are representative of at least three experiments. (C) 2-D Western blot: 50 μg protein were separated by 2-DE using a pH 6–10 gradient for the first dimension, followed by the second dimension on a 12%T SDS-PAGE. Spots identified by MS are indicated in circles. Data are representative of three experiments. (D) mRNA expression was analysed by RT-qPCR. *UBE2D2* was used as endogenous control, expression levels were calculated relative to untreated WT cells. Mean values ±SE from three independent experiments are depicted. * $p \leq 0.05$, ** $p \leq 0.01$.

increase in total PRDX1 protein expression upon LPS treatment using 1-D Western blot analysis (Fig. 5B). Similarly, no difference in PRDX1 expression between wild-type and Tyk2$^{-/-}$ cells was detectable.

Figure 1B illustrates that PRDX1 is a multiple spot protein in 2-DE (spots 9 and 10), which all have a similar M_r, thus resulting in the detection of one single band on 1-D Western blots. To get more insight into the protein heterogeneity, we performed 2-D Western blot analysis to determine the number of detectable PRDX1 spots and their relative abundances. As shown in Fig. 5C, three spots were present before and five after LPS treatment in whole cell lysates from both genotypes. Consistent with the 2-D DIGE

data, spot 9 increased clearly after LPS treatment and this was considerably lower in Tyk2$^{-/-}$ than in wild-type cells. In contrast, differences in spot 10 intensities were not apparent. Apart from spots 9 and 10, one additional spot was detected in 2-D Western blot analysis in untreated cells (probably the counterpart of spot 11 identified in nuclear extracts, see Figs. 1B and D). Two further spots appeared upon LPS treatment (Fig. 5C), both with a more acidic p*I* than spot 10. As spot 9, both showed reduced increase in the absence of Tyk2. They were also calculated from 2-D DIGE data (Table 3 and data not shown) and results confirmed the partially Tyk2-dependent acidic spot shift. Although we could not see increased total PRDX1 protein (Fig. 5B) upon LPS treatment,

PRDX1 mRNA expression increased around four-fold with no differences between wild-type and Tyk2$^{-/-}$ cells (Fig. 5D). Thus, Tyk2 deficiency does neither influence total PRDX1 protein nor PRDX1 mRNA expression. Instead, our results indicate that Tyk2 influences the LPS-mediated changes in the PRDX1 spot pattern.

3.3.4 Tyk2 affects elongation factor 2 (EF2) subcellular levels

EF2 was found in nuclear extracts as differentially regulated spot with elevated amounts in Tyk2$^{-/-}$ macrophages independent of LPS treatment (spot 17 in Table 3, Figs. 1D, 2 and 6A). Enhanced expression of EF2 protein in the absence of Tyk2 was also readily detectable by Western blot analysis (Fig. 6B) and, also consistent with the 2-D DIGE data, LPS treatment did not result in any change of protein expression. Interestingly, differential EF2 protein expression between wild-type and Tyk2$^{-/-}$ cells was only found in nuclear extracts and not in whole cell lysates (Figs. 6B and C).

4 Discussion

In this report, we have used a proteomics approach in order to find novel functions of Tyk2 in the response to LPS in primary murine macrophages. Using 2-D DIGE technology for the comparative analysis of whole cell lysates as well as nuclear extracts from wild-type and Tyk2$^{-/-}$ cells, we achieved high reproducibility between biological replicates allowing us to detect differences in protein expression as low as 30%.

Proteomics studies on the LPS response of murine macrophages have been performed in a few older studies [22, 23, 41], but at that time 2-DE patterns were characterised solely by physicochemical properties of the obtained spots (pI, M_r). More recent studies including identification of intracellular LPS responsive proteins employed cell lines rather than primary cells and, in addition, used different comparative 2-DE approaches [42–44]. Accordingly, the sets of proteins identified show generally little overlap with ours. Interestingly, five of the proteins identified in our study (IFIT3, PRDX1, IRG1, vimentin and EF2) have also been described as LPS regulated in microglia cells, a macrophage-like cell type of the CNS [45].

Our results show that absence of Tyk2 significantly alters the overall protein expression pattern at basal conditions and affects changes in expression levels in response to LPS treatment, whereby the former effect predominates. We found 119 spots (corresponding to 3–6% of spots analysed) that showed at least 40% difference in expression values either before or after LPS treatment. We identified 21 different proteins in 25 of these spots which were either up- or downregulated in the absence of Tyk2. The proteins belong to several different functional categories suggesting that the absence of Tyk2 affects many distinct cellular processes. These include oxidative stress and immune response, metabolism, transcription, translation and cytoskeleton architecture.

All proteins involved in immune responses identified herein are known IFN regulated proteins. Consistent with the role of Tyk2 in IFN signalling, they showed reduced expression in the absence of Tyk2. Importantly, basal
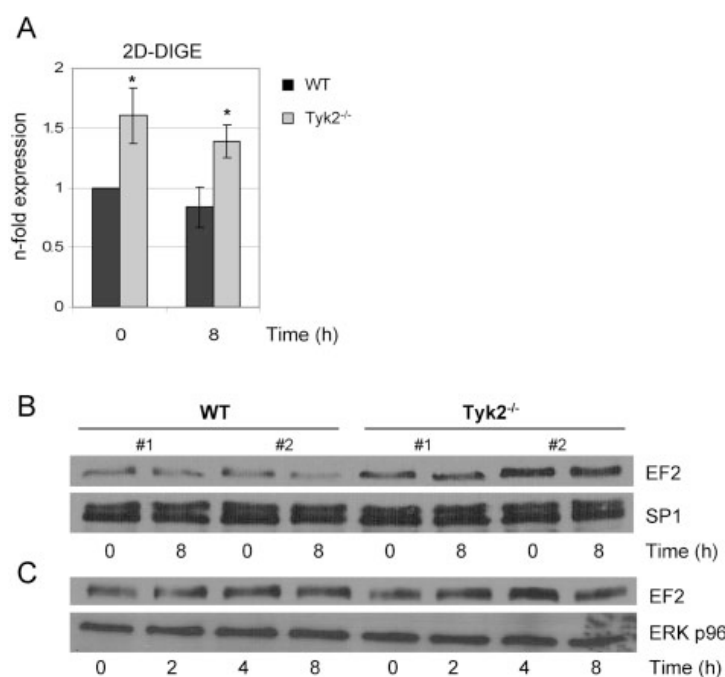
Figure 6. Effect of Tyk2 deficiency on the expression of EF2 protein. Macrophages were treated with LPS for the indicated times and nuclear extracts (A, B) or whole cell lysates (C) were subjected to DIGE analysis (A) or Western blotting (B, C). (A) 2-D DIGE: expression levels are given as fold ratios relative to unstimulated WT cells. Mean values ±SD of three biological replicates are shown. (B) Western blot analysis: 10 μg protein of nuclear extracts were separated by 6.5%T SDS-PAGE. Protein loading was controlled by reprobing with an anti-SP1 antibody. Nos. 1 and 2 indicate that the cells were derived from independent mice. (C) Western blot analysis: 5 μg protein of whole cell lysates were separated by 10%T SDS-PAGE. Protein loading was controlled by reprobing with an anti-panERK antibody. Data are representative of at least three independent experiments. * $p \leq 0.05$, ** $p \leq 0.01$.

expression was already reduced in the absence of Tyk2 in at least one of the spots identified, a phenomenon that has been described previously for two IFN-inducible proteins and some mRNAs [6, 8, 11]. Hence our data support the notion of Tyk2 as an essential component for the maintenance of low-level expression of at least a subset of IFN target proteins. Reduced basal expression of NMI in Tyk2$^{-/-}$ cells (approximately 0.6-fold according to the 2-D DIGE data) was confirmed by Western blot analysis and was also found at the mRNA level. NMI was originally found as a protein that interacts with members of the Myc family of proto-oncogenes [46] and subsequently interaction with several other transcription factors was reported. For example, NMI can interact with all STAT proteins (*e.g.* upon IL-2, IFNγ), except STAT2, and enhance their transcriptional activity by increasing their association with CREB-binding protein (CBP) and p300 co-activators [47]. NMI is homologous to IN35 and both proteins can stabilise each other through their interaction [48], thus crossinfluence might contribute to their similarly reduced expression levels in the absence of Tyk2.

We found several proteins differentially expressed in wild-type *versus* Tyk2$^{-/-}$ macrophages which have not yet been linked to either IFN or Tyk2 (Table 3). Three of them (EF2, PAI2 and PRDX1) were analysed in more detail. We found increased protein expression of EF2 in the absence of Tyk2 specifically in nuclear extracts but not in total lysates, suggesting a difference in subcellular localisation. Due to our relatively crude nuclear extract preparation, the exact localisation cannot be determined and further studies including highly purified organelle preparations will be required. EF2 is critically involved in protein translation where it catalyses elongation of polypeptide chains *via* promotion of ribosomal translocation. EF2 activity is inhibited by PTMs, *e.g. via* phosphorylation by the EF2 kinase [49], which itself is activated by phosphorylation *via* a number of different stimuli, *e.g.* cellular stress. However, we show by 1-D Western blot analysis differences in total EF2 protein levels in Tyk2$^{-/-}$ cells, thereby excluding a potential shift of spots in pI caused by phosphorylation as the sole cause of differential expression patterns found with 2-D DIGE technology.

Catalase and PRDX1 were identified as differentially expressed between wild-type and Tyk2$^{-/-}$ cells. Both enzymes are involved in the detoxification of hydrogen peroxide, which is produced as a result of normal cellular processes that involve oxygen and, importantly, in response to inflammatory stimuli including LPS [50, 51]. We show that although PRDX1 mRNA is modestly upregulated by LPS treatment an increase in PRDX1 protein is detectable neither by 1-D Western blot analysis nor by 2-D DIGE (by adding up spot volumes of all immunoreactive spots shown in Fig. 5C, data not shown). 2-DE reveals a noticeable change in the distribution of different PRDX1 spots, mainly a shift towards more acidic pI in response to LPS. Interestingly, the appearance of the spot with the lowest pI value was less prominent in the absence of Tyk2. Like the other members of the peroxiredoxin family, PRDX1 has a cysteine in its active site

which is reversibly oxidised to a disulfide in the normal catalytic cycle. It can also be hyperoxidised to sulphinic or sulphonic acid, which leads to inactivation of the enzyme [52]. Conway *et al.* [53] described three PRDX1 spots for the mouse macrophage cell line J774. In Western blots the authors proved that these spots correspond to the sulphonic, the sulphenic and the nonoxidised form of PRDX1 (from left to right in 2-DE pattern), and all were increased by chemical oxidation or by challenge with oxidised low density lipoprotein, without additional pattern changes. For human PRDX1, only doublet spots have been shown on 2-DE gels, a native form (basic spot) that shifts nearly completely to the over-oxidised form (acidic spot) upon strong oxidative stress [54, 55]. Although under basal conditions our PRDX1 patterns look similar to those reported for the murine cell line [53], the noticed shift towards lower pI values upon LPS treatment would suggest oxidation of the protein as shown for the human homologue. Our data would then further suggest that lack of Tyk2 results in the suppression of LPS induced (hyper)-oxidation of PRDX1. However, a shift in pI might also be caused by other modifications (*e.g.* phosphorylation). In that context, it is interesting to note that interaction of PRDX1 with the tyrosine kinase c-Abl has been reported [56]. In order to define the exact nature of the modification(s), further and more detailed MS analysis of all five spots seen in our PRDX1 pattern would be required (*e.g.* digest with a different enzyme, high energy CID or multistage CID experiments).

The most dramatic effect on protein expression with respect to differences between genotypes was found for PAI2. Consistent with previous reports [57], PAI2 protein was strongly upregulated by LPS treatment in wild-type cells. Expression of PAI2 was dramatically increased in the absence of Tyk2 as determined by 2-D DIGE and 1-D Western blots analysis. Interestingly, PAI2 mRNA was similarly induced in Tyk2$^{-/-}$ and wild-type cells. This points to the existence of a Tyk2 dependent negative regulatory pathway that limits LPS-induced PAI2 expression at a post-transcriptional level. PAI1 and PAI2 belong to the serpin gene family of protease inhibitors and are the physiological inhibitors of tissue- and urokinase-type plasminogen activator (tPA, uPA) [40]. Although the main proportion of newly synthesised PAI2 remains in the cell, the intracellular function of PAI2 is poorly characterised. There is evidence that PAI2 is involved in multiple cellular processes like proliferation, differentiation, and most consistently, apoptosis [40, 58]. Another important function of PAI2 is the inhibition of cancer metastasis and high PAI2 expression is associated with good prognosis in human cancers [40]. Recently, involvement of Tyk2 in tumour cell invasiveness has been reported [59, 60] and reduced uPA signalling was proposed as the underlying mechanism [59]. The fact that we find increased PAI2 expression in Tyk2$^{-/-}$ cells under inflammatory conditions (*i.e.* LPS treatment) poses the question of whether Tyk2 limits PAI2 expression also during tumour metastasis and whether this contributes to the reduced uPA signalling

described above. Also of relevance in this context is that activation of Tyk2 by uPA has been reported [61–63].

In summary, our data are in line with and further support the role of Tyk2 in the basal and LPS-induced, autocrine/paracrine actions of IFNα/β. We furthermore describe novel positive as well as negative regulatory roles of Tyk2 on protein expression in macrophages and demonstrate that this occurs both at the level of mRNA transcription and post-transcriptionally. As yet unrecognised connections between Tyk2 and diverse cellular proteins reported in this study raise interesting new topics for future research on Tyk2 biology.

5 References

[1] Darnell, J. E., Jr., Kerr, I. M., Stark, G. R., Jak-STAT pathways and transcriptional activation in response to IFNs and other extracellular signaling proteins. *Science* 1994, *264*, 1415–1421.

[2] O'Shea, J. J., Gadina, M., Schreiber, R. D., Cytokine signaling in 2002: New surprises in the Jak/Stat pathway. *Cell* 2002, *109*, S121–S131.

[3] Schindler, C., Cytokines and JAK-STAT signaling. *Exp. Cell Res.* 1999, *253*, 7–14.

[4] Kotenko, S. V., Pestka, S., Jak-Stat signal transduction pathway through the eyes of cytokine class II receptor complexes. *Oncogene* 2000, *19*, 2557–2565.

[5] Watford, W. T., Hissong, B. D., Bream, J. H., Kanno, Y. *et al.*, Signaling by IL-12 and IL-23 and the immunoregulatory roles of STAT4. *Immunol. Rev.* 2004, *202*, 139–156.

[6] Karaghiosoff, M., Neubauer, H., Lassnig, C., Kovarik, P. *et al.*, Partial impairment of cytokine responses in Tyk2-deficient mice. *Immunity* 2000, *13*, 549–560.

[7] Shimoda, K., Kato, K., Aoki, K., Matsuda, T. *et al.*, Tyk2 plays a restricted role in IFN alpha signaling, although it is required for IL-12-mediated T cell function. *Immunity* 2000, *13*, 561–571.

[8] Strobl, B., Bubic, I., Bruns, U., Steinborn, R. *et al.*, Novel functions of tyrosine kinase 2 in the antiviral defense against murine cytomegalovirus. *J. Immunol.* 2005, *175*, 4000–4008.

[9] Schleicher, U., Mattner, J., Blos, M., Schindler, H. *et al.*, Control of *Leishmania major* in the absence of Tyk2 kinase. *Eur. J. Immunol.* 2004, *34*, 519–529.

[10] Aizu, K., Li, W., Yajima, T., Arai, T. *et al.*, An important role of Tyk2 in APC function of dendritic cells for priming CD8+ T cells producing IFN-gamma. *Eur. J. Immunol.* 2006, *36*, 3060–3070.

[11] Karaghiosoff, M., Steinborn, R., Kovarik, P., Kriegshauser, G. *et al.*, Central role for type I interferons and Tyk2 in lipopolysaccharide-induced endotoxin shock. *Nat. Immunol.* 2003, *4*, 471–477.

[12] Costantino, G., Egerbacher, M., Kolbe, T., Karaghiosoff, M. *et al.*, Tyk2 and signal transducer and activator of transcription 1 contribute to intestinal I/R injury. *Shock* 2008, *2*, 238–44.

[13] Kamezaki, K., Shimoda, K., Numata, A., Matsuda, T. *et al.*, The role of Tyk2, Stat1 and Stat4 in LPS-induced endotoxin signals. *Int. Immunol.* 2004, *16*, 1173–1179.

[14] Beutler, B., Rietschel, E. T., Innate immune sensing and its roots: The story of endotoxin. *Nat. Rev. Immunol.* 2003, *3*, 169–176.

[15] Van Amersfoort, E. S., Van Berkel, T. J., Kuiper, J., Receptors, mediators, and mechanisms involved in bacterial sepsis and septic shock. *Clin. Microbiol. Rev.* 2003, *16*, 379–414.

[16] Honda, K., Taniguchi, T., IRFs: Master regulators of signalling by Toll-like receptors and cytosolic pattern-recognition receptors. *Nat. Rev. Immunol.* 2006, *6*, 644–658.

[17] Kawai, T., Akira, S., TLR signaling. *Cell Death Differ.* 2006, *13*, 816–825.

[18] Palsson-McDermott, E. M., O'Neill, L. A., Signal transduction by the lipopolysaccharide receptor, Toll-like receptor-4. *Immunology* 2004, *113*, 153–162.

[19] Chen, C., Boylan, M. T., Evans, C. A., Whetton, A. D. *et al.*, Application of two-dimensional difference gel electrophoresis to studying bone marrow macrophages and their in vivo responses to ionizing radiation. *J. Proteome Res.* 2005, *4*, 1371–1380.

[20] Tannenbaum, C. S., Nurmi-McKernan, L., Largen, M. T., Differential protein synthesis by murine peritoneal macrophages elicited by various stimuli. *J. Leukoc. Biol.* 1987, *41*, 527–538.

[21] Pereira, C. A., Lucchiari, M. A., Modolell, M., Kuhn, L. *et al.*, An attempt to identify gene products related to the induction of an antiviral state in macrophages resistant and sensitive to IFN-gamma. *Res. Virol.* 1993, *144*, 479–486.

[22] Largen, M. T., Tannenbaum, C. S., LPS regulation of specific protein synthesis in murine peritoneal macrophages. *J. Immunol.* 1986, *136*, 988–993.

[23] Hamilton, T. A., Jansen, M. M., Somers, S. D., Adams, D. O., Effects of bacterial lipopolysaccharide on protein synthesis in murine peritoneal macrophages: Relationship to activation for macrophage tumoricidal function. *J. Cell. Physiol.* 1986, *128*, 9–17.

[24] Baccarini, M., Bistoni, F., Lohmann-Matthes, M. L., In vitro natural cell-mediated cytotoxicity against *Candida albicans*: Macrophage precursors as effector cells. *J. Immunol.* 1985, *134*, 2658–2665.

[25] Schreiber, E., Matthias, P., Muller, M. M., Schaffner, W., Rapid detection of octamer binding proteins with 'mini-extracts', prepared from a small number of cells. *Nucleic Acids Res.* 1989, *17*, 6419.

[26] Bradford, M. M., A rapid and sensitive method for the quantitation of microgram quantities of protein utilizing the principle of protein-dye binding. *Anal. Biochem.* 1976, *72*, 248–254.

[27] Miller, I., Radwan, M., Strobl, B., Muller, M. *et al.*, Contribution of cell culture additives to the two-dimensional protein patterns of mouse macrophages. *Electrophoresis* 2006, *27*, 1626–1629.

[28] Laemmli, U. K., Cleavage of structural proteins during the assembly of the head of bacteriophage T4. *Nature* 1970, *227*, 680–685.

[29] Smyth, G. K., Linear models and empirical bayes methods for assessing differential expression in microarray experiments. *Stat. Appl. Genet. Mol. Biol.* 2004, *3*, Article 3.

[30] Miller, I., Gemeiner, M., Two-dimensional electrophoresis of cat sera: Protein identification by crossreacting antibodies against human serum proteins. *Electrophoresis* 1992, *13*, 450–453.

[31] Gharahdaghi, F., Weinberg, C. R., Meagher, D. A., Imai, B. S. *et al.*, Mass spectrometric identification of proteins from silver-stained polyacrylamide gel: A method for the removal of silver ions to enhance sensitivity. *Electrophoresis* 1999, *20*, 601–605.

[32] Shevchenko, A., Wilm, M., Vorm, O., Mann, M., Mass spectrometric sequencing of proteins silver-stained polyacrylamide gels. *Anal. Chem.* 1996, *68*, 850–858.

[33] Grunert, T., Pock, K., Buchacher, A., Allmaier, G., Selective solid-phase isolation of methionine-containing peptides and subsequent matrix-assisted laser desorption/ionisation mass spectrometric detection of methionine- and of methionine-sulfoxide-containing peptides. *Rapid Commun. Mass Spectrom*. 2003, *17*, 1815–1824.

[34] Smirnov, I. P., Zhu, X., Taylor, T., Huang, Y. *et al.*, Suppression of alpha-cyano-4-hydroxycinnamic acid matrix clusters and reduction of chemical noise in MALDI-TOF mass spectrometry. *Anal. Chem.* 2004, *76*, 2958–2965.

[35] Mattow, J., Schmidt, F., Hohenwarter, W., Siejak, F. *et al.*, Protein identification and tracking in two-dimensional electrophoretic gels by minimal protein identifiers. *Proteomics* 2004, *4*, 2927–2941.

[36] Perkins, D. N., Pappin, D. J., Creasy, D. M., Cottrell, J. S., Probability-based protein identification by searching sequence databases using mass spectrometry data. *Electrophoresis* 1999, *20*, 3551–3567.

[37] Zhang, W., Chait, B. T., ProFound: An expert system for protein identification using mass spectrometric peptide mapping information. *Anal. Chem.* 2000, *72*, 2482–2489.

[38] Focking, M., Boersema, P. J., O'Donoghue, N., Lubec, G. *et al.*, 2-D DIGE as a quantitative tool for investigating the HUPO Brain Proteome Project mouse series. *Proteomics* 2006, *6*, 4914–4931.

[39] Laboratory Manual, *Analytical Electrofocusing in Immobiline pH Gradients*, LKB Produkter AB, Bromma, Sweden 1986.

[40] Medcalf, R. L., Stasinopoulos, S. J., The undecided serpin. The ins and outs of plasminogen activator inhibitor type 2. *FEBS J.* 2005, *272*, 4858–4867.

[41] MacKay, R. J., Pace, J. L., Jarpe, M. A., Russell, S. W., Macrophage activation-associated proteins. Characterization of stimuli and conditions needed for expression of proteins 47b, 71/73, and 120. *J. Immunol.* 1989, *142*, 1639–1645.

[42] Zhang, X., Kuramitsu, Y., Fujimoto, M., Hayashi, E. *et al.*, Proteomic analysis of macrophages stimulated by lipopolysaccharide: Lipopolysaccharide inhibits the cleavage of nucleophosmin. *Electrophoresis* 2006, *27*, 1659–1668.

[43] Kovarova, H., Hajduch, M., Macela, A., Natural resistance to infection with intracellular pathogens: Cross-talk between Nramp1 and Lps genes. *Electrophoresis* 1997, *18*, 2654–2660.

[44] Dax, C. I., Lottspeich, F., Mullner, S., *In vitro* model system for the identification and characterization of proteins involved in inflammatory processes. *Electrophoresis* 1998, *19*, 1841–1847.

[45] Lund, S., Christensen, K. V., Hedtjarn, M., Mortensen, A. L. *et al.*, The dynamics of the LPS triggered inflammatory response of murine microglia under different culture and *in vivo* conditions. *J. Neuroimmunol.* 2006, *180*, 71–87.

[46] Bao, J., Zervos, A. S., Isolation and characterization of Nmi, a novel partner of Myc proteins. *Oncogene* 1996, *12*, 2171–2176.

[47] Zhu, M., John, S., Berg, M., Leonard, W. J., Functional association of Nmi with Stat5 and Stat1 in IL-2- and IFNgamma-mediated signaling. *Cell* 1999, *96*, 121–130.

[48] Chen, J., Shpall, R. L., Meyerdierks, A., Hagemeier, M. *et al.*, Interferon-inducible Myc/STAT-interacting protein Nmi associates with IFP 35 into a high molecular mass complex and inhibits proteasome-mediated degradation of IFP 35. *J. Biol. Chem.* 2000, *275*, 36278–36284.

[49] Jorgensen, R., Merrill, A. R., Andersen, G. R., The life and death of translation elongation factor 2. *Biochem. Soc. Trans.* 2006, *34*, 1–6.

[50] Forman, H. J., Torres, M., Reactive oxygen species and cell signaling: Respiratory burst in macrophage signaling. *Am. J. Respir. Crit. Care Med.* 2002, *166*, S4–S8.

[51] Wood, Z. A., Schroder, E., Robin Harris, J., Poole, L. B., Structure, mechanism and regulation of peroxiredoxins. *Trends Biochem. Sci.* 2003, *28*, 32–40.

[52] Rabilloud, T., Heller, M., Gasnier, F., Luche, S. *et al.*, Proteomics analysis of cellular response to oxidative stress. Evidence for *in vivo* overoxidation of peroxiredoxins at their active site. *J. Biol. Chem.* 2002, *277*, 19396–19401.

[53] Conway, J. P., Kinter, M., Dual role of peroxiredoxin I in macrophage-derived foam cells. *J. Biol. Chem.* 2006, *281*, 27991–28001.

[54] Wagner, E., Luche, S., Penna, L., Chevallet, M. *et al.*, A method for detection of overoxidation of cysteines: Peroxiredoxins are oxidized *in vivo* at the active-site cysteine during oxidative stress. *Biochem. J.* 2002, *366*, 777–785.

[55] Chevallet, M., Wagner, E., Luche, S., van Dorsselaer, A. *et al.*, Regeneration of peroxiredoxins during recovery after oxidative stress: Only some overoxidized peroxiredoxins can be reduced during recovery after oxidative stress. *J. Biol. Chem.* 2003, *278*, 37146–37153.

[56] Wen, S. T., Van Etten, R. A., The PAG gene product, a stress-induced protein with antioxidant properties, is an Abl SH3-binding protein and a physiological inhibitor of c-Abl tyrosine kinase activity. *Genes Dev.* 1997, *11*, 2456–2467.

[57] Costelloe, E. O., Stacey, K. J., Antalis, T. M., Hume, D. A., Regulation of the plasminogen activator inhibitor-2 (PAI-2) gene in murine macrophages. Demonstration of a novel pattern of responsiveness to bacterial endotoxin. *J. Leukoc. Biol.* 1999, *66*, 172–182.

[58] Park, J. M., Greten, F. R., Wong, A., Westrick, R. J. *et al.*, Signaling pathways and genes that inhibit pathogen-induced macrophage apoptosis-CREB and NF-kappaB as key regulators. *Immunity* 2005, *23*, 319–329.

[59] Ide, H., Nakagawa, T., Terado, Y., Kamiyama, Y. *et al.*, Tyk2 expression and its signaling enhances the invasiveness of prostate cancer cells. *Biochem. Biophys. Res. Commun.* 2008, *369*, 292–296.

[60] Schuster, C., Muller, M., Freissmuth, M., Sexl, V. *et al.*, Commentary on H. Ide *et al.*, 'Tyk2 expression and its signaling enhances the invasiveness of prostate cancer cells'. *Biochem. Biophys. Res. Commun.* 2008, *366*, 869–870.

[61] Patecki, M., von Schaewen, M., Tkachuk, S., Jerke, U. *et al.*, Tyk2 mediates effects of urokinase on human vascular smooth muscle cell growth. *Biochem. Biophys. Res. Commun.* 2007, *359*, 679–684.

[62] Dumler, I., Kopmann, A., Weis, A., Mayboroda, O. A. *et al.*, Urokinase activates the Jak/Stat signal transduction pathway in human vascular endothelial cells. *Arterioscler. Thromb. Vasc. Biol.* 1999, *19*, 290–297.

[63] Dumler, I., Weis, A., Mayboroda, O. A., Maasch, C. *et al.*, The Jak/Stat pathway and urokinase receptor signaling in human aortic vascular smooth muscle cells. *J. Biol. Chem.* 1998, *273*, 315–321.

PROTEOMICS

Supporting Information
for Proteomics
DOI 10.1002/pmic.200800260

Marta Radwan, Ingrid Miller, Tom Grunert, Martina Marchetti-Deschmann, Claus Vogl, Niaobh O'Donoghue, Michael J. Dunn, Thomas Kolbe, Günter Allmaier, Manfred Gemeiner, Mathias Müller and Birgit Strobl

The impact of tyrosine kinase 2 (Tyk2) on the proteome of murine macrophages and their response to lipopolysaccharide (LPS)

Figure S1
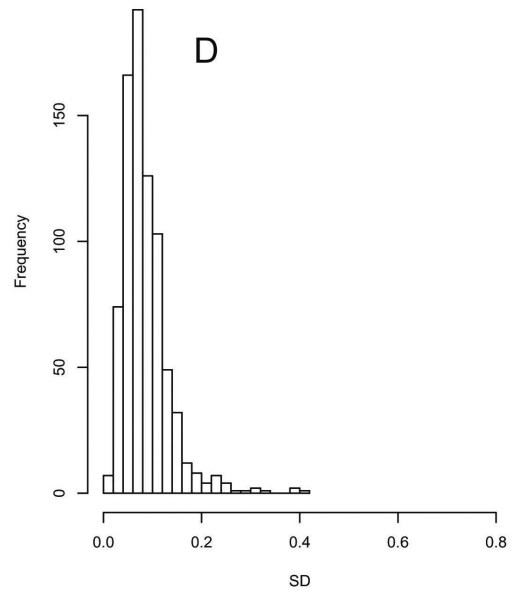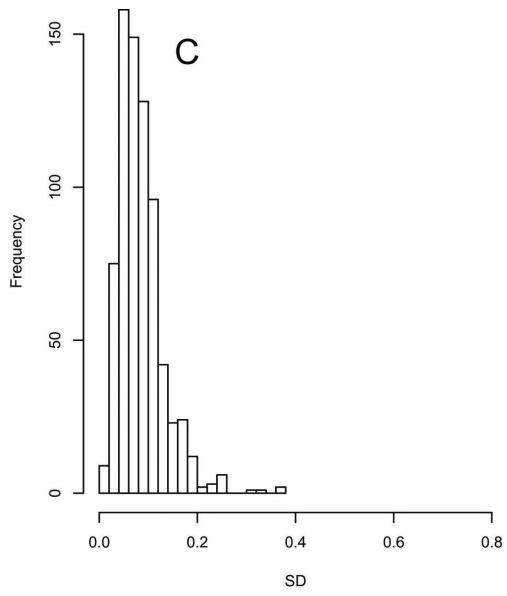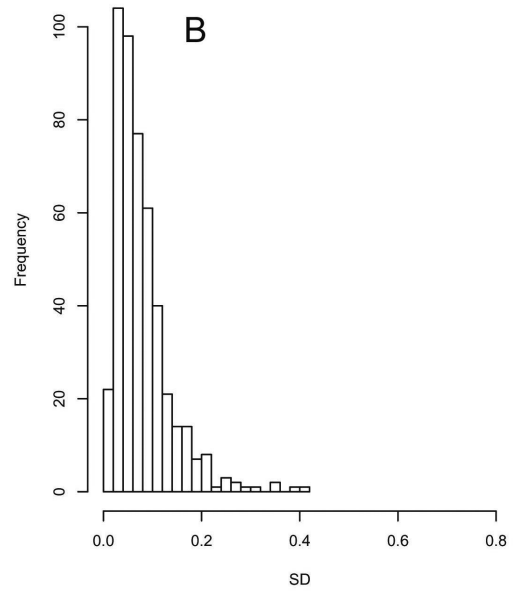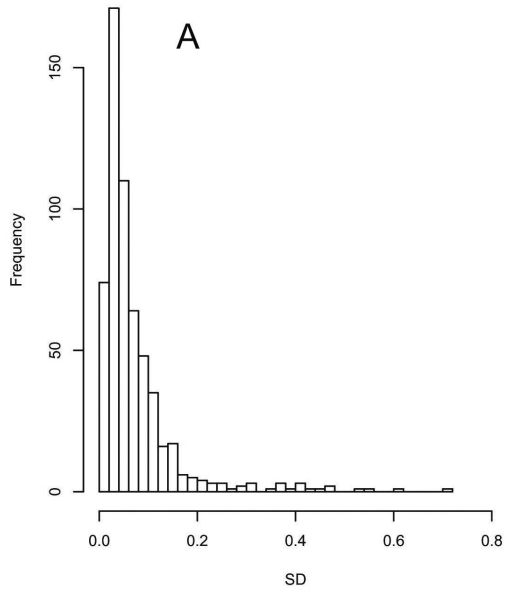
A
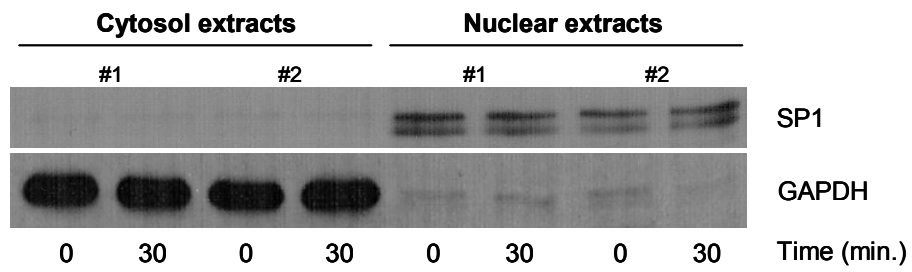
B
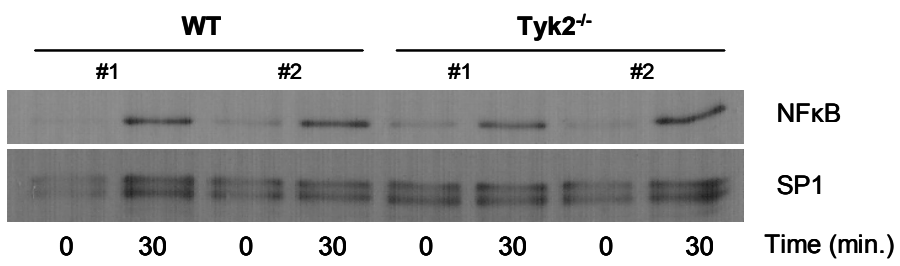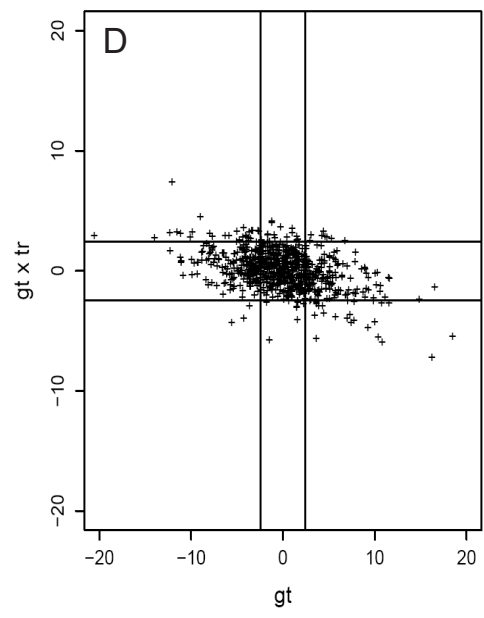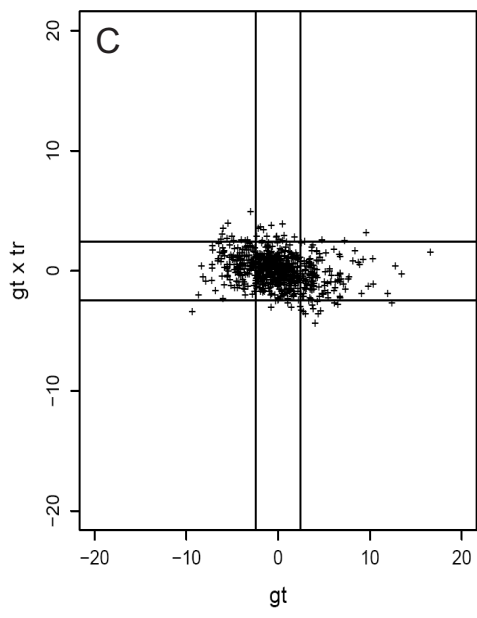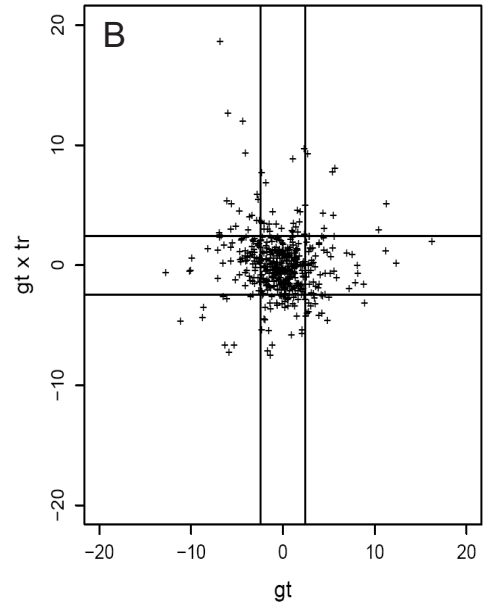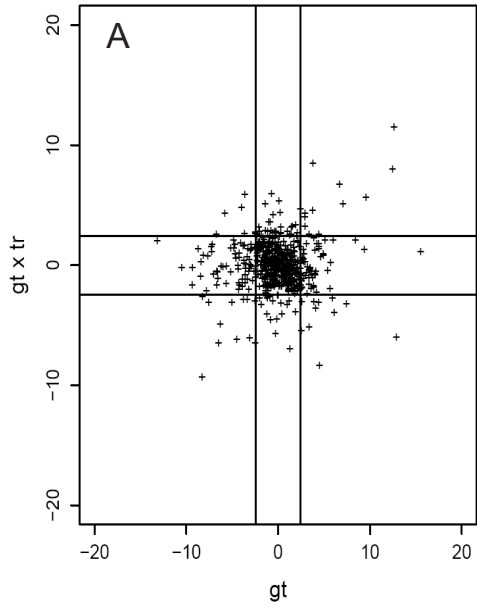
Figure S3

Supplements

Figure S1. 2D-DIGE data are highly reproducible. Histograms show the frequency distribution of SD values over the experiments performed. The SD of spot volume ratios from three biological replicates was calculated for each spot and was plotted against frequencies. (A) whole cell lysates pH 4-7 (n=579 spots), (B) whole cell lysates pH 6-9 (n=478 spots), (C) nuclear extracts pH 4-7 (n=731 spots), (D) nuclear extracts pH 6-9 (n=792 spots).

Figure S2. (A) Nuclear extracts show reproducible enrichment of nuclear proteins. Macrophages were treated with LPS for 30 minutes. 3 µg of nuclear or cytosolic extracts per lane were separated by 8%T SDS-PAGE. GAPDH was used as a cytosolic and SP1 as a nuclear marker. Data are representative of at least three experiments. (B) Translocation of NF-κB is unperturbed in Tyk2$^{-/-}$ macrophages. Macrophages were treated with LPS for 30 minutes. 3 µg of nuclear extract *per* lane were separated by 8%T SDS-PAGE. Protein loading was controlled by re-probing with an anti-SP1 antibody. #1 and #2 indicate that the cells were derived from independent mice.

Figure S3. Tyk2 deficiency significantly alters the proteome pattern of macrophages. The t-values of the genotype effect (*gt*) are plotted against the t-values of the genotype x treatment effect (*gt x tr*). Data include all spots (found in all images) without filtering for minimal differences in the expression values. Values above and below the critical t-values ± 2.306 (indicated by lines) are considered to be significant. Positive t-values indicate decreased and negative t-values increased expression / induction levels in the absence of Tyk2. (A) whole cell lysates pH 4-7 (n=579 spots), (B) whole cell lysates pH 6-9 (n=478 spots), (C) nuclear extracts pH 4-7 (n=731 spots), (D) nuclear extracts pH 6-9 (n=792 spots).

Table S1. Differentially expressed proteins in Tyk2$^{-/-}$ macrophages - detailed MS data.

	Differentially expressed proteins				MS Method	Peptide Mass Fingerprint				Sequencing		
Spot #	Protein Name / Function	Accession #	M$_r$ (kDa)	pI		Probability based MOWSE Score	Sequ. Cov.	Matched peptides	# of peptides for protein ID	Probability based MOWSE Score	Precursor Ion(s) m/z (observed) and charge state [a]	Peptide Sequence(s)
		Swissprot	theor.	theor.			%	matched/ unmatched				
1	Proteasome activator complex subunit 1 (PSME1)	P97371	28.7	5.7	ESI		28		6	237	684.3++ 873.7+++ 853.08+++ 810.32+++ 760.33++ 621.76++	VDVFREDLCSK, VDVFREDLCSKTENLLGSYFPK, KISELDAFLKEPALNEANLSNLK, ISELDAFLKEPALNEANLSNLK, IEDGNNFGVAVQEK, YFSERGDAVAK
2	Interferon-induced protein with tetratripeptide repeats 3 (IFIT3)	Q64345	47.2	5.5	ESI		11		6	164	563.179++ 604.2+ 557.204++ 641.719++ 660.23++	LSEAQAYVDK, QVCQK, APNQTDVLQK, YCNLQEYHR, SIEKEEVKEQT
3	N-myc-interactor (NMI)	O35309	35.2	5	ESI		4		1	36	763.24++	NGGGEVESVDYDRK,
					MALDI	84	30	6/2	2	100	1800.85+ 1921.88+	INVTGIPDELSEEQTR, CSLLDQSFAAYFKEEAR

#	Protein name	Accession										Peptides
4	Interferon-induced protein with tetratripeptide repeats 1 (IFIT1)	Q64282	53.7	7.2	MALDI	21	6	2/2	2	162	1687.07+ 1944.15+	LLFENNDIPDLEVR, GENADGDQVMENLLQLR [b]
5	Interferon-induced protein with tetratripeptide repeats 1 (IFIT1)	Q64282	53.7	7.2	MALDI	147	32	13/4	2	83	1686.88+ 1943.93+	LLFENNDIPDLEVR, GENADGDQVMENLLQLR [b]
6	Interferon-induced protein 35kD homolog (IN35)	Q9D8C4	31.8	5.6	MALDI	58	17	4/2	2	181	756.48+ 2007.18+	QQVLLR; SVTLQTVLYSLQEEQAR [b]
7	Interferon-activable protein 205 (IFI5)	Q08619	47	8.4	MALDI	59	6	4/0	2	60	613.41+ 1181.61+	IVLLR, SQPQNQNIPR
	or Interferon-activable protein 204 (IFI4)	P15092	71.6	9		51	4	4/0	2	60	613.41+ 1181.61+	IVLLR, SQPQNQNIPR
8	Interferon-activable protein 205 (IFI5)	Q08619	47	8.4	MALDI	59	6	4/0	3	101	613.41+ 759.47+ 1181.61+	IVLLR, DLNLER, SQPQNQNIPR
	or Interferon-activable protein 204 (IFI4)	P15092	71.6	9		51	4	4/0	3	101	613.41+ 759.47+ 1181.61 +	IVLLR, DLNLER, SQPQNQNIPR
9	Peroxiredoxin-1 (PRDX1)	P35700	22.2	8.3	MALDI	112	28	7/3	2	124	1225.67+ 1359.81+	QITINDLPVGR, GLFIIDDKGILR
10	Peroxiredoxin-1 (PRDX1)	P35700	22.2	8.3	MALDI	153	41	9/2	2	99	831.46+ 1225.69+	SVDEIIR, QITINDLPVGR
11	Peroxiredoxin-1 (PRDX1)	P35700	22.2	8.3	MALDI	60	20	4/3	2	55	1225.67+ 1359.81+	QITINDLPVGR, GLFIIDDKGILR
12	Catalase (CATA)	P24270	59.8	7.7	MALDI	308	50	26/7	2	100	962.54+ 1276.63+	DAQLFIQK, LAQEDPDYGLR
13	Plasminogen activator inhibitor 2 (PAI2)	P12388	46.3	5	MALDI	70	15	7/5	2	105	1284.87+ 1698.07+	FKEEYIQLSK, VLQFNEIGSYGITTR

#	Protein	Accession	MW	pI	Method	Score	Coverage		Number	m/z		Peptides
14	3-ketoacyl-CoA thiolase A (THIKA)	Q921H8	44	8.7	MALDI	165	44	14/6	2	1379.84+ 2042.12+	212	AEELGLPILGVLR, IAQFLSGIPETVPLSTVNR
	3-ketoacyl-CoA thiolase B (THIKB)	Q8VCH0				65	22	7/13	2	1379.84+ 2042.12+	212	AEELGLPILGVLR, IAQFLSGIPETVPLSTVNR
15	Purine nucleoside phosphorylase (PNPH)	P23492	32.2	5.8	ESI		59		16	935.5++ 907.3+++ 1360.6+++ 681.34+++ 718.4+ 840.96+++ 587.34++ 787.86++ 1221.14++ 814.36+++ 1157.1++ 958.93++ 1125.6+ 563.3++ 1239.62++ 620.3++ 593.32++ 1184.48++ 808.81++ 881.35++	769	MENEFTYEDYETTAK, EAQIFDYNEIPNFPQSTVQGHAGR, EAQIFDYNEIPNFPQSTVQGHAGR, FHMYEGYSLSK, VTFPVR, DHINLPGFCGQNPLR, FPAMSDAYDR, FPAMSDAYDRDMR, KLQEGTYVMLAGPNFETVAESR, KLQEGTYVMLAGPNFETVAESR, LQEGTYVMLAGPNFETVAESR, MLGADAVGMSTVPEVIVAR, VFGFSLITNK, VFGFSLITNK, VVMDYENLEK, VVMDYENLEK, ANHMEVLDAGK, ANHMEVLDAGK, FVSILMESIPLPDR, FVSILMESIPLPDRGS
16	Argininosuccinate synthase (ASSY)	P16460	46.6	8.4	MALDI	117	19	10/2	2	858.47+ 999.55+	89	IDIVENR, RQVEIAQR
17	Elongation Factor 2 (EF2)	P58252	95.3	6.4	MALDI	172	21	16/1	1	1091.64+	43	VNFTVDQIR
18	Phenylalanyl-tRNA-synthase beta chain (SYFB)	Q9WUA2	65.7	6.7	MALDI	57	7	5/2	3	744.46+ 921.47+ 1198.71+	117	LTELLR, TAEFQVAR, VRPFAVAAVLR
19	Staphylococcal nuclease domain-containing protein 1 (SND1)	Q78PY7	102.1	7.1	MALDI	170	17	18/5	3	757.34+ 786.29+ 957.51+	96	AGNLARR, FFTESR, QINLSNIR
20	Vimentin (VIME)	P20152	53.7	5.1	MALDI	124	24	11/4	1	1587.92+	72	TNEKVELQELNDR

21	F-actin capping protein subunit alpha-1 (CAZA1)	P47753	32.9	5.3	MALDI	162	40	11/4	2	155	1197.72+ 2089.02+	LLLNNDNLLR, FITHAPPGEFNEVFNDVR
22	F-actin capping protein subunit beta (CAPZB)	P47757	31.3	5.5	MALDI	133	32	8/0	2	53	786.46+ 1108.64+	DIVNGLR, RLPPQQIEK
23	Adenyl cyclase-associated protein 1 (CAP1)	P40124	51.6	7.2	MALDI	110	21	9/4	2	55	1515.74+ 1958.08+	ADMQNLVERLER [b] LGLVFDDVVGIVEIINS
24	EF-hand domain containing protein 2 (EFHD2)	Q9D8Y0	26.8	5	MALDI	83	21	7/1	3	137	755.37+ 937.53+ 973.54+	NFFEAK, EFLLIFR, VQAINVSSR
25	Immune-responsive protein 1 (IRG1)	P54987	53.8	7.1	MALDI	126	30	12/12	2	64	1168.63+ 1852.97+	ALFPADHIER, RFHPPSVVGTLGSAAAASK

a) Monoisotopic; + singly; ++ doubly and +++ triply charged peptide

b) Acetylation at protein N-terminus

3. Comparing the applicability of CGE-on-the chip and SDS-PAGE for fast pre-screening of mouse serum samples prior to proteomics analysis

Tom Grunert[1,2,3]*
Martina
Marchetti-Deschmann[1]*
Ingrid Miller[4]
Mathias Müller[2,3]
Günter Allmaier[1]

[1]Institute of Chemical
 Technologies and Analytics,
 Vienna University of
 Technology, Vienna, Austria
[2]Institute of Animal Breeding and
 Genetics, Veterinary University
 of Vienna, Vienna, Austria
[3]University Centre Biomodels
 Austria, Veterinary University of
 Vienna, Vienna, Austria
[4]Institute of Medical Chemistry,
 Veterinary University of Vienna,
 Vienna, Austria

Research Article

Comparing the applicability of CGE-on-the-chip and SDS-PAGE for fast pre-screening of mouse serum samples prior to proteomics analysis

In this comparative study, a set of 13 mouse sera was investigated, which had to be checked in a fast way for homogeneity prior to complex, time-consuming and expensive proteomics analysis. SDS-PAGE and CGE-on-the-chip were compared in terms of handling, time consumption and significance of detecting differences. SDS-PAGE was a system giving good information on the samples at first sight and discrepancies for one sample were observed immediately after staining. The time consumption of up to 20 h was rather high (separation and staining procedure with 14 × 14 cm gels) in SDS-PAGE. CGE-on-the-chip system exhibited differences for two samples and, most important, analysis time was reduced to only 1 h. Of importance is that the serum protein pattern obtained by both methods may not represent the same proteins. Sample preparation was equal for both analytical techniques but necessary sample amount was only half of the material in the case of CGE-on-the-chip. Statistical evaluation indicated highly critical values for only one sample in SDS-PAGE and for two samples in the CGE-on-the-chip system, both in good agreement with visual observations. Three samples showed limited homogeneity with both methods. Five and six samples, respectively, were indicated as noticeable with one of the used methods.

1 Introduction

Mouse models increase our understanding of human physiology, particularly immunology and cancer biology. Effects on protein expression and alteration due to genetic modification or physiological stimulus are increasingly studied using complex proteomic tools such as 2-DE or multi-dimensional liquid chromatography coupled to MS [1–4]. Serum presents an easily accessible source to gain information about the *in vivo* status of the living organism. But serum samples themselves are of high complexity and comprise a wide dynamic range for the concentration of proteins. For example the concentration range of albumin in human serum is 34–54 mg/mL (approx. 60%) of 60–83 mg/mL total protein concentration; thus it represents

a so-called high-abundance protein [5, 6]. In contrast to serum albumin, interleukin 6 is present only in very low concentrations, up to 5 pg/mL (0.000000007%) during the acute phase of inflammation and is therefore considered as low-abundance or low-copy protein. Overall it can be said that the range of serum protein concentrations can vary by ten orders of magnitude [7, 8]. It is important to note that only a few proteins occur at higher concentrations, but the diversity of proteins increases significantly for low-abundant proteins [9]. Currently widespread proteomic strategies and tools for investigation of serum samples enable the identification of proteins at sensitivity limits of 10^{-7}–10^{-8} M under certain conditions [9]. For the detection of known proteins, sensitivities down to 10^{-9}–10^{-14} M in plasma can be achieved utilizing very specific methods, *e.g.* enzyme-linked immunosorbent assay [7] or electrochemical nano-wire detectors used for serum and cell extracts [10].

By using these complex strategies and highly sophisticated analytical instrumentation it seems, at the first glance, to marginalize the importance of sample preparation itself and the control of sample quality at the very first beginning of the analytical process. Thus, knowledge about the

Correspondence: Dr. Martina Marchetti-Deschmann, Institute of Chemical Technologies and Analytics, Vienna University of Technology, Getreidemarkt 9/164-IAC, A-1060 Vienna, Austria
E-mail: martina.marchetti@tuwien.ac.at
Fax: +43-1-58801-15199

Abbreviations: IQR, interquartile range; M_r, molecular weight

*Both authors contributed equally to the paper.

number, relative concentrations of proteins or, generally spoken, the distribution of the various constituents of a well-defined and constant starting biomaterial is substantial for a successful analysis. It is a well-known but also under-estimated fact that sample preparation and handling play a crucial role for subsequent protein identification and relative or absolute quantification [11]. In a worst case scenario inhomogeneous serum samples (*e.g.* incomplete clotting, proteolysis) or samples that have been reanalysed (*e.g.* alteration during storage) without checking the initial state can lead to wrong data resulting in false theories about biological correlations. Therefore a fast pre-screening evaluation of almost unprocessed serum samples prior to applying any proteomics strategy (*e.g.* measuring protein differential expressions using 2-DE and MS) is advisable. This can be done by evaluating protein patterns of high-abundance serum proteins (only they can be analysed reliably enough) by using fast and easy-to-handle methods optimally with a high throughput method. Although these methods may exhibit only protein profiling of lower resolution, they may already show major differences in the starting serum material due to technical and biological variations. These variations are key factors that have to be considered during experimental design to provide statistically significant results in subsequent quantitative proteomics [12]. Factors of biological variance are mainly mouse strains, age, sex, animal keeping conditions and feeding/nutrition [13]. Blood-collection procedures (tail vein, cardiac or orbital sinus puncture), use of anaesthetics, serum preparation (type of clot activation, centrifugation speed and duration, separation of serum from cells) and storage conditions (temperature, freeze–thaw cycles) were recognized as important factors of technical variance for serum samples [14–18]. Both biological and technical influences affect the starting quality of serum samples independent of any prior biological or pharmacological manipulation. The use of reference materials for calibration, control and traceability can help to improve reproducibility and strengthen comparisons between experiments and laboratories but are useless if the sample has already decomposed during storage [16].

In this study, the suitability of two methods for fast low-resolution protein profiling was evaluated. A CGE-on-the-chip (lab-on-the-chip) system with an LIF detector was compared with the well-established 1-D planar gel electrophoretic method, SDS-PAGE, to indicate the quality of serum samples by evaluating the protein pattern of high-abundant serum proteins before complex proteomics studies are started. Thirteen different mouse sera were collected from healthy mice with the same genetic background, sex and age to reduce the biological variation of the sera. Blood-taking procedure, serum preparation and storage were standardized for all samples in order to minimize technical variabilities from this side. CGE-on-the-chip was selected because of potential advantages compared with previously used techniques such as small-scale SDS-PAGE, size exclusion chromatography and MS [19, 20] including

minimal sample and test reagent requirement, ease of use, short analysis time, high reproducibility and automated data analysis as well as the potential of a high throughput system [21].

2 Materials and methods

All chemicals were of analytical grade except otherwise stated. Serum samples were obtained from 13 male, weight-matched, 7–8-week-old C57BL/6 mice (Biomodels, Vienna, Austria) and collected in three different batches (three days); batch 1: mice 1–6, batch 2: mice 7–12 and batch 3: mouse 13. Blood was drawn from tail veins directly into serum tubes (Sarstedt Microvette 500, Nümbrecht, Germany) and was allowed to clot at room temperature for 1 h; it was subsequently centrifuged at 4°C for 10 min at $9.300 \times g$ (Eppendorf, Hamburg, Germany) and stored at −80°C until analysis. All animal experiments were carried out in accordance with protocols approved by institutional ethics committee, the Austrian laws (GZ 68.205/67-BrGT/2003) and European Directives.

SDS-PAGE was performed according to Laemmli [22] on gels of $140 \times 140 \times 1.5$ mm (separation: %T = 10–15, %C = 2.7) in a Hoefer SE 600 vertical electrophoresis chamber (Hoefer Scientific Instruments, San Francisco, CA, USA). Freshly thawn serum samples were diluted by a factor of 10 with 0.9% NaCl solution; 5 μL (= 0.5 μL undiluted serum) of the diluted solution were mixed with 5 μL Laemmli sample buffer containing 0.02 mg/mL DTT, reduced for 10 min at 95°C, and 5 μL glycerine (75%) were added. In total 15 μL were loaded onto each lane (= 0.5 μL undiluted serum). After electrophoresis, proteins were stained overnight with 0.05% CBB R-250 in 14% TCA in water/methanol (70/30 v/v). Background was decreased by washing with ethanol/acetic acid/water (30/10/60 v/v/v and 5/7/88 v/v/v, 2 h each). Gels were scanned (JX-330 flatbed scanner, Sharp, Osaka, Japan) using the software Quantity One version 2.7 (PDI, Huntington Station, NY, USA). Images were qualitatively and quantitatively evaluated using ImageMaster^TM TotalLab software (GE Healthcare Life Sciences, Munich, Germany) applying manual lane detection (half lane width 13 pixels), automatic background subtraction (valley-to-valley) and manual peak detection. For molecular weight (M_r) calibration a protein marker (LMW-SDS Marker, GE Healthcare Life Sciences) was used.

CGE-on-the-chip separations were performed on the Agilent 2100 Bioanalyzer System (Agilent Technologies, Waldbronn, Germany) using the Protein 80 Kit (Agilent Technologies). All CGE-on-the-chips were prepared according to the manufacturer's instructions. Briefly, 2 μL of mouse serum were diluted with 30 μL water; 4 μL (= 0.25 μL undiluted serum) were mixed with 2 μL of the provided sample buffer including 0.0052 mg/mL DTT. Sample buffer contains a low (1.6 kDa) and a high (95 kDa) M_r protein used for internal calibration. The solution was heated for 5 min (95°C) and further diluted with 84 μL

water; 6 µL of the final sample were pipetted into the designated sample well on the CGE-chip and electrokinetically injected (= 0.017 µL undiluted serum). For M_r sizing a protein ladder (= well-defined proteins, Agilent Technologies kit) was treated in the same way. Peak detection, quantification and qualitative analysis were performed manually (valley-to-valley integration) using the Protein assay software 2100 expert (Version B.02.02.SI238). Statistical evaluation of all data was performed using SPSS Version 14.0 (SPSS, Chicago, IL, USA).

3 Results and discussion

In SDS-PAGE the electrophoretic mobility of each protein molecule is interfered with by the molecular sieving matrix, a networked structure of polyacrylamide/bis-acrylamide, resulting in different migration distances on the gel. The M_r of separated proteins is determined after visualization using the linear correlation between the relative migration distance and the logarithm of M_r. Contrary to SDS-PAGE in CGE-on-the-chip a fluorescence dye is added to the protein sample forming a protein-dodecyl sulphate-dye complex, which is subsequently analysed in a channel containing a linear sieving polymer and finally detected by a laser-induced fluorescence unit. Obtained migration times are used for M_r sizing based on well-defined external and internal protein standards [20, 21, 23].

Under reducing conditions most of the abundant serum proteins are expected to be present in the lower M_r range since many of these proteins consist of more than one subunit covalently linked by disulphide bridges, which are destroyed during sample preparation. Possible differences in the serum protein pattern, indicating adulterated sample material, are therefore expected in an M_r range between 10 and 100 kDa. The chosen gel composition for SDS-PAGE (%T 10–15) compromises a sufficient resolution for these proteins but also shows additionally bands above 100 kDa. The separation gel performs very well for proteins between 14.4 and 97 kDa, determined by the chosen M_r marker. Therefore further analysis was restricted to that specific mass range. The CGE-on-the-chip protein 80 kit is dedicated to the separation of proteins between 5 and 80 kDa. Although both methods were not compared in exactly the same M_r range, the general applicability of the investigated systems could be studied, as the M_r ranges exhibited good performances for each system within its well-defined M_r range (determined by the M_r markers) and cover the M_r range most important for the mouse serum proteome.

The first overview of the serum composition was obtained by comparing the protein pattern of mouse serum samples directly on the SDS-PA gel and by arranging the electropherograms of the CGE-on-the-chip system in a simulated gel-like image (Fig. 1). Tracing the sample quality of more than one sample requires a more detailed analysis including the relative quantification for each band/peak and
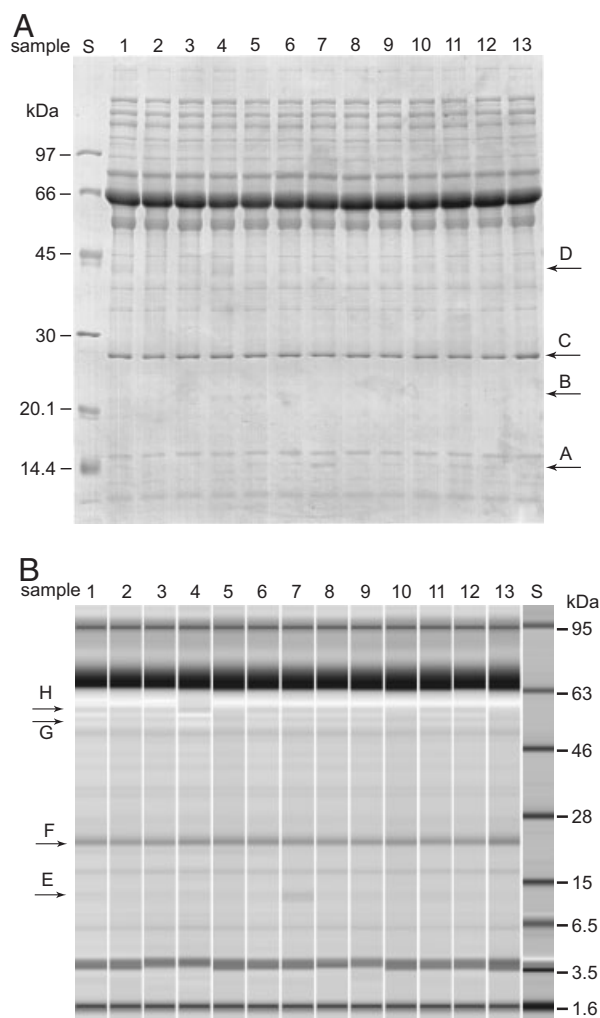
Figure 1. Image of SDS-PAGE and gel-like image (CGE-on-the-chip) obtained from 13 different mouse serum samples under reducing conditions. Differences in protein peak pattern are assigned with an arrow (A) SDS-PAGE: arrow A – samples 7 and 11, arrow B – samples 4 and 5, arrow C – sample 13 and arrow D – samples 1 and 4; (B) CGE-on-the-chip: arrow E – samples 7 and 11, arrow F – sample 13, arrow G – samples 4, 5, 10, 13 and arrow H – sample 4; S, M_r standard proteins (kDa).

measuring variations by comparing protein band volumes or peak areas, expressed by relative abundances. The relative abundance of each signal was calculated as a percentage of the sum of all selected protein bands/peaks. Usually the SD is used to describe the dispersion within data sets. Because the aim is the comparison of SDs across a broad range of relative abundances, the use of the CV is required. Data interpretation using these classic statistical methods without data transformation is based on the assumption of normal distribution, which is unknown for the specific data set. Therefore the more reliable method "box plot" was applied. Box plots are less affected from extremes and without any predisposed statistical distribution [24]. In box plots the mean value is replaced by the median and the length of the box is equivalent to the interquartile range (IQR) and

represents the middle 50% of the ranked data. Whiskers (vertical line with small horizontal line) indicate the range of the data which are not more than $1.5 \times$ IQR away from both ends of the box. All values above $\pm 1.5 \times$ IQR are extreme values or outliers. Data marked with an open circle (°) range between $1.5 \times$ IQR and $3 \times$ IQR and are close extreme values. Far away extreme values are marked with an asterisk (∗) and exceed $3 \times$ IQR.

3.1 SDS-PAGE

After visualizing protein bands with CBB on the SDS-PAGE a first overview of the protein composition of each sample was obtained by comparing protein pattern between the 13 serum samples directly on the gel (Fig. 1A) without the assistance of software. A particularly remarkable difference, namely a quite abundant band, was observed at 14 kDa for sample 7, assigned with arrow A in Fig. 1A. Alteration in protein pattern at the same M_r was also found for sample 11. At 21 kDa (arrow B) a prominent band was observed in samples 4 and 5 and the protein bands at 27 kDa (arrow C) in sample 13 and at 44 kDa (arrow D) in samples 1 and 4 seemed to be more intense than in the other mouse serum samples. Visually observed differences between all 13 mouse serum samples directly after staining on the gel were therefore limited to four protein bands: 14, 21, 27 and 44 kDa.

For a more exact analysis, the corresponding signals of the CBB-stained protein bands were densitometrically determined and exemplarily one analysis is shown for sample 1 in Fig. 2A. The densitograms of all serum samples contained 13 well-defined protein bands between 97 and 14.4 kDa of which the average M_r was calculated.

In total the obtained protein pattern showed one very intensive band (65 kDa) and three bands of medium intensity (27, 57, 76 kDa). All other peaks were of lower intensity with an S/N of 3–5 except for the protein band at 21 kDa where S/N was below 2 for most of the samples. However this protein band was included in the examination based on already recognized differences by eye for samples 4 and 5 on the gel (Fig. 1A, arrow B).

Relative abundances of the protein bands were determined as the percentages of volumes of each band *versus* total volume of all analysed 13 protein bands. The volume of a densitometrically detected protein band is defined as the peak area of a band, displayed by the number of pixels, multiplied with the intensity, reflecting the concentration of the protein at that specific point, of each pixel. The average relative abundance for each protein band was calculated for all 13 serum samples (Table 1a) and relative abundances between 0.52 and 67% were observed. On the basis of these analyses protein bands could be classified into three groups: one protein band with 67%, three above and nine protein bands below 2% of relative abundance.

The variation of relative abundances composed of technical and biological variation of each protein band was determined and expressed by the CV as described above. The CVs for the selected protein bands were between 5 and 57%. Reasons for high CVs can be one or more extreme value(s) or a high variation of all values. To estimate the reliability of the SDS-PAGE for serum samples the technical variation for the system was evaluated using two independent samples. Average CVs of 7.06% (intra-gel comparison) and 12.83% (inter-gel comparison) were found comparing relative abundances and an average CV of 1.46% was calculated for the overall sizing reproducibility (for details see Supporting Information data). For the protein bands at 14, 21 and 44 kDa differences were already observed on the gel without the help of software and exhibited CVs > 40% after statistical evaluation. For these cases the box plot showed the distribution of the 13 serum samples for each protein band (Fig. 2C). A far away extreme value was found for the protein band at 14 kDa in sample 7. This confirmed the first finding of a visually observable discrepancy in the protein pattern at that position on the gel. All other values for this protein band are in a range of variation of $\pm 1.5 \times$ IQR, interestingly also sample 11, which was first considered as an outlier. For the protein band at 21 kDa, sample 5 showed a close extreme value that was already recognized by visual examination (Fig. 1C; arrow B). Despite similar visually observed band intensities for samples 4 and 5 a close extreme or even extreme value could not be observed for sample 4 as it was assumed before statistical analysis. However the second highest value was calculated for sample 4, represented by the upper whisker in the box plot diagram. This is supposed to be a result of the chosen band width for evaluation, which was not identical with the actual lane width to avoid errors for relative protein quantification due to randomized edge effects. In contrast to the gel view no extreme value was determined for the protein band at 27 kDa where evidence of a more intense band was recognized for sample 13. It was represented in the box plot diagram by the upper whisker and therefore still in the range of variation of $\pm 1.5 \times$ IQR. At 44 kDa the assumed outliers for samples 1 and 4 could be verified with the box plot analysis. Both samples were marked as close extreme values. A noticeable low CV of 5%, far below the expected overall biological variance, was found for the highest abundant protein band at 65 kDa. This is due to the statistic correlation derived from the formula for the CV ((SD/mean of relative abundance) $\times$ 100) and the fact that the calculated values for SDs do not increase in the same degree as mean values of relative abundances.

Statistical evaluation of each single protein band within the 13 mouse sera confirmed conclusions drawn after visual examination of the SDS-PAGE except for sample 4 at 21 kDa and sample 13 at 27 kDa, which were not statistically marked as outliers. In addition extreme values were found in the box plot diagram at 15 kDa for sample 6, at 35 kDa for sample 4, at 48 kDa for sample 3, at 76 kDa for samples 6, 7, 9 and 10 and at 84 kDa for sample 7.
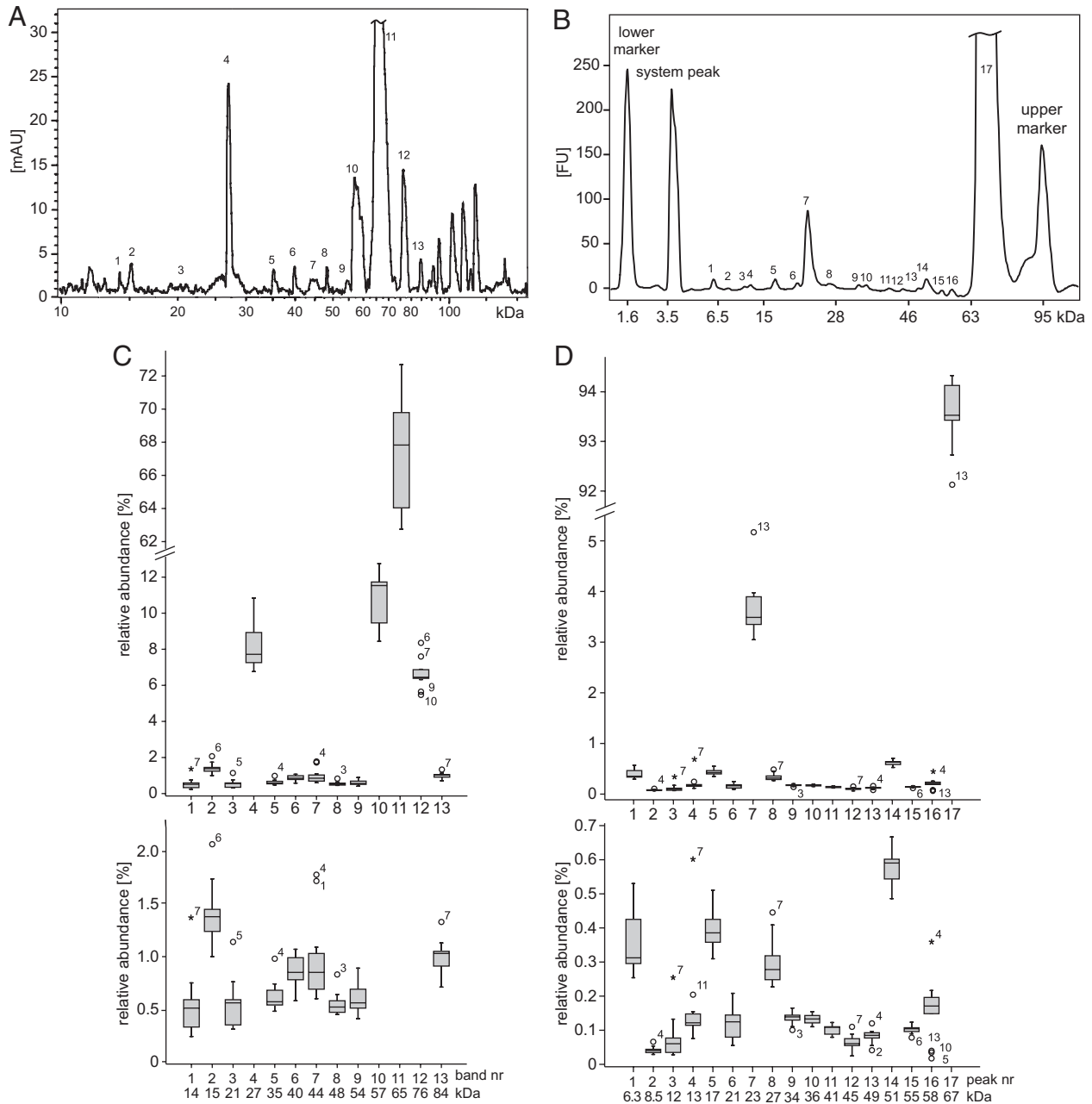
Figure 2. Comparison of the peak profile of serum sample 1. (A) Densitogram obtained from SDS-PAGE (AU, absorbance units) and (B) electropherogram obtained from the CGE-on-the-chip (FU, fluorescence units) each assigned with the corresponding peak numbers used throughout the discussion. (Peak numbers of (A) and (B) are independent). Box plot diagrams show the distribution of the relative abundances of each band/peak of 13 mouse serum samples for the (C) SDS-PAGE and the (D) CGE-on-the-chip system. Numbers alongside the extreme values indicate sample numbers.

3.2 CGE-on-the-chip

CGE-on-the-chip allows the analysis of a maximum of ten samples on one single chip. As for SDS-PAGE the technical variation of the system was investigated using two independent samples. Average CVs of 5.96% (intra-chip) and 11.14% (inter-chip) were calculated. The overall sizing reproducibility was even better (CV of 0.53%, for details see

Supporting Information data). The very good inter-chip reproducibility allows the comparison of the 13 mouse serum samples even run on two different chips. A so called "gel-like" image allows the visualization of the raw data, electropherograms (Fig. 2B), in a way comparable to well-accepted SDS-PAGE images. As an internal M_r standard for every single analysis, an upper and lower M_r marker protein of defined concentration is added to the sample buffer to

Table 1. Summarized statistics of each selected protein band/peak of (a) SDS-PAGE and (b) CGE-on-the-chip

(a)

Band	Retardation factor (Rf) mean	M_r mean (kDa)	Band volume mean	Relative abundance mean (%)	SD of relative abundances (%)	CV (%)
1	0.87	14	468	0.52	0.30	57
2	0.84	15	1264	1.4	0.28	20
3	0.73	21	492	0.58	0.23	41
4	0.64	27	7375	8.2	1.2	15
5	0.54	35	562	0.63	0.14	22
6	0.50	40	780	0.86	0.14	17
7	0.46	44	849	0.95	0.39	41
8	0.43	48	494	0.55	0.10	19
9	0.39	54	539	0.60	0.14	24
10	0.37	57	9808	11	1.5	14
11	0.33	65	61 022	67	3.4	5.0
12	0.27	76	5971	6.6	0.73	11
13	0.23	84	901	1.0	0.16	16

(b)

Peak	Aligned migration time mean (s)	M_r mean (kDa)	Peak area mean	Relative abundance mean (%)	SD (%)	CV (%)
1	19.7	6.3	6.0	0.36	0.090	25
2	20.8	8.5	0.7	0.041	0.010	24
3	22.1	12	1.3	0.076	0.061	80
4	22.5	13	2.7	0.16	0.14	84
5	24.4	17	6.5	0.39	0.057	14
6	26.2	21	2.0	0.12	0.053	44
7	26.9	23	60	3.6	0.54	15
8	28.7	27	5.0	0.30	0.071	23
9	30.9	34	2.2	0.14	0.017	12
10	31.4	36	2.2	0.13	0.014	10
11	33.2	41	1.7	0.10	0.014	14
12	34.3	45	1.1	0.065	0.021	33
13	35.5	49	1.4	0.082	0.019	23
14	36.1	51	9.6	0.58	0.054	9.4
15	37.3	55	1.7	0.10	0.013	12
16	38.0	58	2.6	0.16	0.090	57
17	40.1	67	1546	94	0.66	0.7

allow M_r determination independent of even small migration variations (this is in contrast to standard SDS-PAGE). In case of the complex serum samples, an overlapping of the signals of the M_r marker with some serum components was observed (Fig. 2B) but the determination of the molecular weights of the serum components was not interfered because of sufficient intensity and therefore distinct peak maximum of the upper marker. In total 17 distinct protein signals between 5 and 80 kDa were found. At this point it has to be mentioned that protein signals beyond 67 kDa, clearly detected by SDS-PAGE, are in some cases hardly detectable on the CGE-on-the-chip system as the signal of the high-abundance protein at 67 kDa superimposes them. In addition the high concentration of this protein influences the migration behaviour of the low-abundance proteins in the capillary resulting therefore in altered migration times and sometimes co-migration of these proteins with the internal calibrant at 95 kDa. To eliminate interpretation

uncertainties concerning peak number, peak shape or resolution, all probably arising from irregular overloading of the capillary system, dilution experiments with water were performed with one exemplary sample. No significant changes in peak pattern and relative peak intensities were observed, leading to the conclusion that the sample amount did not influence the overall CGE-on-the-chip analyses. At first sight differences in the protein pattern were recognized at approx. 12 kDa in samples 7 (abundant new protein was detected) and 11 (Fig. 1B; arrow E), at 23 kDa (variations in protein abundance) in sample 13 (Fig. 1B, arrow F), at approx. 58 kDa in samples 4, 5, 10 and 13 (Fig. 1B; arrow G) and at approx. 60 kDa in sample 4 (Fig. 1B; arrow H). The overall peak pattern (Fig. 2B) showed one very intensive peak at 67 kDa, one peak of medium intensity at 23 kDa and 15 peaks with at least an S/N of 3; 7 out of 17 protein peaks were baseline separated compared with 13 out of 13 protein bands on the SDS-PAGE after densitometry. Peaks were

manually integrated and the relative abundance of each peak was calculated based on peak area *versus* the total area of all 17 peaks (Table 1b). Based on these calculations relative abundances in the range of 0.04% to 94% were observed (Table 1b) and the peaks could be classified into three groups: one protein peak with 94%, one protein peak with 3.6% and 15 protein peaks below 1% relative abundance.

The variation of relative abundances was in the range between 0.7 and 84%. CVs above 40% were observed for peaks at M_r 12, 13, 21 and 58 kDa. The CV of 40% was chosen because it represents obvious outliers in SDS-PAGE. However on the gel-like image of the CGE-on-the-chip system the signal at 21 kDa (CV 44%) seemed to be inconspicuous. Box plot diagrams (Fig. 2D) showed far away extreme values at 12 and 13 kDa for sample 7 and one close extreme value for sample 11 at 13 kDa confirming the first findings. Interestingly the protein peak at 21 kDa with a CV of 44% did not show extreme values in the box plot diagram pointing out a possibly broader distribution of all individual data. Actually individual data can be divided into two groups according to their biological origin: group 1 containing samples 1–6 (batch 1) and group 2 with samples 7–12 (batch 2). A highly significant variation was determined, estimated by Student's 2-tail test (*t*-test) for independent samples ($p<0.001$) and a 2.3-fold increase between batches 2 and 1. Additionally a significant variation between batches 2 and 1 could be identified on the CGE-on-the-chip system for peak 7 at 23 kDa (1.1-fold increase, $p = 0.012$). Relative abundances of mouse sera grouped in batches 1 and 2 also showed in SDS-PAGE for the bands at 21 kDa (1.8-fold, $p = 0.02$), 27 kDa (1.2-fold, $p = 0.0002$), 57 kDa (1.3-fold, $p = 0.001$) and 65 kDa (1.1-fold, $p = 0.003$) a significant statistical variation between batches 2 and 1. On the basis of these results in retrospect both methods showed slight differences at 21 kDa between samples 1– 6 (batch 1) and samples 7–12 (batch 2) (Fig. 1A and B).

For sample 13 one close extreme value at 23 kDa confirmed the first result observed. Sample 4 showed one far away extreme value at 58 kDa, three close extreme values were found for samples 5, 10 and 13 at the same M_r. At approx. 46 kDa a descending detector signal was observed in all electropherograms dropping sometimes below the zero line. This effect can be observed in the gel-like view as a white region (Fig. 1B, arrows G and H). Nevertheless significant peaks, as 51, 55 and 58 kDa, were found and further interpreted. As an additional effect it was observed that serum albumin (60% of the total protein content) tends to give rise to an instrumental artefact also expressed by a decreasing baseline negatively influencing the resolution in the discussed mass range [25]. The close extreme values in the box plot diagram for samples 5, 10 and 13 at 58 kDa can be explained by very low protein concentrations and therefore very small peaks adjacent to that very abundant serum albumin. Peak integration became difficult and maybe less precise. Similar to the observation at the SDS-PAGE a very low CV (0.7%) for the highest-abundant protein at 67 kDa was observed.

Summarized, visible variations on the gel-like image (CGE-on-the-chip) for protein peaks at 12 kDa for sample 7, at 13 kDa for samples 7 and 11, at 23 kDa for sample 13 and at 58 kDa for samples 4, 5, 10 and 13 were nicely corresponding to extreme values in the box plot diagram. Additionally extreme values were found in box plot diagram at 8.5 kDa for sample 4, at 27 kDa for sample 7, at 34 kDa for sample 3, at 5 kDa for sample 7, at 49 kDa for samples 2 and 4, at 55 kDa for sample 6 and at 67 kDa for sample 13.

3.3 Comparison of SDS-PAGE and CGE-on-the-chip

SDS-PAGE and CGE-on-the-chip are based on a similar separation principle, but on different detection principles resulting in different relative band/peak intensity patterns [26]. Therefore it is important to mention that band/peak numbers, their corresponding M_r and the signal/band intensities obtained from SDS-PAGE and CGE-on-the-chip are not directly comparable. Nevertheless both methods were used to compare the specific protein peak pattern of 13 serum samples, which were then evaluated using box plot diagrams reflecting therefore the total (biological and technical) variation of the pre-screening experiment. But from our data for serum samples we can conclude that the technical variation of both systems, expressed by CVs for sizing accuracy and relative peak intensities (CVs < 15%), is far below those values considered to be alarming (CV > 40%). Based on the two levels of extreme values, close and far away extreme value generated in the box plot analysis, mouse serum samples were divided into the following groups: (i) far away extreme values: sample 7 (SDS-PAGE) and samples 4 and 7 (CGE-on-the-chip), (ii) close extreme values: samples 1, 3, 4, 5, 6, 7, 9 and 10 (SDS-PAGE) and 2, 3, 4, 5, 6, 7, 10, 11 and 13 (CGE-on-the-chip) (Fig. 2C and D) and (iii) in conspicuous data: samples 2, 8, 11, 12 and 13 (SDS-PAGE) and, 8, 9 and 12 (CGE-on-the-chip). In case of sample 13 initially recognized differences on the gel and gel-like image were only seen in the box plot diagram of CGE-on-the-chip (Fig. 2D). The value found for sample 13 in SDS-PAGE was in fact the highest measured value of all 13 samples, but still below the inner fence of $1.5 \times IQR$. Based on the statistical evaluation for both systems, 7 out of 13 samples were detected as extreme values, whereupon 6 samples were marked as noticeable with both analytical methods. Samples 4, 6 and 7 exhibited more than one extreme value in SDS-PAGE and samples 4, 7 and 13 in the CGE-on-the-chip system. Sample 7 showed the highest number of extreme values in both methods (SDS-PAGE: 3; CGE-on-the-chip: 4). A rather poor sample quality compared with the other serum samples can be supposed for sample 7 justified by this cross-correlated information. However such samples, showing several extreme values, should not be eliminated in the pre-screening process itself as they may represent part of a significant biological population. Only the knowledge of particular reasons (*e.g.* instrumental malfunction, technical

reasons from pre-analytical steps and well-known artefacts from sample preparation) would allow the deletion of these data from the set. Otherwise, samples should be marked as extremes but have to be still processed and reconsidered if they would shift the subsequently obtained result to an important biological or medical implication [24, 27]. In our case we know from ongoing studies including mass spectrometric protein identification after in-gel digestion that far extreme values assigned to samples 4 and 7 may be explained by haemolysis. Haemolysis can either be explained by a sample preparation error that is readily observed only if it exceeds a certain extent (sample turns slightly reddish). So haemolysis can easily be overlooked as the red colour is not always observable in yellowish samples making a pre-screening, as we present within these data, indispensable. On the other hand, haemolysis also arises from certain diseases corroborating our approach not to eliminate the affected samples on all accounts but to mark them as peculiar.

In multi-component mixtures with a wide dynamic range (*e.g.* high- and low-abundance proteins), the calculation of relative abundances of single bands or peaks gives rise to systematic errors. Since relative abundances are reliant on each other, a small change in the value of the very abundant component shifts the values of other low-abundant constituents to a great extent. Statistical data transformation (*e.g.* using square or cubic root or logarithmic transformation) before calculating the relative abundance based on the sum of all selected protein bands/peaks would be an alternative handling of the original data (in this case volume and area) avoiding overemphasis of a dominant peak. Another possibility would be the simple multiplication of original data of high-abundant proteins with an empirical factor [28]. But an empirical factor is a critical issue to figure out for biological samples as certain knowledge about the material has to be available. Subtraction of the mean value after data transformation (*e.g.* square root transformation) would terminate the dependency of the data, but an exact amount of sample applied to the analysis is indispensable since fluctuating protein concentrations would result in wrong extreme values and CVs. This can be achieved by using exactly the same sample volume and the exact total protein concentration. Besides these statistical problems one has to consider that sample inherent protein signals are not qualified for this kind of study because it requires an unvaried protein composition. Typically used internal standards for quantification cannot be applied since a peak overlap of sample and standard proteins occurs.

Comparing instrumental parameters and sample characteristics the optimal absolute protein amount (18 µg total protein) required for the CGE-on-the-chip system was only half of the amount necessary for SDS-PAGE; sizing reproducibility was much better for the capillary system but the reproducibility for the relative peak abundances were comparable. The absolute limit of detection is much lower, but the sample amount cannot be further reduced, since too much information concerning low-abundance proteins might get lost (S/N < 3). On the other hand increasing sample amount to gain more information on these specific peaks has a bad influence on migration behaviour (SDS-PAGE: forming of micelles during sample handling, streaking and inhomogeneous conductivity across the gel; CGE-on-the-chip: indistinct peaks for low and/or upper M_r marker, baseline drift or late migration). A compromise must be found for gathering maximum information and technical drawbacks of the chosen system.

Time consumption for sample preparation itself, manual peak assignment and data examination accounts for both methods equally. All serum samples have to be reduced and heated in a sample buffer system before analysis and after analysis data have to be evaluated statistically. The most obvious difference in time-consumption is the analysis run time itself. For one chip, containing up to ten samples, only 30 min including protein separation, staining and detection are required. For 13 samples, two chips were required resulting in 1 h total analysis time. The protocol for SDS-PAGE, as it was used in this study, consisted of protein separation (approx. 4 h), staining (overnight) and scanning (15 min) procedure, resulting in a total time of approx. 20 h without gel casting. Or 4.5 h taking only the separation and scanning into account as staining procedures can be significantly shortened (*e.g.* heat mediated Coomassie staining). In the latter case all 13 samples could be run at the same time. Fewer reagents for the CGE-on-the-chip method compared with the SDS-PAGE protocol were necessary and are beneficial in environmental terms.

4 Concluding remarks

Pre-screening of serum samples is essential prior to complex proteomic analysis to achieve valuable biological data. A good sample control has to be available particularly for samples prone to technical artefacts like samples of body fluids, pre-fractionated samples or samples with inherent proteolytic activity. Having a fast and easy-to-handle analytical method to evaluate the starting material establishes the possibility of delving into suspect samples. The presented study shows that SDS-PAGE and CGE-on-the-chip are both suitable pre-screening methods for serum samples to identify possible outliers or samples that have to be considered during the proceeding proteomics study within a comprehensive sample pool and both are useful for optimizing analytical strategies when conclusions have to be drawn solely from protein pattern without any knowledge of the separated proteins. Besides identical time consumption for sample preparation and final data evaluation, the sample requirement was only half for the CGE-on-the-chip system, the technical variation in terms of sizing reproducibility was much better and the absolute time needed for analysis was considerably reduced in case of CGE-on-the-chip compared with SDS-PAGE. Comparing serum samples based on the obtained images, differences appear more clearly on SDS-PAGE than on the gel-like image. Considering the statistical

evaluation of the serum samples the CGE-on-the-chip system is a faster and more stringent system (two samples were marked as problematic) with a lower technical variation than SDS-PAGE.

5 References

[1] Hood, B. L., Zhou, M., Chan, K. C., Lucas, D. A. *et al.*, *J. Proteome Res.* 2005, *4*, 1561–1568.

[2] Griffin, J. L., *Curr. Opin. Chem. Biol.* 2006, *10*, 309–315.

[3] Righetti, P. G., Castagna, A., Antonucci, F., Piubelli, C. *et al.*, *J. Chromatogr. A* 2004, *1051*, 3–17.

[4] Liu, H., Lin, D., Yates 3rd, J. R., *Biotechniques* 2002, *32*, 898–911.

[5] A.D.A.M. *Medical Encyclopedia* 2005, updated September 19, 2007. http://www.nlm.nih.gov/medlineplus/ency/ article/003480.htm.

[6] A.D.A.M. *Medical Encyclopedia* 2005, updated September 19, 2007. http://www.nlm.nih.gov/medlineplus/ency/ article/003483.htm.

[7] Anderson, N. L., Anderson, N. G., *Mol. Cell. Proteomics* 2002, *1*, 845–867.

[8] Jacobs, J. M., Adkins, J. N., Qian, W. J., Liu, T. *et al.*, *J. Proteome Res.* 2005, *4*, 1073–1085.

[9] Archakov, A. I., Ivanov, Y. D., Lisitsa, A. V., Zgoda, V. G., *Proteomics* 2007, *7*, 4–9.

[10] Zheng, G., Patolsky, F., Cui, Y., Wang, W. U., Lieber, C. M., *Nat. Biotechnol.* 2005, *23*, 1294–1301.

[11] Skoog, D. A., Holler, F. J., Crouch, S. R. *Principles of Instrumental Analysis*, Thomson Learning, London 2006.

[12] Molloy, M. P., Brzezinski, E. E., Hang, J., McDowell, M. T., VanBogelen, R. A., *Proteomics* 2003, *3*, 1912–1919.

[13] Gaines Das, R. E., *Ilar J.* 2002, *43*, 214–222.

[14] Van Herck, H., Baumans, V., Brandt, C. J., Boere, H. A. *et al.*, *Lab. Anim.* 2001, *35*, 131–139.

[15] West-Nielsen, M., Hogdall, E. V., Marchiori, E., Hogdall, C. K. *et al.*, *Anal. Chem.* 2005, *77*, 5114–5123.

[16] Rai, A. J., Gelfand, C. A., Haywood, B. C., Warunek, D. J. *et al.*, *Proteomics* 2005, *5*, 3262–3277.

[17] Hsieh, S. Y., Chen, R. K., Pan, Y. H., Lee, H. L., *Proteomics* 2006, *6*, 3189–3198.

[18] Ferguson, R. E., Hochstrasser, D. F., Banks, R. E., *Proteomics Clin. Appl.* 2007, *1*, 739–746.

[19] Scherberich, J. E., Fischer, P., Bigalke, A., Stangl, P. *et al.*, *Electrophoresis* 1989, *10*, 58–62.

[20] Goetz, H., Kuschel, M., Wulff, T., Sauber, C. *et al.*, *J. Biochem. Biophys. Methods* 2004, *60*, 281–293.

[21] Kuschel, M., Neumann, T., Barthmaier, P., Kratzmeier, M., *J. Biomol. Techniques* 2002, *13*, 172–178.

[22] Laemmli, U. K., *Nature* 1970, *227*, 680–685.

[23] Bousse, L., Mouradian, S., Minalla, A., Yee, H. *et al.*, *Anal. Chem.* 2001, *73*, 1207–1212.

[24] Massart, D. L., Smeyers-Verbeke, J., Capron, X., Schlesier, K., *LC-GC Europe* 2005, *18*, 215–218.

[25] Deasai, S., Barthmaier, P., *Agilent Technologies Application Note* 2003, *59*, 5988-9911EN.

[26] Anonymous, Agilent *Technologies Application Note* 2001, 5988-3160EN.

[27] Burke, S., *LC-GC Europe Online Supplement* 2002, *59*, 19–24.

[28] Nelsestuen, G. L., Zhang, Y., Martinez, M. B., Key, N. S. *et al.*, *Proteomics* 2005, *5*, 4012–4024.

Supplementary Information

Comparing the applicability of CGE-on-the-chip and SDS-PAGE for fast pre-

screening of mouse serum samples prior to proteomics analysis

Tom Grunert[1-3*], Martina Marchetti[1*#], Ingrid Miller[4], Mathias Müller[2,3], Günter

Allmaier[1]

[1] *Institute of Chemical Technologies and Analytics, Vienna University of Technology, Vienna, Austria*

[2] *Institute of Animal Breeding and Genetics, Veterinary University of Vienna, Vienna, Austria*

[3] *University Centre Biomodels Austria, Veterinary University of Vienna, Vienna, Austria*

[4] *Institute of Medical Chemistry, Veterinary University of Vienna, Vienna, Austria*

[*] Both authors contributed equally to the paper

Corresponding author:

Address: Martina Marchetti, Ph.D.

Institute of Chemical Technologies and Analytics

Vienna University of Technology,

Getreidemarkt 9/164-AC, A-1060 Vienna, Austria

E-mail: martina.marchetti@tuwien.ac.at

Tel: +43 1 58801 15162, Fax: +43 1 58801 15199

Study design to estimate the technical variation of SDS-PAGE and CGE-on-the-chip for mouse serum samples

To evaluate the technical variation of SDS-PAGE and the CGE-on-the-chip system, mouse serum of two samples (sample 7 and 5 from mouse 7 and 5 respectively) was used. Sample preparation was done as described in the original article. After that both samples were applied three times on three different gels and three times on three different CGE chips. Gel staining and evaluation was performed as it is described in the original article. This also applies for the capillary system.

Results and Discussion

To estimate the technical variations of the analytical methods two representative mouse serum samples were chosen. Sample 7 is a candidate for the sample group showing at least one far extreme value in box plot analysis pointing out that this sample has to be considered a critical sample in terms of biological variation within the genetic mouse pool or serum preparation. Supplementary Table 1 shows the results for the intra-gel (three identical samples on one gel) and inter-gel (three identical samples on three different gels) analysis. CV values for the relative peak abundances of each peak vary between 1.3 and 12.06 % giving an average CV of 6.72 % for the intra-gel analysis and 2.38 and 26.20 % resulting in an average CV of 11.11 % for the inter-gel comparison. Supplementary Table 2 shows the results for the CGE-on-the-chip analysis for the same sample. Intra-chip reproducibility for relative peak abundances varies between 0.13 and 15.65 % (average 5.25 %) and inter-chip variation between 0.30 and 35.66 % (average 12.07 %). Supplementary Table 3 and 4 represent the same calculations for sample 5, a representative sample for the sample group giving close extreme values in box plot analysis. For the intra-

gel analysis the CVs range from 1.43 to 12.35 % (average 7.22 %) and the calculated CVs for inter-gel analysis vary between 3.95 and 36.20 % (average 13.75 %). Better results were obtained for the CGE-on-the-chip system. Intra-chip variation ranges from 0.20 to 15.76 % (average 6.67 %) and inter-chip variation is represented by CVs between 0.25 and 20.34 % (average 10.21 %).

For our pre-screening approach we pointed out that CV values for single bands/peaks above 40 % are an indication for particular variations. The technical variations of relative peak abundances are clearly below that critical value for the CGE-on-the-chip system. As we only compare only intra-gel runs in the presented study the CVs are also below that threshold.

Additionally sizing reproducibility was calculated for SDS-PAGE and CGE-on-the-chip to point out that peak assignment is not a critical issue. Supplementary Table 5 and 6 sum up these data. Technical variation for sizing reproducibility turned out to be below 1 % and 3.3 % for intra-gel and inter-gel analysis respectively. For CGE-on-the-chip technical variation was better, below 1 % and 1.5 % for intra-chip and inter-chip analysis.

Supplementary Table 1: Summarised statistics of relative abundances for sample 7.1. Results for the intra-gel and inter-gel comparison of each selected protein band of SDS-PAGE**.**

intra-gel analysis				
Band	M_r mean [kDa]	Relative abundance mean [%]	SD of relative abundances [%]	CV [%]
1	14	3.28	0.14	4.32
2	15	1.58	0.12	7.40
3	21	0.23	0.03	12.06
4	27	9.44	0.38	4.05
5	35	0.78	0.05	6.99
6	40	1.41	0.13	9.23
7	44	1.23	0.14	11.91
8	48	1.14	0.07	5.97
9	54	0.51	0.04	8.68
10	57	13.50	0.52	3.74
11	65	57.88	0.76	1.30
12	76	7.88	0.38	4.71
13	84	1.13	0.08	6.91
inter-gel analysis				
Band	M_r mean [kDa]	Relative abundance mean [%]	SD of relative abundances [%]	CV [%]
1	14	3.28	0.21	6.44
2	15	1.58	0.13	8.14
3	21	0.23	0.05	22.20
4	27	9.44	0.58	6.09
5	35	0.78	0.06	7.16
6	40	1.41	0.20	14.03
7	44	1.23	0.32	26.20
8	48	1.14	0.08	6.93
9	54	0.51	0.08	16.30
10	57	13.50	1.25	9.27
11	65	57.88	1.38	2.38
12	76	7.88	0.96	12.12
13	84	1.13	0.08	7.15

Supplementary Table 2: Summarised statistics of relative abundances for sample 7.1. Results for the intra-chip and inter-chip comparison of each selected protein peak of CGE-on-the-chip**.**

intra-chip analysis			
Band	M_r mean [kDa]	Relative abundance mean [%]	SD of relative abundances [%]	CV [%]
1	6.3	0.37	0.02	4.54
2	8.6	0.05	0.01	11.25
3	11.8	0.37	0.01	2.69
4	12.9	0.62	0.01	2.34
5	17.3	0.53	0.02	2.98
6	21.5	0.05	0.01	12.53
7	23.3	3.78	0.06	1.71
8	27.6	0.42	0.03	6.13
9	34.2	0.16	0.01	4.31
10	35.9	0.15	0.01	3.53
11	41.5	0.16	0.01	6.15
12	46.1	0.06	0.01	15.65
13	49.3	0.18	0.01	5.82
14	51.0	0.69	0.02	2.63
15	55.1	0.07	0.00	5.63
16	58.3	0.33	0.00	1.25
17	67.8	92.00	0.12	0.13

inter-chip analysis			
Band	M_r mean [kDa]	Relative abundance mean [%]	SD of relative abundances [%]	CV [%]
1	6.3	0.37	0.03	7.82
2	8.6	0.05	0.01	15.19
3	11.8	0.37	0.02	4.00
4	12.9	0.62	0.05	7.30
5	17.3	0.53	0.02	4.34
6	21.5	0.05	0.01	19.52
7	23.3	3.78	0.09	2.37
8	27.6	0.42	0.03	6.26
9	34.2	0.16	0.01	8.41
10	35.9	0.15	0.01	9.99
11	41.5	0.16	0.03	21.81
12	46.1	0.06	0.01	20.22
13	49.3	0.18	0.01	7.03
14	51.0	0.69	0.09	13.44
15	55.1	0.07	0.02	35.66
16	58.3	0.33	0.07	21.57
17	67.8	92.00	0.27	0.30

Supplementary Table 3: Summarised statistics of relative abundances for sample 5.1. Results for the intra-gel and inter-gel comparison of each selected protein band of SDS-PAGE**.**

intra-gel analysis				
Band	M_r mean [kDa]	Relative abundance mean [%]	SD of relative abundances [%]	CV [%]
1	14	0.80	0.08	10.29
2	15	1.62	0.14	8.36
3	21	0.46	0.05	11.09
4	27	10.29	0.62	5.74
5	35	0.83	0.07	8.81
6	40	1.42	0.10	6.40
7	44	1.72	0.20	11.96
8	48	1.06	0.07	6.24
9	54	0.58	0.07	12.35
10	57	15.73	0.60	3.79
11	65	54.99	0.78	1.43
12	76	9.08	0.36	4.11
13	84	1.42	0.08	5.55
inter-gel analysis				
Band	M_r mean [kDa]	Relative abundance mean [%]	SD of relative abundances [%]	CV [%]
1	14	0.80	0.12	15.47
2	15	1.62	0.33	20.59
3	21	0.46	0.21	46.63
4	27	10.29	1.01	9.83
5	35	0.83	0.08	8.95
6	40	1.42	0.18	12.71
7	44	1.72	0.35	20.44
8	48	1.06	0.09	8.83
9	54	0.58	0.08	14.66
10	57	15.73	1.08	6.84
11	65	54.99	2.17	3.95
12	76	9.08	1.03	11.38
13	84	1.42	0.13	8.97

Supplementary Table 4: Summarised statistics of relative abundances for sample 5.1. Results for the intra-chip and inter-chip comparison of each selected protein peak of CGE-on-the-chip.

intra-chip analysis				
Band	M_r mean [kDa]	Relative abundance mean [%]	SD of relative abundances [%]	CV [%]
1	6.3	0.43	0.02	4.46
2	8.6	0.06	0.01	13.73
3	11.8	0.10	0.01	9.33
4	12.9	0.20	0.01	6.39
5	17.3	0.61	0.03	4.71
6	21.5	0.20	0.01	5.71
7	23.3	4.17	0.09	2.11
8	27.6	0.41	0.04	8.54
9	34.2	0.18	0.01	5.03
10	35.9	0.13	0.01	4.46
11	41.5	0.16	0.01	5.44
12	46.1	0.04	0.01	15.76
13	49.3	0.14	0.02	11.68
14	51.0	0.75	0.02	2.17
15	55.1	0.16	0.02	8.37
16	58.3	0.42	0.02	5.36
17	67.8	91.83	0.18	0.20

inter-chip analysis				
Band	M_r mean [kDa]	Relative abundance mean [%]	SD of relative abundances [%]	CV [%]
1	6.3	0.43	0.03	6.98
2	8.6	0.06	0.01	19.59
3	11.8	0.10	0.01	11.56
4	12.9	0.20	0.02	11.68
5	17.3	0.61	0.04	6.61
6	21.5	0.20	0.02	8.67
7	23.3	4.17	0.11	2.52
8	27.6	0.41	0.03	7.91
9	34.2	0.18	0.01	7.27
10	35.9	0.13	0.02	16.78
11	41.5	0.16	0.01	6.93
12	46.1	0.04	0.01	20.34
13	49.3	0.14	0.02	11.37
14	51.0	0.75	0.05	6.49
15	55.1	0.16	0.03	17.30
16	58.3	0.42	0.05	11.37
17	67.8	91.83	0.23	0.25

Supplementary Table 5: Summarised sizing statistics for sample 7.1 and 5.1. Results for the intra-gel and inter-gel comparison of each selected protein band of SDS-PAGE.

Band	intra-gel analysis for sample 7.1			intra-gel analysis for sample 5.1		
	M_r mean [kDa]	SD of M_r [kDa]	CV [%]	M_r mean [kDa]	SD of M_r [kDa]	CV [%]
1	14.3	0.1	0.4	14.4	0.1	0.5
2	15.2	0.1	0.4	15.3	0.1	0.7
3	20.7	0.1	0.4	20.7	0.1	0.6
4	25.3	0.1	0.4	25.4	0.1	0.4
5	33.8	0.1	0.2	33.9	0.1	0.3
6	39.0	0.1	0.3	39.0	0.1	0.3
7	43.7	0.1	0.3	43.7	0.2	0.4
8	47.3	0.4	0.4	47.3	0.1	0.3
9	54.4	0.3	0.3	54.6	0.1	0.2
10	57.9	0.5	0.5	57.8	0.2	0.3
11	64.8	0.5	0.5	65.2	0.2	0.3
12	76.8	0.4	0.2	77.1	0.2	0.2
13	84.6	0.2	0.2	85.0	0.2	0.2

Band	inter-gel analysis for sample 7.1			intra-gel analysis for sample 5.1		
	M_r mean [kDa]	SD of M_r [kDa]	CV [%]	M_r mean [kDa]	SD of M_r [kDa]	CV [%]
1	14.3	0.32	2.2	14.4	0.4	3.0
2	15.2	0.34	2.2	15.3	0.5	3.2
3	20.7	0.40	1.9	20.7	0.3	1.6
4	25.3	0.31	1.2	25.4	0.4	1.4
5	33.8	0.32	1.0	33.9	0.3	0.9
6	39.0	0.36	0.9	39.0	0.4	0.9
7	43.7	0.39	0.9	43.7	0.4	0.9
8	47.3	0.45	1.0	47.3	0.5	1.0
9	54.4	0.55	1.0	54.6	0.5	0.9
10	57.9	0.69	1.2	57.8	0.6	1.1
11	64.8	0.75	1.2	65.2	0.9	1.3
12	76.8	0.94	1.2	77.1	1.3	1.6
13	84.6	1.58	1.9	85.0	2.2	2.5

Supplementary Table 6: Summarised sizing statistics for sample 7.1 and 5.1. Results for the intra-chip and inter-chip comparison of each selected protein peak of CGE-on-the-chip.

Band	intra-chip analysis for sample 7.1			intra-chip analysis for sample 5.1		
	M_r mean [kDa]	SD of M_r [kDa]	CV [%]	M_r mean [kDa]	SD of M_r [kDa]	CV [%]
1	6.3	0.0	0.3	6.3	0.0	0.6
2	8.5	0.0	0.0	8.6	0.1	0.8
3	11.7	0.0	0.3	11.8	0.0	0.3
4	12.8	0.1	0.4	12.9	0.1	0.7
5	17.2	0.0	0.2	17.3	0.1	0.3
6	21.5	0.0	0.2	21.5	0.1	0.3
7	23.2	0.1	0.2	23.3	0.1	0.4
8	27.5	0.1	0.2	27.6	0.1	0.3
9	34.0	0.0	0.1	34.2	0.1	0.4
10	35.7	0.1	0.2	35.9	0.1	0.3
11	41.4	0.1	0.2	41.5	0.1	0.2
12	46.6	0.4	0.9	46.1	0.1	0.3
13	48.9	0.1	0.1	49.3	0.2	0.4
14	50.6	0.0	0.1	51.0	0.1	0.2
15	54.9	0.0	0.1	55.1	0.1	0.2
16	58.0	0.1	0.2	58.3	0.1	0.2
17	67.5	0.1	0.1	67.8	0.1	0.2

Band	inter-chip analysis for sample 7.1			intra-chip analysis for sample 5.1		
	M_r mean [kDa]	SD of M_r [kDa]	CV [%]	M_r mean [kDa]	SD of M_r [kDa]	CV [%]
1	6.3	0.0	0.5	6.3	0.1	0.8
2	8.5	0.1	1.0	8.6	0.1	1.3
3	11.7	0.1	0.7	11.8	0.1	0.6
4	12.8	0.1	0.7	12.9	0.1	0.8
5	17.2	0.1	0.5	17.3	0.1	0.5
6	21.5	0.1	0.6	21.5	0.1	0.3
7	23.2	0.1	0.5	23.3	0.1	0.4
8	27.5	0.1	0.3	27.6	0.1	0.5
9	34.0	0.2	0.5	34.2	0.2	0.6
10	35.7	0.1	0.4	35.9	0.2	0.4
11	41.4	0.3	0.7	41.5	0.2	0.4
12	46.6	0.7	1.4	46.1	0.2	0.4
13	48.9	0.2	0.5	49.3	0.3	0.6
14	50.6	0.2	0.4	51.0	0.2	0.4
15	54.9	0.1	0.3	55.1	0.2	0.3
16	58.0	0.1	0.2	58.3	0.1	0.2
17	67.5	0.1	0.1	67.8	0.1	0.2

Curriculum vitae

Name: Tom Grunert
Address: Aegidigasse 19/18,
                  1060 Vienna, Austria
Birth: Dresden, 26 February 1972
Nationality: German

Education

2005-present   Doctoral thesis
                 Title: The effect of tyrosine kinase 2 (Tyk2) deficiency on primary murine macrophages monitored by qualitative and quantitative proteomic analysis. Joint project of the Institute of Chemical Technologies and Analytics, *Prof. G. Allmaier*, Vienna University of Technology and the Institute of Animal Breeding and Genetics, *Prof. M. Müller*, Veterinary University of Vienna, Austria.

1995-2003   M.Sc. in Biology, Institute of Analytical Chemistry, *Prof. G. Allmaier*, University of Vienna, Austria.
                 Diploma thesis
                 Title: Characterisation of the glycoprotein antithrombin using affinity chromatography and MALDI-MS.
                 Grade: Excellent.

1999-2000   School for Artistic Photography in Vienna, Austria.

1991-1994   Graduate (FH) in Business Administration, College of the Federal Bank of Germany, Frankfurt/ Main, Germany.

Work experience

2004-2005   Digital photo archivist at the International Workgroup for Indigenous Affairs, Copenhagen, Denmark.

1999-2004   Technician (part-time), Research and Development, Octapharma Pharmazeutika Produktionsgesellschaft m.b.H., Vienna, Austria.

1994-1995   Official in charge of personnel administration, Federal Bank of Germany, Berlin, Germany.

1990-1991   Laboratory assistant, Institute of Medical Microbiology and Epidemiology, University Clinical Centre, Dresden, Germany.

Publications

1) <u>Grunert T</u>, Marchetti-Deschmann M, Miller I, Müller M, Allmaier G.
Comparing the applicability of CGE-on-the-chip and SDS-PAGE for fast pre-screening of mouse serum samples prior to proteomics analysis.
Electrophoresis. 2008 Nov;29(21):4332-40

2) Radwan M, Miller I, <u>Grunert T</u>, Marchetti-Deschmann M, Vogl C, O'Donoghue N, Dunn M, Kolbe T, Allmaier G, Gemeiner M, Müller M, Strobl B.
The impact of Tyrosine kinase 2 (Tyk2) on the proteome of murine macrophages and their response to lipopolysaccharide (LPS).
Proteomics. 2008 Sep;8(17):3469-85

3) Kremser L, Bruckner A, Heger A, <u>Grunert T</u>, Buchacher A, Josic D, Allmaier G, Rizzi A.
Characterization of antithrombin III from human plasma by two-dimensional gel electrophoresis and capillary electrophoretic methods.
Electrophoresis. 2003 Dec;24(24):4282-90.

4) <u>Grunert T</u>, Pock K, Buchacher A, Allmaier G.
Selective solid-phase isolation of methionine-containing peptides and subsequent matrix-assisted laser desorption/ionisation mass spectrometric detection of methionine- and of methionine-sulfoxide-containing peptides.
Rapid Commun Mass Spectrom. 2003;17(16):1815-24.

5) Heger A, <u>Grunert T</u>, Schulz P, Josic D, Buchacher A.
Separation of active and inactive forms of human antithrombin by heparin affinity chromatography.
Thromb Res. 2002 Apr 15;106(2):157-64.

Oral presentations

6th Austrian Proteome Research Symposium; Sep 2008; Vienna, Austria.
The effect of Tyk2 on cellular response in activated murine macrophages monitored by quantitative proteomics analysis
<u>Grunert T</u>, Strobl B, Marchetti-Deschmann M, Miller I, Radwan M, Vogl C, Gemeiner M, Allmaier G, Müller M.

Conference posters

3. ESF Functional Genomics Conference; Oct 2008; Innsbruck, Austria.
The impact of Tyrosine Kinase 2 (Tyk2) on the proteome of murine macrophages and their response to lipopolysaccharide (LPS).
<u>Radwan M</u>, Miller I, Grunert T, Marchetti-Deschmann M, Vogl C, O'Donoghue N, Dunn MJ, Kolbe T, Allmaier G, Gemeiner M, Müller M, Strobl B.

HUPO 2008 7th World Congress; Aug 2008; Amsterdam, Netherlands.
Proteomic study of Tyk2 deficient murine macrophages in response to poly I:C.
<u>Grunert T</u>, Strobl B, Marchetti-Deschmann M, Miller I, Radwan M, Vogl C, Gemeiner M, Allmaier G, Müller M.

Annual International Society for Interferon and Cytokine Research Meeting, Oxford, UK, 2007.
The influence of Tyk2 deficiency on the murine macrophage proteome.
Radwan M, Miller I, Strobl B, Grunert T, Dunn M, Vogl C, Marchetti M, Allmaier G, Gemeiner M, Müller M.

3rd Summer School in Proteomic Basics - Exploring the Diversity of Proteins, Brixen/ Bressanone, Italy, 2006.
Role of Tyk2 in systemic responses to endotoxin: a serum proteomics study.
Grunert T, Marchetti M, Miller I, Strobl B, Karaghiosoff M, Gemeiner M, Allmaier G and Müller M.

20th International Symposium on the separation and analysis of proteins, peptides and polynucleotides, Ljubljana, Slovenia, 2000.
Separation of active and inactive forms of human antithrombin III by heparin affinity chromatography.
Kovac A, Grunert T, Buchacher A, Schulz P, Josic D.

Scholarship

ERASMUS scholarship at the School of Biological Sciences, University of Manchester, UK, 1998-1999.